# SUB-MODELING OF THERMAL MECHANICAL FATIGUE CRACK PROPAGATION

**by**

**Valeriy Krutiy**

**A Thesis Submitted to the Graduate**
**Faculty of Rensselaer Polytechnic Institute**
**in Partial Fulfillment of the**
**Requirements for the degree of**
**MASTER OF SCIENCE**
**Major Subject: MECHANICAL ENGINEERING**

Approved:

_____
**Dr. Alexander Staroselsky, Thesis Advisor**

Rensselaer Polytechnic Institute
**Hartford, Connecticut**
December, 2009

# CONTENTS

Page

# LIST OF SYMBOLS

Nomenclature

| | | |
|---|---|---|
| **Δ** | [-] | delta or change in the subsequent symbol |
| **Δσ** | [MPa] | stress range |
| **σ** | [MPa] | mechanical stress |
| $\sigma_{max}$ | [MPa] | max mechanical stress |
| **ε** | [-] | engineering strain |
| **ν** | [-] | Poisson's ratio |
| **E** | [MPa] | modulus of elasticity |
| **h** | [W/(m$^2$K)] | heat transfer coefficient |
| **N** | [-] | number of cycles |
| **T** | [°C] | temperature |
| **t** | [s] | time |
| $K_I$ | [Mpam$^{1/2}$] | mode I stress intensity factor |
| $K_{IC}$ | [MPam$^{1/2}$] | critical mode I stress intensity factor |
| $K_{II}$ | [MPam$^{1/2}$] | mode II stress intensity factor |
| $K_{III}$ | [MPam$^{1/2}$] | mode III stress intensity factor |
| J | [J/m$^2$] | J integral |
| $K_{eff}$ | [MPam$^{1/2}$] | effective stress intensity factor |
| $\Delta K_{eff}$ | [MPam$^{1/2}$] | change in effective stress intensity factor |
| **a** | [m] | crack length |
| **b** | [-] | FRANC3D power law growth factor |
| **α** | [grad] | angle |
| ***G*** | [MPa] | shear modulus |
| R | [-] | stress ratio |
| **Q** | [*J*] | thermal energy |
| **q** | [W] | heat transfer rate |
| **K** | [W/mK] | thermal conductivity |
| **A** | [m2] | surface area |
| **CTOD** | [m] | crack tip opening displacement |

Subscripts

| | |
|---|---|
| FEA | finite element analysis |
| LEFM | linear elastic fracture mechanics |
| UX | displacement at node X |
| FX | force at node X |
| ASTM | American Society of Testing and Materials |
| BE | boundary element |
| BEA | boundary element analysis |
| BES | boundary element system |
| FCG | fatigue crack growth |
| FCP | fatigue crack propagation |
| FE | finite element |
| FEA | finite element analysis/analyses |
| FLAGRO | fracture mechanics and fatigue crack growth analysis software |
| FRANC | FRacture ANalysis Code (2D or 3D) |
| HCF | high cycle fatigue (stress based or load controlled fatigue) |
| SIF | stress intensity factor (K) |
| 1D | one-dimensional |
| 2D | two-dimensional |
| 3D | three-dimensional |
| LCF | low-cycle fatigue |
| TMF | thermal mechanical fatigue |

# LIST OF TABLES

Table Page

# LIST OF FIGURES

Figure Page

# ACKNOWLEDGMENT

I would like to thank my advisor Professor Alexander Staroselsky for his time and support. In addition, I would like to thank my co-workers Kaliya Balamurugan and Peter Tomeo for sharing their experience in Ansys. Finally, I would like to thank my friends and family for their support and putting up with me for these past few months.

I would also like to thank my dear wife Iouliia for her love and support during the past years. Without her patience and encouragement, this work would not have been possible.

# ABSTRACT

This thesis outlines a framework for damage tolerance assessment using computational mechanics software. This framework is presented through the methodology for simulating of through cracks growth in the walls of turbine blade structures. A CAD model of the airfoil was created. Geometry derived from this model was used to construct a finite elements model. Crack trajectories have been computed during simulation. The analysis was conducted under combined effects of thermal and mechanical loads. Data similar to a typical turbine blade were used to run a heat transfer analysis and, subsequently, a thermal structural analysis, finally the incremental thermal structural fracture mechanics analysis have been performed. The interaction between the thermal-mechanical loads acting on the superstructure and the local structural response near the crack tips is accounted for by employing a hierarchical sub-modeling and interpolation strategy. Stress intensity factors are computed using an extension of the M-integral method embedded in Franc3D/NG. Crack trajectories are determined by applying the maximum stress criterion. Crack growth results in localized mesh of local element and the deletion regions are remeshed automatically using a newly developed all-quadrilateral meshing algorithm. The predicted mixed-mode fatigue crack propagation results of the proposed methodology compares well with published in-field observations of failed blades. The effectiveness of the methodology, and its applicability to performing practical analyses of realistic structures, is demonstrated by simulating curvilinear crack growth in a airfoil wall from cooling hole which represents a typical turbine blade microfeature. Finally, a damage tolerance design methodology is proposed; where the effects of thermal mechanical fatigue are based on the combine respond the both uncracked and cracked blade geometry. The advantages of the proposed methodology are that it can accurately and parametrically vary different inputs (temperatures/temperature gradients, complex model geometry, and material properties) to show the impact on the stresses and strains, as well as crack behavior. The prediction results can estimate the severity of damage based on specific conditions in turbine engines and facilitate a damage tolerance approach toward the maintenance of an engine.

# 1. Introduction

## 1.1 Turbine blades used in aircraft engines.

Turbine blades and vanes used in aircraft engines are typically the most demanding structural applications for high temperature materials due to combination of high operating temperature, corrosive environment, high monotonic and cyclic stresses, long expected component lifetimes, and the enormous consequence of structural failure.

In a basic turbojet engine, Figure 1-1 air enters the engine and passes through the compressor where it is pressurized and then mixed with fuel. The fuel burner ignites the high-pressure mixture of fuel and air causing temperatures above 1500°C in the combustion chamber. This hot, fast-moving air then enters the turbine section, where stationary vanes direct the air into a turbine is turned as the hot air flows around the turbine blades. The turbine turns the shaft that is connected to the compressor so that the cycle continues. After passing through the turbine, hot air accelerates through the nozzle and exits the engine. The overall acceleration of air causes a thrust force on the engine in the direction opposite the airflow. The average pressure and temperature distribution expose on Figure 1-1.

The higher the operating temperature of an engine, the greater its efficiency, and the more power it can produce from each gallon of fuel. There is, therefore, an incentive to operate such engines at as high a temperature as possible. Among the critical limitations on the operating temperature of an engine are the materials used for applications in the hottest regions of the engine, such as turbine airfoils.

The material of jet engine turbine blades used in today's airplane applications is subjected to very high temperatures and mechanical loads. Especially in the high pressure region behind the combustion chamber the turbine blades are made of monocrystalline nickel-base super alloys in order to withstand the very high thermal as well as mechanical loads. The loading conditions vary drastically during starting and landing cycles of the airplane, with operational temperatures reaching up to 1100° C, imposing a thermo-mechanical loading on the material.

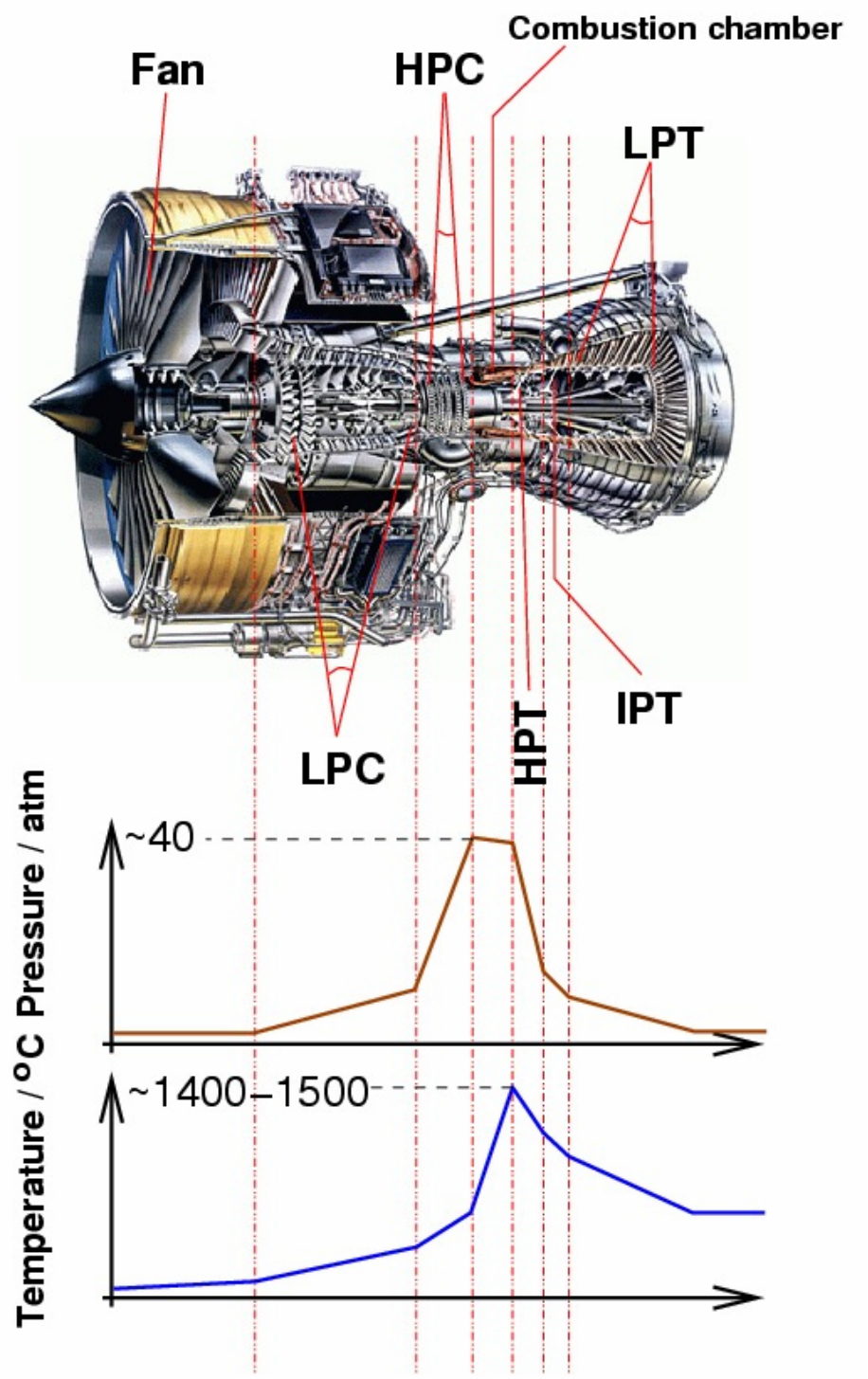


**Figure 1-1 A jet engine (Rolls-Royce Trent 800), showing the different stages: intermediate pressure compressor (IPC), high pressure compressor (HPC), high pressure turbine (HPT), intermediate pressure turbine (IPT), low pressure turbine (LPT), and the pressure and temperature profiles along the engine. Image of the Trent 800 courtesy Rolls-Royce Plc. Diagrams after Michael Cervenka, Rolls-Royce [47]**

Currently the most widely used single crystal turbine blade superalloys are PWA 1480/1493, PWA 1484, RENE N-5 and CMSX-4. These alloys play an important role in commercial, military and space propulsion systems. Single crystal materials have highly orthotropic properties making the position of the crystal lattice relative to the part geometry a significant factor in the overall analysis. The failure modes of single crystal turbine blades are complicated to predict due to the material orthotropy and variations in crystal orientations. Fatigue life estimation of single crystal turbine blades represents an important aspect of durability assessment. [2]

Extreme temperature gradients and transients thermally induce the most severe cyclic stresses encountered by turbine airfoils. These thermal stresses combine with mechanically induced centrifugal and bending loads to produce thermo mechanical fatigue (TMF) of the airfoil. Anisotropic material properties of advanced turbine blade alloys further complicate analysis and life prediction for these complex loading conditions.

It is therefore of interest to develop a robust design approach, so that the effects of defects and damages can be evaluated with great accuracy. In the design phase, where the structural design of blade is made, models of the entire blade are used to assess production, stiffness and strength aspects. Several load cases are analyzed. Models of perfect blades are used. The purpose of the latter is to generate a damage tolerant design, to establish criteria for position, size and type of defects as well as to determine critical initial crack locations for the preliminary damage detection. A novel approach to provide a desired fatigue life and crack tolerance is introduced.

## 1.2 Problem statement

It is the intention of this thesis to develop a novel sub-model methodology of advanced materials TMF crack propagation. This method enables prediction of a crack growth rate and trajectory. It is important to emphasize the sub-modeling approach to greatly reduce the amount of processed data. We will implement this new method into finite element software through development of user subroutines. The developed crack propagation framework and model predictions would lead to the formulation of damage tolerant failure criteria and possible design optimization.

## 1.3 Research objectives

The life prediction and damage tolerant failure criteria of engine components require the consideration of thermal-mechanical fatigue (TMF) cycles. The problem of thermal mechanically driven crack growth in the presence of significant inelastic strains is a challenging problem. In order for a novel sub-model methodology to be useful for predicting thermal-mechanical crack growth in components, it should satisfy the following conditions. 1) should predict crack growth rate of a single crack, 2) correctly predict fatigue crack growth rates independently of part geometry and 3) be calculable for complex real part geometry. Obviously, parameters not satisfying the above requirements would be of limited value, since component or simulated component testing be required to obtain crack growth rate information. [1]

The objective of this thesis is a development of methodology for the fatigue life prediction based on damage-tolerant approach. More specific attention of framework should be given to sub-modeling of TMF crack propagation in turbine blade to achieve both computational efficiency and accuracy. The methodology should combine CAD modeling; finite element analysis, fracture mechanics, meshing, sub-modeling and interpolation for functional workflow and accurate prediction of crack growth. Our research will concentrate on developing three-dimensional elastic finite element model and 3D mixed-mode fatigue crack propagation model to calculate stress intensity factors [44]. The effects of temperatures/temperature gradients distribution, complex model geometry, material properties, initial crack size, location and orientation should be investigated using the proposed model.

## 1.4 Assumptions/limitations

The predictions of fatigue crack growth in a structure are based on the similarity principle. The value of $\Delta$K, Range of Stress Intensity Factor, is used as the crack driving force to obtain the corresponding da/dN from the basic material fatigue crack growth data of the material.

Depending on the purpose of the predictions, some simplifications of the prediction procedure can be justified to obtain estimates of $\Delta$K values. However, more accurate

predictions require that data on the K variation along the crack front, which implies that FE calculations should be made.

The plastic field ahead of the crack tip significantly limits the applicability of the linear elastic fracture mechanics. It is especially important for small cracks and high temperatures applications.

## 1.5 Thesis layout

The following chapters will go step by step through the research performed for this thesis. Chapter two is a review of the fatigue failure, thermal mechanical fatigue research and turbine blade design approach description. Chapter three is a discussion of the completed thermal-mechanical analysis with a review of build models and applied loading schemes. The analytical and finite element solutions for the crack nucleation are introduced. Chapter four includes the numerical fracture mechanics analysis. The chapter concludes with a discussion of fatigue and fracture mechanics interaction and the methods are used in this research to analyze crack propagation. The models description and boundary conditions setup and software selection used for crack propagation simulation are presented. Chapter five is a discussion of results and data analysis. This chapter contains proposed crack propagation methodology and makes recommendations for future research.

# 2. Background and literature review

The primary goal of this thesis is to develop a methodology that accurately characterizes a crack growth resulting from TMF in turbine blades. To date, there has not been comprehensive research published in open literature which addresses this specific problem. To the best of our knowledge this is the first systematic study on this subject. However, when separating this problem into the general engineering issues that are connected to the application, some published researches are applicable.

For example, any material undergoing cyclic loading involves fatigue research. When heat is also cyclically applied, the study of thermo-mechanical fatigue (TMF) research as is reasonable. Crack resulting from TMF involves a study of the effects of thermal gradients distribution, any study related to cracking concerns fracture mechanics and fatigue crack growth. Additionally, modeling each of these types of the problems with FEA can be a research area by itself. So once these contributing subjects have been identified, a survey of the previous research in each of these areas should be done before investigating the more specific problem. Thus we will analyze: 1) thermal fatigue and TMF research, 2) fracture mechanics and fatigue crack growth, 3) the foundations of blade design requirements, materials, cooling; and 4) fracture analysis, FEA modeling

## 2.1 Fatigue of materials review

Fatigue research is normally classified today by either a lifing approach (estimating the total cycles until fracture of a material for a range of cyclic stresses) or a fatigue crack growth/damage tolerance approach. The roots of lifing date back to the early 1900. Basquin [48] suggested that the true, elastic stress amplitude ($\Delta\sigma/2$) of fatigue had a linear relationship on a log-log scale with cycles-to-failure ($N_f$), thus defining the modern-day S-N curve. Coffin [49] and Manson [50] have developed a power-law function for plastic strain-life. Basquin's and the Coffin-Manson's fatigue life representations were combined to form the total strain-life equation and are graphically shown in Figure 2-1 as the strain-life curve.

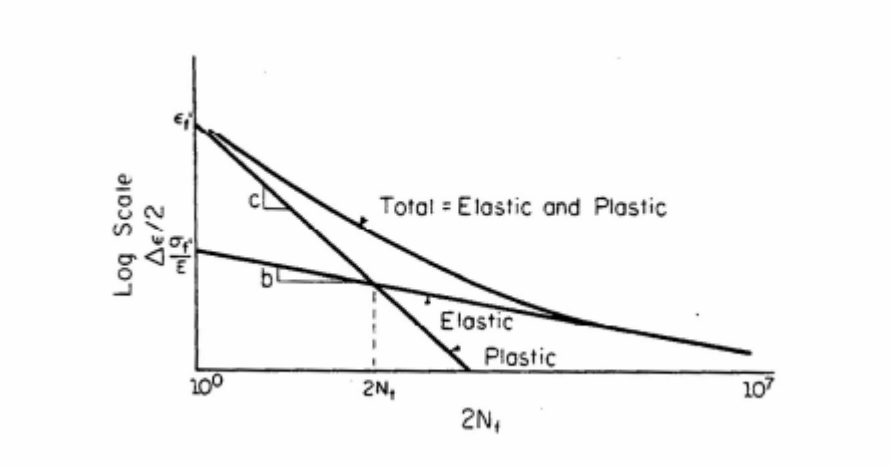


**Figure 2-1 Total Strain-life Curve [51]**

While this relationship represents the general trend of most metals and is still used as the baseline for strain-life relationships, the study of TMF requires a more detailed analysis of the specific damage mechanisms involved.

It is important to note that during the low-cycle fatigue (LCF) regime, plasticity is a dominant deformation mode. This determination of the dominant damage mode becomes crucial in determining the subsequent propagation and ultimate failure of the damage. In 1971, Manson, Halford, and Hirschberg [52] proposed strain range partitioning (SRP) as a means of quantifying the specific damage mechanisms involved in strain-life determination. By assuming that each partition can model a specific damage type with a specific number of life cycles, a Palmgren [53]-Miner [54] type life prediction can be used.

The fatigue mechanism in metallic materials should basically be associated with cyclic slip and the conversion into crack initiation and crack extension. The fatigue life until failure comprises two periods, the crack initiation period and the crack growth period. The crack initiation period includes crack nucleation at the material surface and crack growth of micro-structurally small cracks. The crack growth period usually is covered by Paris equation [70]. In many cases the crack initiation period covers a relatively large percentage of the total fatigue life.

Micro-structurally small cracks can be nucleated at stress amplitudes below the fatigue limit. Crack growth is then arrested by micro-structural barriers. The fatigue limit as a threshold property is highly sensitive to various surface conditions. At high stress

amplitudes, and thus relatively low fatigue lives, the effect of the surface conditions is much smaller.

In view of possible effects during the crack initiation period, it can be understood that scatter of the fatigue limit and large fatigue lives at low stress amplitudes can be large, whereas scatter of lower fatigue lives at high amplitudes will be relatively small.

### 2.1.1 Fracture mechanics and crack growth

The ultimate failure in fatigue is always precipitated by fatigue cracking at some level. This cracking, also known as fatigue crack growth (FCG), has become a foundational area of study as it pertains to damage-tolerant design. Damage tolerance is a mechanistic philosophy and methodology whereby the remaining strength and/or life of a component is determined after measurable damage. According to this type of methodology, one deems a certain amount of damage to a component acceptable for use if it can be quantified at a non-critical stage. More specifically in regards to fracture mechanics and fatigue design, a certain known crack length, a, is acceptable up to a certain critical length, ac.

The starting point of this study has its pedigree fracture mechanics and a review of the work done in this field along with FCG is very significant to this research. This section will survey Linear Elastic Fracture Mechanics (over 95% of blade design in the turbine engine industry is accomplished via 3D elastic anisotropic FEA, although crystal plasticity analysis is becoming a common tool for research applications, it is still not practical for blade design because of complex 3D geometry and loading involved [44]), Nonlinear Fracture Mechanics (theoretical aspects only), and a section on how to model LEFM areas using FEA.

### 2.1.2 Linear elastic fracture mechanics

Systematic analysis of the mechanical failure started in 15$^{th}$ century by Leonardo da Vinci. He has studied mechanical strength of metal wires. However only in 18$^{th}$ century invention of steam machine and following industrialization brought the extensive studies of the failure behavior of metals. Brittle fracture testing was first performed by Inglis [64] in 1913 and was finally quantified by Griffith [65] in 1920 using the First Law of

Thermodynamics and an energy balance in looking at the stress analysis of an elliptical hole. Later, Irwin [66] and Orowan [67] introduced local plasticity, thereby representing cracking in metals more accurately.

In 1958 Irwin proposed the stress-intensity factor K for static fracture analysis.

$$K = \sigma\sqrt{\pi a}Y \tag{2.1}$$

K became a universal parameter. It depends on crack length, mechanical stress and geometry function. In spite of the significance of plastic deformation in the crack tip zone, the linear elastic fracture mechanics (LEFM) became a foundation to the study of fracture and damage tolerant design. Westergaard [68], Dugdale [69], and others followed as modifications to LEFM continued in efforts to more rigorously account for the mechanics of cracked materials.

In 1961 Paris [70] applied LEFM concept by introducing simple empirical equation (2.1).When plotting a fatigue crack growth rate curve, it is common to plot the log (da/dN) versus log (ΔK) and the result is a sigmoidal shape as seen in Figure 2-6. Paris offered a mathematical approximation of the linear portion of this curve in Region II known as the Paris Law as listed in Equation 2.1.

$$\frac{da}{dN} = C(\Delta K)^n \tag{2.1}$$

C and n are material constants that are determined based on the fit of experimental data. Paris' low has become the corner stone of the use of fracture-mechanical methods in the aviation and automotive industries.

Paris' law is an overestimation for many problems of fatigue crack propagation, since are many important parameters are neglected. There have been many modifications which depend upon the specific type of loading of the material. Forman [72] incorporated the applied stress ratio, R and took into consideration Region III of the FCG curve, where crack growth is rapid as K approaches the fracture toughness of the material, $K_c$. (Equation 2.3)

$$\frac{da}{dN} = \frac{C(\Delta K)^m}{(1-R)K_c - \Delta K} \tag{2.3}$$

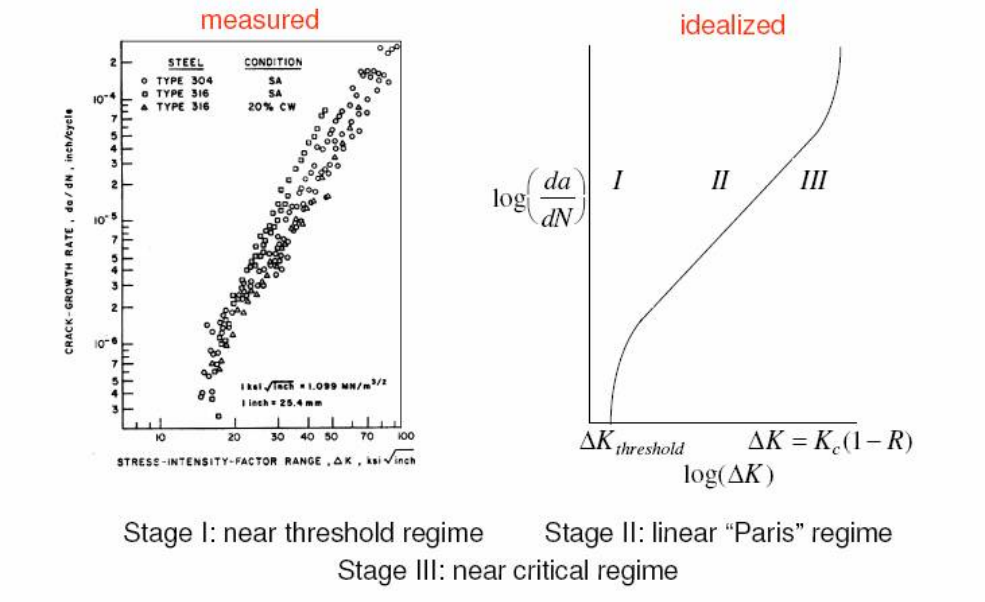


**Figure 2-2 Typical FCG data as represented by log da/dN vs. log ΔK [47]**

Walker [73] incorporated ratio R into FCG estimation. Based on two different aluminum alloys, Walker developed equation (2.4), which modifies Forman's work using an additional exponent, m.

$$\frac{da}{dN} = C[(1-R)^m K_{\max}]^n \tag{2.4}$$

The crack closure phenomena has resulted the equation improvements. As a result of the plastic zone that is created at the crack tip, some additional amount of material plastically deformed. This additional material closes the crack before the applied stress has reached its minimum. This crack closure results in a decreased ΔK, known as the "effective" stress intensity range. The $\Delta K_{eff}$ equals the difference between the maximum $K_{max}$ and the $K_{op}$ when the crack begins to open. (Equation 2.5) [74, 75]

$$\Delta K_{\text{eff}} = \Delta K_{\max} - \Delta K_{\text{op}} \tag{2.5}$$

Even though LEFM became a well-established approach in particular for structural integrity of constructions, the need to develop and use high performance materials and to reasonably define there fatigue-strength limits. The extensive crack-tip plasticity has to be evaluated. The elastic plastic fracture mechanics (EPFM) have been introduced.

### 2.1.3 Elastic plastic fracture mechanics

Elastic-plastic fracture mechanics (EPFM) approaches like cyclic crack-tip opening (ΔCTOD) and the cyclic J-integral became important parameters to describe crack propagation.

Irwin [104] introduced plastic zone correction to physical crack length. Dugdale [69] and other researches [80], [81] proposed and developed yield-strip model. Later, it became the crack tip opening displacement (CTOD) analysis as a measure of crack tip blunting.

Rice [76] suggested the nonlinear energy-released rate, in form of a path independent line integral around the cracked region. The energy release rate, J-integral, accounts the change in the potential energy due to crack growth. Hutchinson [77] and Rice and Rosengren [78] used the Ramberg-Osgood equation [103] for monotonic loading conditions to define the stresses and strains ahead of the crack tip for elastic-plastic material behavior (Equations 2.6 and 2.7).

$$\sigma_{ij} = k_1 \left( \frac{J}{r} \right)^{\frac{1}{n+1}} \tag{2.6}$$

$$\varepsilon_{ij} = k_2 \left( \frac{J}{r} \right)^{\frac{1}{n+1}} \tag{2.7}$$

Dowling and Begley [79] applied the J-integral concept to cyclic-loading conditions (Equation 2.8).

$$\frac{da}{dN} = C'(\Delta J)^{m'} \tag{2.8}$$

Staroselsky, Vestergaard, Anniggery and Favrov [100] following similarity with linear fracture mechanics and taking into account that $\Delta \mathrm{K} = \mathrm{K}_{\max} - \mathrm{K}_{\min} = \mathrm{K}_{\max}(1-R)$, expressed the crack growth rate as following power function (Equation 2.9).

$$\frac{da}{dN} = A' J_{\max}^{q} (1-R)^{m} \tag{2.9}$$

Shih [82] determined a relationship between the CTOD and the J-integral.

Various approaches to determine elastic-plastic material behavior at crack tip are proposed in a literature. Micro-crack propagation models to include creep and/or plasticity, but without J-integrals were introduced [83] with a new FCG approach for the plastic strain range-based growth law. At [84] modified the Paris' Law introduced for FCG through a cavitated material, as induced by creep. Landes and Begley [85], and later Saxena [86], correlated C* and Ct to crack data.

The J-integral is most commonly used to quantify nonlinear fracture. Further modifications have been made to extend the scope of the J-integral to more accurately represent the nature of FCG for the given TMF test environment and material. Blackburn [87] J* and Kishimoto [88] J^ path independent integral approaches permitted a wider range of loading and of materials response. Summary path integrals properties have been represented by [89] Under NASA's HOST Program (HOt Section Technology), the study of eight path-independent integrals shows the J* and J^ proved to accurately predict FCG behavior of Inconel 718. The T* parameter [90] proved to model all conditions as well, except time dependent conditions. Kim and Van Stone [91] found that both J* and J^ parameters describe crack growth behavior well for elevated temperatures with a hold time for Alloy 718. They later found [92] that these integrals correlate well to FCG under isothermal conditions when the crack tip deformation has large-scale plasticity.

Predictions on fatigue properties are basically different for the crack initiation life and for the crack growth period. The various characteristics of fatigue fractures can be understood in terms of crack initiation and crack growth mechanisms. These characteristics are essential in failure analysis, but they are also relevant to understand the significance of technically important variables of fatigue properties.

## 2.2 Thermal mechanical fatigue research

People used TMF effects in pre-historic time by fire heating and water cooling stones which resulted in the stone fractures. However, the study of thermal effects on mechanical behavior dates back to 1838 when J. Duhamel [55] published equations for

thermal stresses resulting from non-uniform heating. In 1894, Winkelmann and Schott [56] investigated thermal shock in ceramics, linking thermal stresses to fracture, quantitatively. In 1935, Schmid and Boas [57] researched thermal strain-induced plasticity in crystals. Bollenrath and coworkers [58] published work on thermal shock in ductile metals.

The behavior of materials under TMF conditions have been predicted by using and modifying many of the research works. The nature of high temperature, strain-induced plasticity was studied to separate, measure, and predict TMF damage. Millenson and Manson [59] explained the reason of thermally induced cracking in welded turbine wheels as consequential from cyclic plastic strains. Another part of research has been focused on the microstructural properties of materials on TMF. Sehitoglu [60] suggested the microstructural mechanisms carrying out in TMF. In [61] the study was completed to describe the isothermal TMF in various environments. The effects of oxidation-induced crack nucleation were defined; the transgranular and intergranular cracking in creep conditions were also observed. Remy [62] completed TMF study on the nickel-based superalloy, IN-100, modeling interdendritic oxidation and quantifying its effect on fatigue crack growth for CT specimens. These loads are normally applied in-phase (IP), whereby a specimen is put into tension when at high temperature, or out-of-phase (OP) with high-temperatures applied when the specimen is at its low load. Remy's view on TMF is a useful starting-point for investigating phenomena, and some classical TMF data acquired in. [63] must be noted as well. The current researches involve a more complex interaction of thermal and mechanical behavior than simply IP and OP TMF.

### 2.2.1 Thermal mechanical fatigue cracking

TMF cracking occurs at many locations on turbine airfoils, including pressure and suction sides and both leading and trailing edges [2]. In anisotropic structures, cracks are observed both parallel and normal to the casting growth direction (Figure 2-4). Biaxial loading conditions can cause cracking in orientations counter-intuitive to historical conditions. The anisotropic nature of single crystal and directionally solidified blades make it necessary to perform 3D stress analysis on the airfoil design. Figure 2-3

TMF cracking observed on anisotropic turbine blades can occur parallel and perpendicular to the casting solidification direction.

Fatigue cracks are nucleated at the blade leading edge cooling hole locations (Figure 2-3) due to a combination of mechanical and thermal cyclic stresses and strains. There is considerable blade-to-blade variation in the region where fatigue cracks are initiated at the cooling holes because of geometry properties and BC variations.

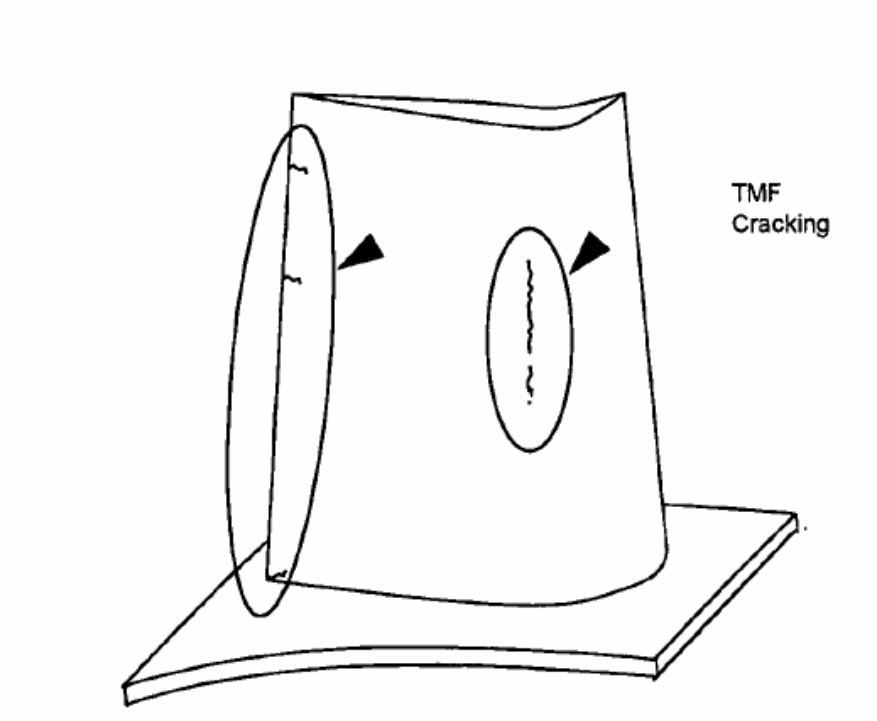


**Figure 2-3 TMF cracking observed on anisotropic turbine blades [2]**

Cracking adjacent to the cooling holes resulted from thermal stresses. Such cracks usually show sub-critical growth behavior.

The critical stress state variables such as temperatures, stress and strain components are usually obtained by finite element analysis (FEM). The complexity of turbine blade design makes an elastic-plastic finite element analysis very expensive and time consuming. Generally, the analysis is limited to elastic properties. Over 95% of blade design in the turbine engine industry is accomplished via 3D elastic anisotropic finite element analysis. Although creep and plasticity analysis are becoming a common tool for research applications, it is still not practical for blade design because of complex 3D

geometry and loading involved. [44] Elastic 3D finite element analysis results in a prediction of the full states of stress and strain in the part due to the thermal and mechanical loadings of the mission point being analyzed.

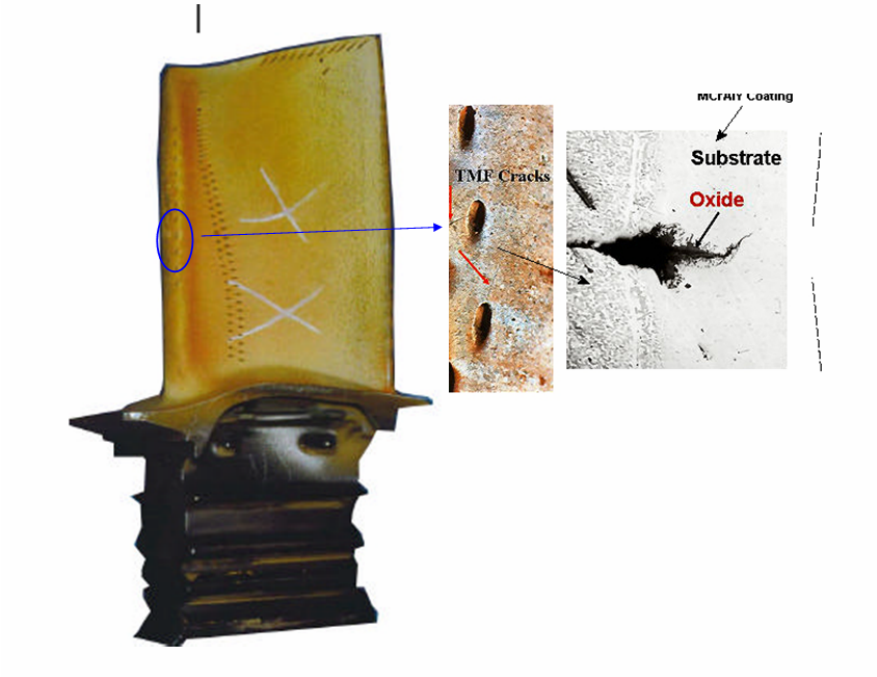


**Figure 2-4 Fatigue cracks typically nucleate at the blade leading edge cooling hole locations[48]**

### 2.2.2 Thermal mechanical fatigue of the turbine blades

There are 2 types of TMF – Cycle I and Cycle II. Cycle I, or the linear out of phase cycle, has a strain temperature profile characterized by the simultaneous occurrence of minimum strain and maximum temperature. Cycle I is generally the more damaging of the two for high strength, low ductility materials because the compressive mechanical strains in conjunction with elevated temperatures may promote compressive creep, thereby causing the mean stress to shift upwards during each cycle and cause fatigue damage to increase. Rotor TMF crack initiation, if it does occur, is generally similar to a Cycle I type (Figure 2-5) since fatigue capability under this condition may be less than that determined isothermally.

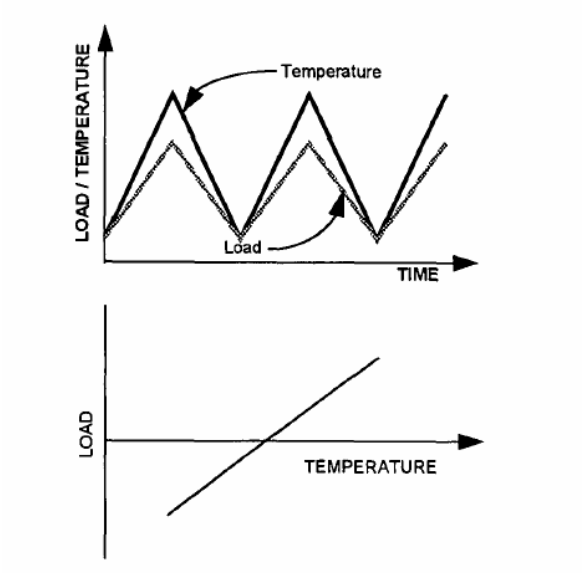


**Figure 2-5 In-phase load and temperature waveform [20]**

Cycle II, or in-phase TMF, occurs when the maximum strain is directly in phase with the maximum temperature. In these conditions, the mean stress can relax towards compression, which may delay crack formation and propagation depending on the damage mode (e.g., transgranular or intergranular). This type of cycle often occurs

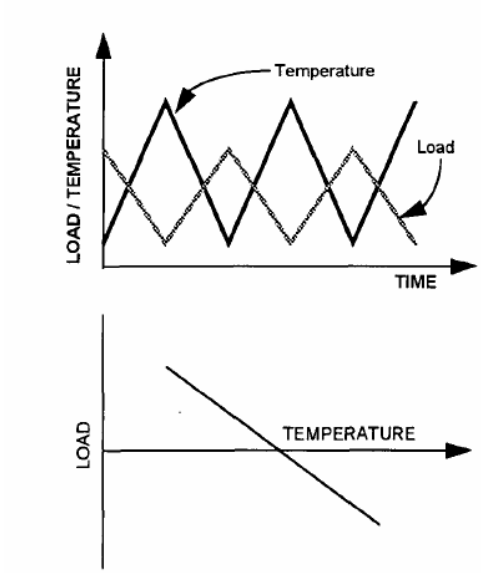


**Figure 2-6 Out-of phase load and temperature waveforms [20]**

in conditions where thermal expansion is not controlled by the adjacent material (Figure 2-6) or in cases where the rotational speed, as opposed to gas path temperature, dominates the total stress response. A wide variety of thermal and mechanical loading

cycles are experienced by turbine airfoils. These are dependent on the location along the airfoil and the speed of the particular power transient. The phasing between thermal and mechanical loads defines the TMF response of the airfoil [20]. The extremes of load-temperature phasing are in-phase (Figure 2-5) and out-of-phase (Figure 2-6). In-phase cycles occur when an unconstrained local area of the blade is mechanically loaded at the same time the temperature increases. Out-of-phase cycling occurs when a locally constrained area of the blade tries to expand both mechanically and thermally as temperature increases. This usually causes the blade to go into compression. Out-of-phase cycling is generally the most harmful because stress relaxation at the maximum temperature develops high mean stresses. While actual turbine blade TMF cycles are a combination of in-phase and out-of-phase cycles, TMF characterization of turbine blade materials is generally performed using out-of-phase cycles [20].

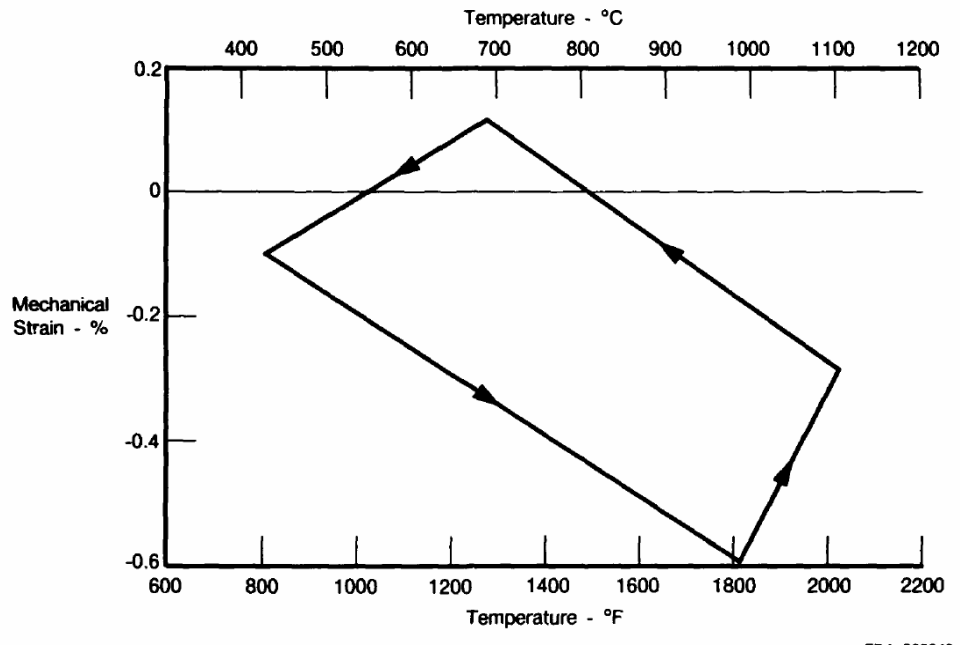


**Figure 2-7 Typical Quadrilateral TMF Cycle [20].**

Figure 2-7 An Typical strain and temperature cycle similar to those seen in turbine blade analysis. Temperature and strain are nearly out-of-phase. The points are individual time steps in the mission.

However, during in-phase TMF cycles the high temperature creep is much more pronounced. The creep induced damage and creep induced residual stresses play the key role in IP TMF.

TMF life prediction in turbine blades commonly begins with 3D elastic finite element stress analysis. The elastic stresses and strains are combined in a TMF parameter to predict TMF life. Often the finite element analysis identifies the high strain locations within the blade and focuses detailed stress-strain constitutive analysis on those areas. The hysteresis loop predictions are used to define the shakedown stress state which can be applied to an appropriate TMF life prediction technique

Thermal-mechanical fatigue damage mechanisms may occur in locations undergoing constrained thermal growth. Since environmental and creep damage can become active under these conditions with high temperatures, isothermal life predictions can be inadequate. The interaction of these effects needs to understand to develop a reliable and physically based predictive methodology for components that are subject to TMF conditions.

In summary [24], the following general rules apply for the TMF of nickel-base super alloys:

- The greatest TMF resistance has been obtained in the [001] direction. The elastic modulus (and thus the stresses) developed is lower than in other directions for single crystals.
- The mean stresses to be sustained and do not relax because of the TMF unsteadiness during the inelastic deformation. The mean stresses play a considerable role at finite lives, because the plastic strain range is smaller than the elastic strain range.
- Complex chemistries of oxides form with properties different from those of the substrate, resulting in internal stresses and oxide fracture that channels the crack into the material.
- TMF results display strain-rate sensitivity generally for the majority of nickel-base alloys at temperatures above 700° C. If the strain rate is reduced or hold periods are introduced, the cycles to failure are lowered.

- TMF IP damage is larger than TMF OP damage at high strain amplitudes, whereas the trend is reversed at long lives for most nickel superalloys. The diamond cycle often produces lives that fall between the TMF IP and TMF OP extremes.

## 2.3 The airfoil design approach

Turbine blades and vanes used in aircraft engines, typically the most demanding structural applications for high temperature materials due to combination of high operating temperature, corrosive environment, high monotonic and cyclic stresses, and long expected component lifetimes, and the enormous consequence of structural failure.

**Figure 2-8 A jet engine HPT blade. Photo courtesy S.Tin, Rolls-Royce [48]**

There are several consideration involved in designing turbine blades. The basic blade design factors are given in [15]. The aerofoil design is probably the primary deliberation since it is essential for the blade to generate sufficient power to drive the compressor at maximum efficiency. Aspects that influence design include the aircraft role, (civil or military application), and the number of stages required in the proposed design configuration. Within the context of the current paper it is sufficient to note that aerodynamic factors influence blade lives by dictating blade geometry, thus fixing the level of induced stresses and thereby ultimately determining the failure modes and

failure locations. For advanced gas turbine engines, where turbine entry temperatures can be significantly above the incipient melting temperatures of available blade materials, cooling of first stage nozzle guide vanes and HP turbine rotor blades is an essential requirement.

However compromises again have to be made between the ideals of cooling design and the requirements of blade manufacture. As well as introducing stress concentration features, cooling passages contribute to the substantial variations in temperatures which occur over small regions of the blade cross section. Both aspects compound the difficulties of accurate blade life determination.

Mechanical integrity is the final design consideration since having met aerodynamic and blade cooling requirements, the blade must have the ability to withstand the imposed static and cyclic stresses. Although many factors affect mechanical design the two of importance in respect to the current paper are (i) the combined thermo mechanical load state within the blade and (ii) the crack propagation process.

The turbine blade general cooling solution has received attention in a blade design. Thermal efficiency of a gas turbine engine can be improved by increasing the turbine inlet gas temperature. As turbine inlet temperature is increased, there is a greater need for more efficient cooling. A turbine blade operates typically at temperature 1300°-1400° C, pressure 1.20-1.70 Mpa and in addition to that it rotates at the speeds greater than 3000 rpm. The efficient cooling mechanisms are needed to improve blade life and overall efficiency of the turbine. Present material cannot withstand such high thermal stresses in this extreme operating environment of pressure and temperature. Therefore, for the Nickel-based Single Crystal Superalloy blades the sophisticated cooling techniques have been employed in order to maintain safe and long operation of the turbines under extreme operating conditions.

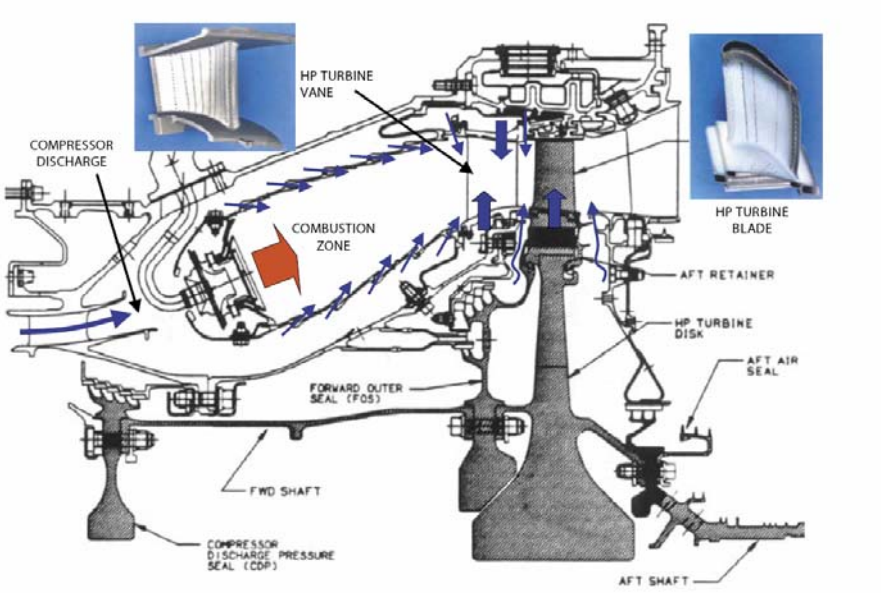


**Figure 2-9 Aero-engine High Pressure Turbine and Combustor [104]**

Figure 2-10 illustrates currently used methods of cooling a blade, so the engine can operate at higher temperatures. The first is through film cooling techniques which protect the external surfaces of the blade from the hot gases of the combustor. By injecting air diverted from the compressor into the mainstream flow through strategically located holes, a layer of cool air can be formed around the blade. A number of factors go into just how effectively the outer blade is cooled such as the location and shape of the hole and the blowing ratio. The hole location and shape determine the areas of the blade that are cooled and how well the coolant spreads upon injection. The blowing ratio is a measure of the mass flux of the injected coolant in relation to that of the mainstream flow. Generally, film cooling is improved with higher blowing ratios. However, the blowing ratio could be so large that coolant is lifted off the blade surface into the mainstream flow, so that no cooling is gained.

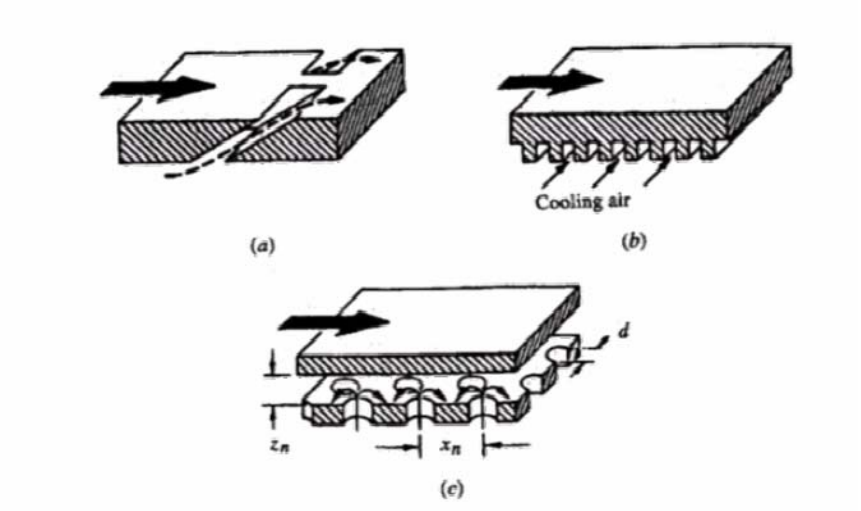


**Figure 2-10 Methods of blade cooling are a) film cooling, b) internal convection, and c) impingement (Mattingly, 1996) [104].**

Another method of blade cooling is through internal convective cooling, which occurs inside the blade as shown in Figure 2-10b. Heat conducted through the blade walls can be removed through serpentine passages inside the blade. A third form of blade cooling is impingement, shown in Figure 2-10c. Impingement builds off of convective cooling techniques by modifying internal passages to accelerate cool air through small holes. The jet of air created by the smaller flow area impinges upon the inside blade wall resulting in localized cooling. This method can be used to cool spots that get particularly hot.

Figure 2-11 A modern multi-pass turbine blade cooling scheme [104] shows a modern multi-pass turbine blade that incorporates film cooling, convective cooling, and impingement cooling

Turbine blade lifing based on TMF is very difficult due to the difficulties of predicting the state of stress and strain caused by the intricate geometrical features such as internal passages and film cooling holes and by uncertainties in transient temperature distributions. pointed out that any model aimed at producing acceptable turbine blade life predictions must examine the loading cycles in detail, and take into account how variables such as the stress and inelastic strain at each area of the blade varies with time[20].

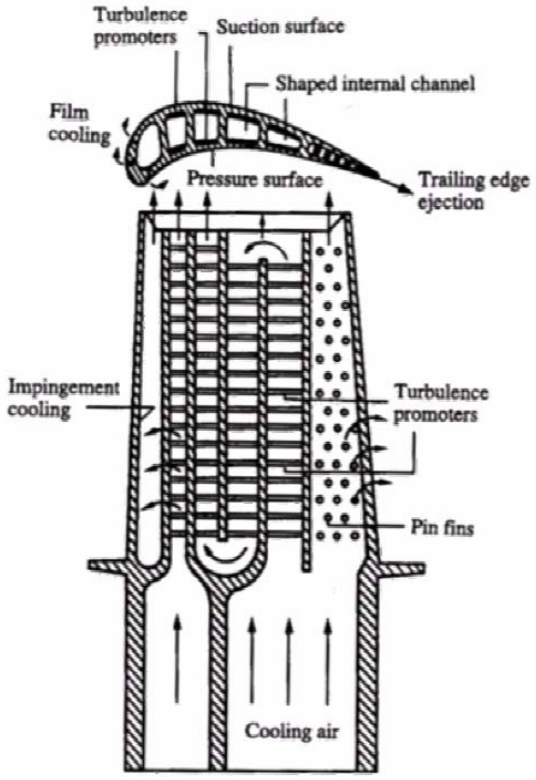


**Figure 2-11 A modern multi-pass turbine blade cooling scheme [104]**

# 3. Thermal-stress analysis.

The finite element analysis results are critical for identifying crack propagation parameters during a TMF cycle. The methodology is sensitive to the finite element modeling procedure. Care must be taken in controlling the element selection, material properties definition and applied boundary condition evaluation. The singularity issues, the size of the finite element mesh can affect simulation results as well.

The thermal portion of the analysis should consist at least of two steps. The first step is a steady-state analysis in which the blade is brought from an initial temperature of 70°F to a steady operating temperature distribution and than second step simulates the cool down. The transient response of the blade is then monitored for flight time. Temperatures from thermal analysis interpolated through ANSYS onto structural finite element mesh. Analysis performed using ANSYS. Initial linear analysis is completed for yield assessment. Nonlinear analysis is performed using temperature-dependent material properties (elastic modulii and coefficients of thermal expansion).The temperature-dependent stress/strain curves should used in nonlinear solutions for materials experiencing yield. Than discrete flight trajectory points are analyzed to determine worst case loads for strain and deflection (not always the hottest case).

For our task we analyzed one of the worst load case based on sensitivity studies of temperature distribution and boundary conditions at cooling hole location. The thermal cycle for our study is simplified to Cycle II, or in-phase TMF, that occurs when the maximum strain is directly in phase with the maximum temperature, Chapter 2.2.2.

The general thermal–stress problem separates into two distinct problems to be solved consecutively. The first is a problem (thermal analysis) in what is generally termed the theory of heat conduction and requires the solution of a boundary-value problem. When the temperature distribution has been found, the determination of the resulting stress distribution (thermal-stress analysis) is a problem in what is termed the non linear uncoupled quasi-static theory of thermoelasticity.

### 3.1.1 Modeling process for thermal-structural analysis

The best results for the crack propagation prediction are the precise modeling of geometry, material, load and boundary conditions. The modeling technique for the crack growth prediction was shown in [30, 31]. The crack simulation analysis should be completed based on final blade airfoil analysis, using ANSYS (or another applicable finite elements code) and proven methodology.

For our study a simplified 3D section of the blade was modeled. The airfoil solid model is shown in Figures 3-1 and 3-2; whereas, the finite element ANSYS model is shown in Figure 3-3

The generic blade is cooled by convection with cavity wall trip strips, not shown, and with a set of pedestals in the trailing edge. While external surfaces are locally film cooled from the leading edge with three rows of showerhead holes, there are film cooling holes on either the pressure or suction surfaces of the airfoil. The trailing edge has a centerline cooling flow ejection.

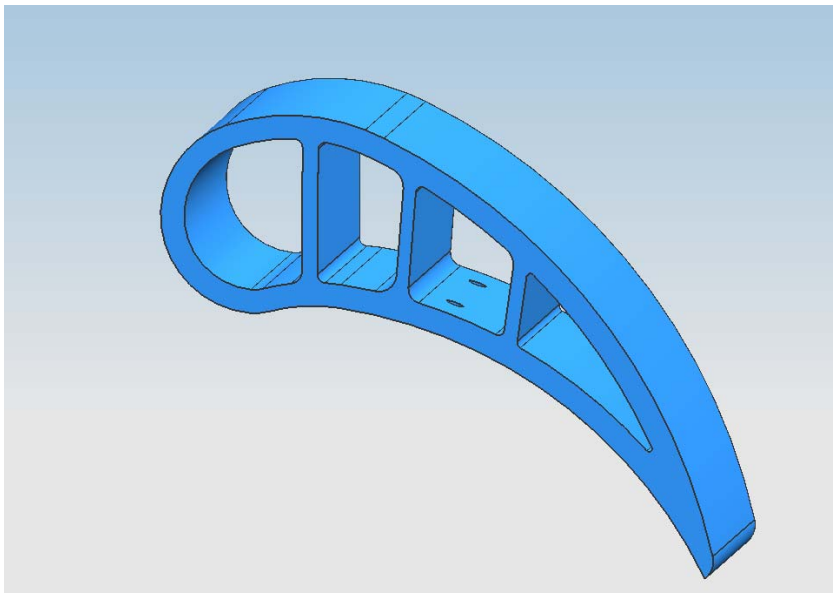

**Figure 3-1 Simplified 3D fragment of blade airfoil**

The study model ANSYS 3D model, depicted in Figure 3-7, has a two film cooling holes on suction surface. During the failure examination the most fatigue cracks have been related to the film cooling holes.

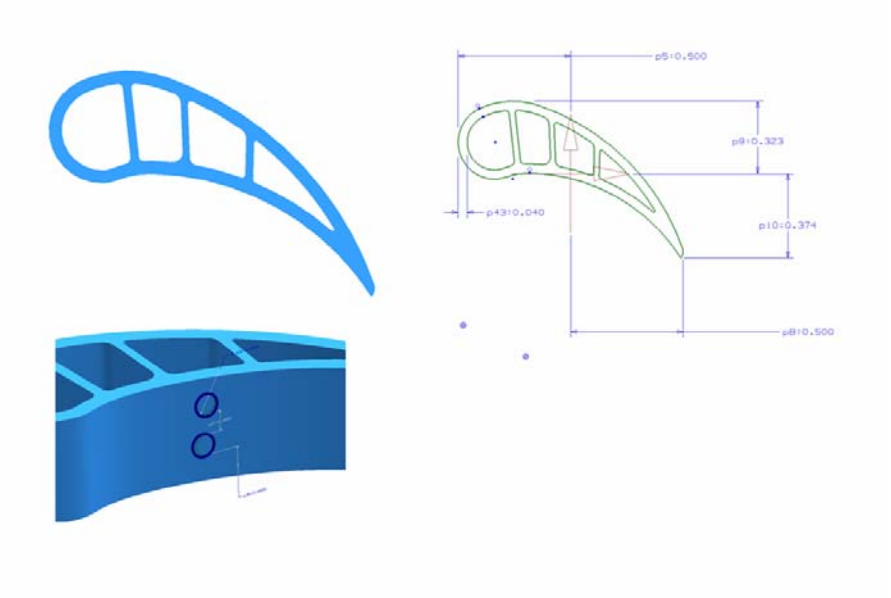

**Figure 3-2 The UG/NX 3D model created for crack simulation study**

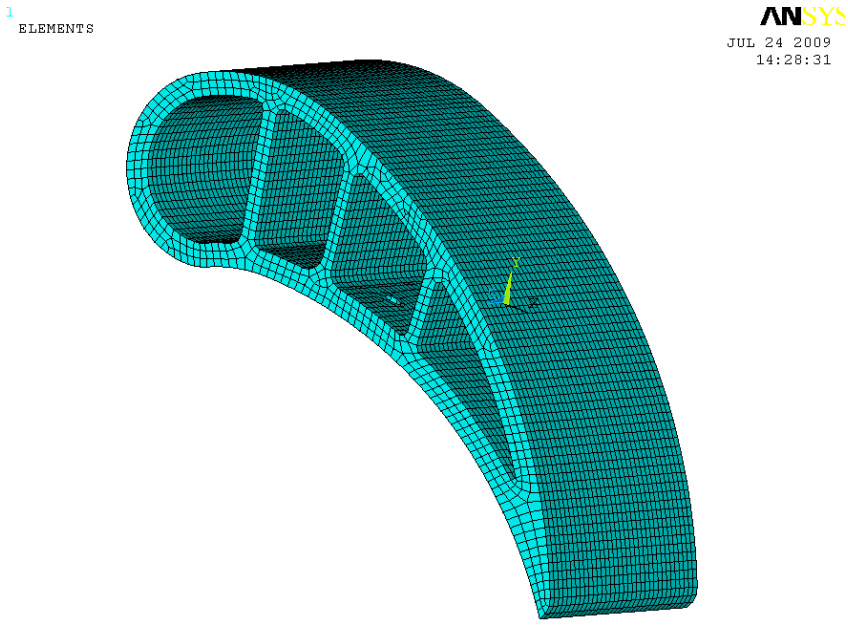


**Figure 3-3 The 3D finite element ANSYS model**

### 3.1.2 An airfoil thermal analysis and sensitivity study

The 3D-20 node tetrahedral thermal solid elements Quadratic Solid90 and Mesh200 (we use this pseudo-element to help define our overall 3D mesh) were used for the

thermal analysis, and then transition to the Solid95 element type for structural analysis. Solid95 is only 20 node element compatible with Franc3D/NG.

After the solid and mesh models have been developed the material properties are specified as a function of temperature.

The general thermal–stress problem separates into two distinct problems to be solved consecutively. The first is a problem in what is generally termed the theory of heat conduction and requires the solution of a boundary-value problem. For the temperature distribution definition the prediction of the local heat transfer coefficients and local airfoil metal temperatures is critical.

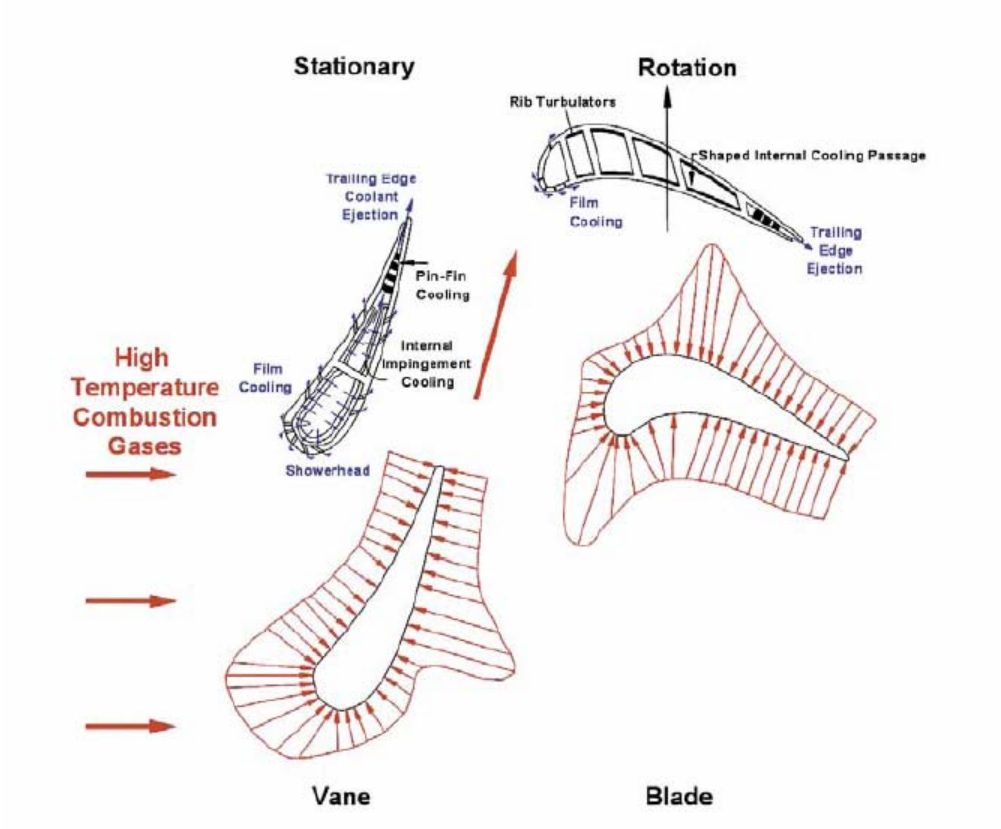


**Figure 3-4 Cross-Sectional View and Heat Flux Distribution of a Cooled Vane and Blade [104]**

Figure 3-4 shows the heat flux distribution around an inlet guide vane and a rotor blade. At the leading edge of the vane, the heat transfer coefficients are very high, and as the flow splits and travels along the vane, the heat flux decreases. Along the suction side of the vane, the flow transitions from laminar to turbulent, and the heat transfer

coefficients increase. As the flow accelerates along the pressure surface, the heat transfer coefficients also increase. The trends are similar for the turbine blade: the heat flux at the leading edge is very high and continues decrease as the flow travels along the blade; on the suction surface, the flow transitions from laminar to turbulent, and the heat flux sharply increases; the heat transfer on the pressure surface increases as the flow accelerates around the blade.

Defining boundary conditions become the first step in the analysis to simulate the thermal and mechanical loads that the part experiences throughout the mission profile. The set-up of thermal boundary conditions for the model is a very laborious process. For the real model on the external side, computational fluid dynamic codes are used to set-up external pressure and Mach number distributions for free-stream conditions with specified turbulence intensity levels. Boundary layer programs are used to establish the external heat transfer coefficients based on expected wall roughness. Gas recovery temperatures and film cooling effectiveness, usually obtained from previous testing, are used to determine the adiabatic wall (film) temperatures.

Different coating systems can be modeled as modified equivalent heat transfer coefficients. External heat transfer coefficients and film temperatures are specified as external boundary conditions for the model. Inside the airfoil, flow network models are used to determine internal pressure drops and Mach number distributions. Heat transfer correlations based on previous testing can be used to determine the internal heat transfer characteristics of the blade cooling system under the effects of rotation. The network flow analysis provides the means to determine internal heat transfer coefficients and coolant temperatures as internal boundary conditions for the model.

The thermal portion of the analysis consists of two steps. The first step is a steady-state analysis in which the blade is brought from an initial temperature of 70°F to a steady operating temperature distribution based. The second step simulates the cool down in to the 70°F.

Thermal analysis completed based on the steady-state heat transfer problem. The assumptions are transient analysis was completed and critical thermal BC were defined. For a steady-state (static) thermal analysis heat conduction problem with convection boundary conditions analyzed using ANSYS.

For the convection heat transfer heat flux is given by Newton's Law of Cooling:

$$[K(T)]\{T\} = \{Q(T)\}$$

Some assumptions applied to problem solution. There are no transient effects are considered in a steady-state analysis; [K] can be constant or a function of temperature {Q} can be constant or a function of temperature

In our case the convection is basic mode for the heat transfer, the energy exchange between a blade body and surrounding fluid. Convention applied to surfaces only (edges in 2D analyses). Convection is defined by heat flow rate per unit area between surface and fluid $q^*$. It depends on a film coefficient h, the surface area A, and the difference in the surface temperature $T_{surface}$ & ambient temperature $T_{ambient}$ (Eqs. 3-9)

$$q^* = hA(T_{surface} - T_{ambient}) \tag{3.9}$$

The convention film coefficients and ambient temperatures are user input values. The film coefficient *h* can be constant or temperature dependent. Input consists of external heat transfer coefficients, film temperatures and internal heat transfer coefficients, coolant temperatures.

For the conduction heat transfer heat flux is given by Fourier's law of conduction

$$q^* = -k_{nn}\frac{\partial T}{\partial n} \tag{3.10}$$

Conduction is defined by heat flow rate per unit area in direction *n* - $q^*$. It depends on $k_{nn,}$ the thermal conductivity in direction *n; T,* the temperature, and $\frac{dT}{dn}$, the thermal gradient in direction *n.* See equation (3-10).

The procedure to do a steady – state thermal analysis with ANSYS consists from a few steps. They are preprocessing (CAD and FE models definition and meshing), solution (material properties and boundary condition definition and problem characterization) and, finally postprocessing (results review and solution validation).

By creating geometry we start the ANSYS preprocessing mode. The geometry can be imported or created within ANSYS. For our task the 3D and 2D models were created using CAD software (Unigraphics/NX software) and than imported. For the real case the best solution to use a sub modeling technique and import part of blade airfoil.

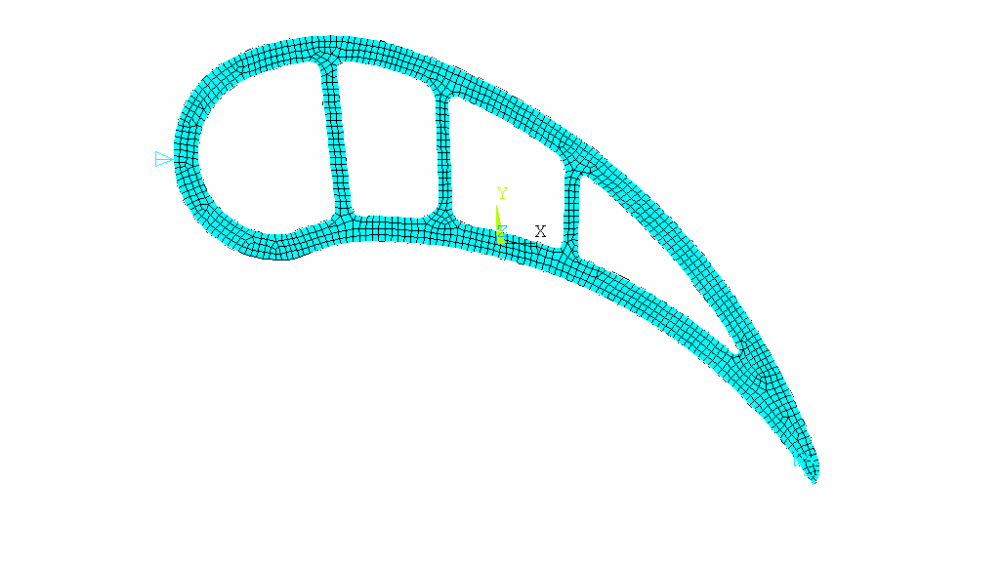


**Figure 3-5 The2D Model dimensionally equal to 3D Model cross section created in Unigraphics/NX software imported and meshed in ANSYS.**

For the meshing approach the elements selection was made. The thermal element for the 2D analysis is PLANE77. It is an eight-node quadrilateral element used in modeling two-dimensional heat conduction problems; this element more capable of modeling problems with curved boundaries. At each node, the element has a single degree of freedom, the temperature. Output data include nodal temperatures and element data, such as thermal gradient and thermal flux components. For the 3D analysis SOLID90 was selected. It is a twenty – node brick element used to model steady-state or transient conduction heat transfer problems. Each node of the element has a single degree of freedom-temperature. This element well suited to model problems with curved boundaries. The solution output consists of nodal temperatures and other information, such as average face temperature, temperature-gradient components and the heat-flux components. Also Mesh200 element was used; this pseudo-element helps define our overall 3D mesh. To define the material properties, the thermal conductivity was averaged over the temperature range being analyzed and the real work temperatures were used. For our task the material library file was created to simulate structural and material properties of Ni based single crystal alloys. The real problem will be required the real material property file. The MeshTool was used create the mesh. For the 3D

model the process of meshing an existing volume by sweeping an area mesh were used. This completes the preprocessing step.


**Figure 3-6 The lines (components) on 2D thermal model representing model boundary**

For the solution phase the convective loads were applied. The nodal components representing lines (2D model) Figure 3-6, and areas (3D model) Figure 3-8 were created.

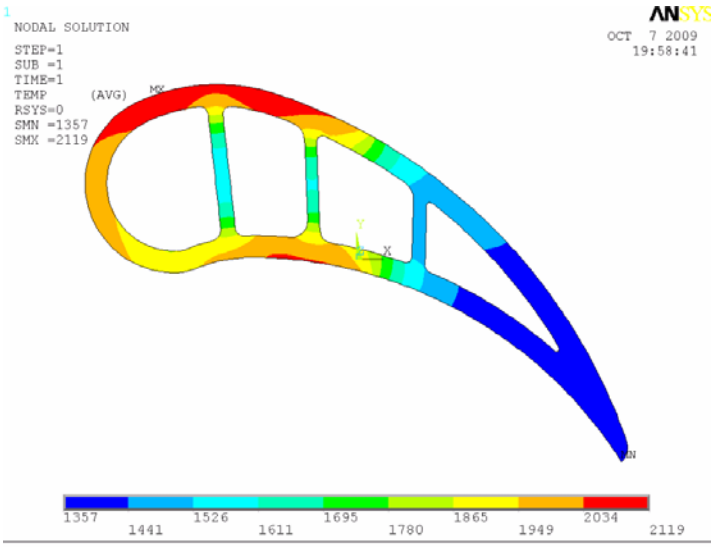


**Figure 3-7 The auxiliary 2D model selected thermal fields distribution for 2D thermal-structural analysis**

For the postprocessing step the primary data items, nodal temperatures were received (TEMP). The solution was validated on expected temperature range principal. For our model we are looking 1300°F-2000°F (700°C-1000°C). The nodal (averaged) and element (unaveraged) thermal gradients were examined to remesh a model.

For the study model the 2D ANSYS auxiliary thermal/structural model Figure 3-5 was created to facilate sensitivity study. The original model were created with blade stacking axis or the z-direction; one node near the middle of an aft internal rib remains fixed in space for all three directions , also a few schemes for different heat transfer coefficients and bulk temperature of the surrounding fluid $T_b$ were reviewed to investigate the thermal field distribution. Nonlinear analysis performed using temperature-dependent material properties (elastic modulii and coefficients of thermal expansion). By using the new ranges of convention coefficients implicitly and by interpolating the values of bulk temperatures inputted into the system the results were much improved over the initial analysis.

For the heat transfer correlations surface zones (nodal components) on the model were defined (Figure 3-8) By applying different heat transfer coefficients and bulk temperatures to simulate and modify thermal loads and solving thermal problem the thermal fields distribution were observed. The Figure 3-9 represents a thermal fields distribution.

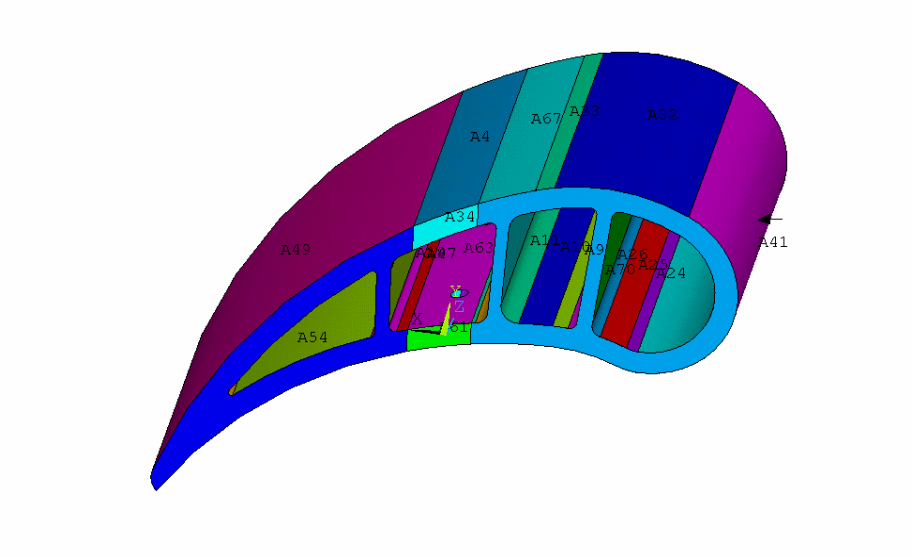


**Figure 3-8 3D Model Thermal zones distribution**

A few thermal conduction studies were performed using ANSYS for 3D Models based on 2D models thermal-structural analysis. The study of a dependency between thermal boundary conditions and temperature fields distribution. Figures 3-7, 3-9 presented a few possible thermal fields distributions related to the defined flight points.

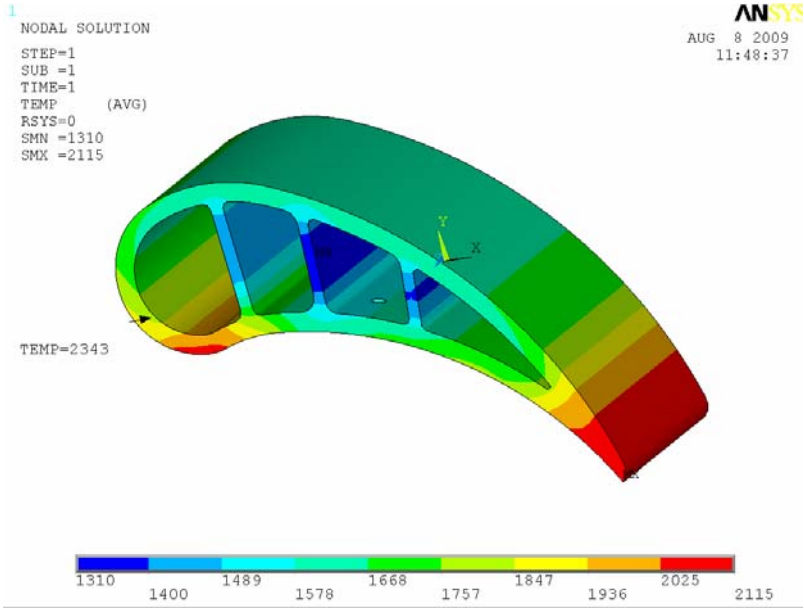


**Figure 3-9 Possible Temperature distribution at point A**

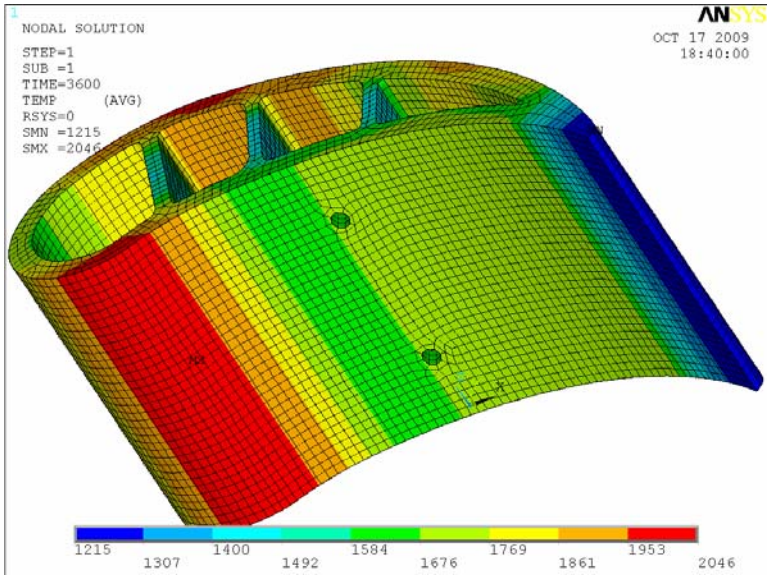


**Figure 3-10 The temperature distribution resulting solution**

For the model simplification we are not completed study of a dependency between thermal boundary conditions and temperature fields' distribution inside cooling holes. The thermal-structural effect of cooling holes is important on a crack nucleation phase, see next chapters for more details. The influence on a crack propagation stage more depends on global model condition and will be reviewed in future works.

While this depiction of the temperature and heat transfer coefficients over the airfoil surfaces being analyzed is a helpful indication that the modifications being made are allowing for a more realistic solution. The resulting solutions are shown in Figure 3-10 and are able to obtain a similarly accurate answer for the thermal-structural analysis.

### 3.1.3 Thermal-stress analysis procedure

When a blade is heated or cooled, it deforms by expanding or contracting, if the deformation is restricted by displacement constrains (i.e. blade geometry and assembly condition) thermal stresses are induced. The non –uniform temperature distribution also causes the thermal stresses. Temperatures from thermal analysis interpolated through ANSYS onto structural finite element mesh.

For the thermal-stress analysis the sequential method is used. The method involves two types of analyses:

1. First do a steady-state thermal analysis.

For the real model transient thermal analysis to select flight point that causes Max deformation. The method includes model with thermal elements, the thermal loading, solution and results review. The details are covered in previous paragraph.

2. Second complete a structural analysis.

According to Chapter 2 of the ANSYS Coupled-Field Guide, "A sequentially coupled physics analysis is the combination of analyses from different engineering disciplines which interact to solve a global engineering problem. For convenience, the solutions and procedures associated with a particular engineering discipline will be referred to as a physics analysis. When the input of one physics analysis depends on the results from another analysis, the analyses are coupled."

Thus, each different physics environment must be constructed separately so they can be used to determine the coupled physics solution. However, it is important to note that a single set of nodes will exist for the entire model. By creating the geometry in the first physical environment, and using it with any following coupled environments, the geometry is kept constant. For our case, we will create the geometry in the Thermal Environment, where the thermal effects were applied.

Structural Analysis Steps:

- Switching element types. The Solid95 element type is only 20 node element compatible with Franc3D/NG. The current default element type for switching is Solid186.
- The material properties are defined by using material property file
- Specify static analysis type (this step not use for steady state analysis, however we need for real model transient analysis)
- Applying the structural displacement loads, including temperatures as a part of the loading.
- Solution
- Review the stress results

### 3.1.4 Analytical elasticity based solution for the crack nucleation.

One of cause because of which stresses may be set up in an elastic body is the unequal heating of different parts of the body. With a few exceptions, the elements of a body expand as the temperature is increased. If the element is allowed to expand freely, the body will be strained but there will not be any stress due to such an expansion. However, if the temperature rise in the body is not uniform and the body is continuous, the expansion of the elements cannot proceed freely and thermal stresses are produced.

Let us consider first an unstrained elastic body with a uniform temperature $T_0$. Now imagine that the body is heated to some temperature $T_1$ above $T_0$. The body will be stressed if T varies from point to point in the body. The strain of an element may be considered as consisting of two parts. One part is due to the expansion of the element because of the change of its temperature. If α is the coefficient of linear expansion of the material, which is defined as the change in length per unit length per degree rise in temperature, this part of longitudinal strain will be αT. There will be no shearing strains produced, because the expansion of a small element, due to change of temperature, will not produce angular distortion in an isotropic material. If the element is allowed to expand freely, this is the only component of strain and the element will not be stressed. Now, if the element is not allowed to expand freely, stresses will be produced and the total strain of the element must be the sum of that part due to the stresses and that due to the change of the temperature. Now let us consider a thin circular disk with uneven temperature distribution. Figure 3-11.

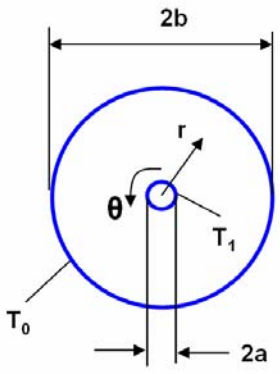


**Figure 3-11 Thin circular disk geometry.**

Assume the temperature T is a function of the radial distance r only. We have a case of plane stress with rotational symmetry. In terms of cylindrical coordinates, we find,

$$\varepsilon_r = \frac{1}{E}(\sigma_r - \nu\sigma_\theta) + \alpha T$$
$$\varepsilon_\theta = \frac{1}{E}(\sigma_\theta - \nu\sigma_r) + \alpha T \tag{3.1}$$

The equilibrium equation,

$$r\frac{d\varepsilon_\theta}{dr} - \varepsilon_\theta - \varepsilon_r = 0 \tag{3.2}$$

is identically satisfied if we introduce the stress function Φ such that

$$\sigma_r = \frac{\phi}{r} \qquad \sigma_\theta = \frac{d\phi}{dr} \tag{3.3}$$

Substituting (3.1) and (3.2) into the compatibility equation

$$\frac{d\sigma_r}{dr} + \frac{\sigma_r - \sigma_\theta}{r} = 0$$

and simplifying, we find

$$\frac{d^2\phi}{dr^2} + \frac{1}{r}\frac{d\phi}{dr} - \frac{\phi}{r^2} = -\alpha E\frac{dT}{dr}$$

$$\text{or} \quad \frac{d}{dr}\left[\frac{1}{r}\frac{d}{dr}(r\phi)\right] = -\alpha E\frac{dT}{dr} \tag{3.4}$$

This equation can be easily integrated, and the solution is

$$\phi = -\frac{\alpha E}{r}\int_a^r Trdr + \frac{c_1 r}{2} + \frac{c_2}{r} \tag{3.5}$$

where the lower limit *a* in the integral can be chosen arbitrarily. For a disk with a hole, it may be the inner radius. For a solid disk we may take it as zero.

The stress components can now be found by substituting (3.5) into formulas (3.3). Hence

$$\sigma_r = -\frac{\alpha E}{r^2}\int_a^r Trdr + \frac{c_1}{2} + \frac{c_2}{r^2}$$

$$\sigma_\theta = \alpha E\left(-T + \frac{1}{r^2}\int_a^r Trdr\right) + \frac{c_1}{2} - \frac{c_2}{r^2} \tag{3.6}$$

Consider a thin disk which receives heat over its faces and rejects it at its circumference in such a way that the temperature at any point in the disk is essentially uniform through the thickness. If $T_0$ is the temperature at the edge of the disk and $T_1$ is the temperature at the center, the temperature rise at a radius $r$ is given by

$$T = (T_1 - T_0) - (T_1 - T_0)\frac{r^2}{b^2}$$

Substituting the expression of $T$ given by the above formula into Eqs. (3.6) and integrating, we obtain

$$\sigma_r = -\frac{1}{4}\alpha E\left(T_1 - T_0\right)\left(1 - \frac{r^2}{b^2}\right) \qquad \sigma_\theta = -\frac{1}{4}\alpha E\left(T_1 - T_0\right)\left(1 - \frac{3r^2}{b^2}\right)$$

If there is a circular hole of radius a at the center of the disk and the edges are free of external forces, we have

$\sigma_r = 0$ at r = b and r = a

Then

$$\frac{c_1}{2} + \frac{c_2}{b^2} = -\frac{\alpha E}{b^2}\int_a^b Trdr \qquad \frac{c_1}{2} + \frac{c_2}{b^2} = 0$$

From which it follows that

$$\frac{c_1}{2} = -\frac{\alpha E}{b^2 - a^2}\int_a^b Trdr \qquad c_2 = -\frac{a^2\alpha E}{b^2 - a^2}\int_a^b Trdr$$

And

$$\sigma_r = \alpha E\left[-\frac{1}{r^2}\int_a^r Trdr + \frac{1}{b^2 - a^2}\int_a^r Trdr - \frac{a^2}{r^2(b^2 - a^2)}\int_a^r Trdr\right]$$

(3.7)

$$\sigma_\theta = \alpha E\left[-T - \frac{1}{r^2}\int_a^r Trdr + \frac{1}{b^2 - a^2}\int_a^r Trdr - \frac{a^2}{r^2(b^2 - a^2)}\int_a^r Trdr\right]$$

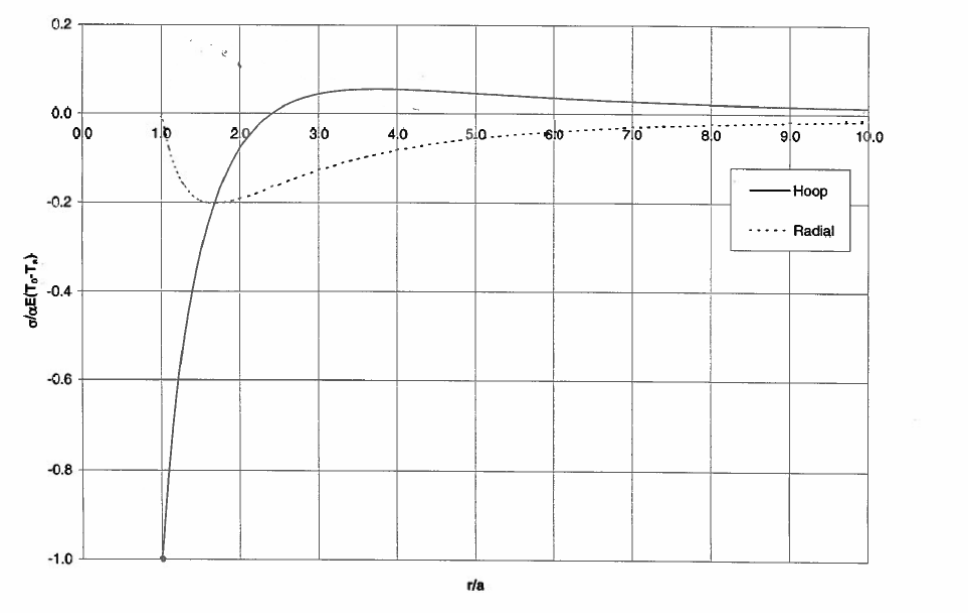


**Figure 3-12 Thermal stress components plot**

The plot of induced stresses shows that areas adjacent to the cooling holes always under tensile condition. Figure 3-12. The results reveal that the existence of cooling holes causes the stress and strain concentrations near the holes. Tensile stresses develop around the hole during cooling, as the area near the hole cools faster than the periphery. Therefore the hole is not allowed to shrink freely by the hotter material surrounding it. These conditions provoke crack initiation; because of tensile hoop stresses.

### 3.1.5 Finite element solution for the crack nucleation

#### 3.1.5.1 CAD and FE geometry, thermal analysis

A few 2D models were created. The square plates with hole diameters 0.160” and side sizes 0.5”,1”,2”,4” and 2” disk with 0.160” hole were meshed, the 300°F were applied to the hole edge and 1000 °F to the outer edge.

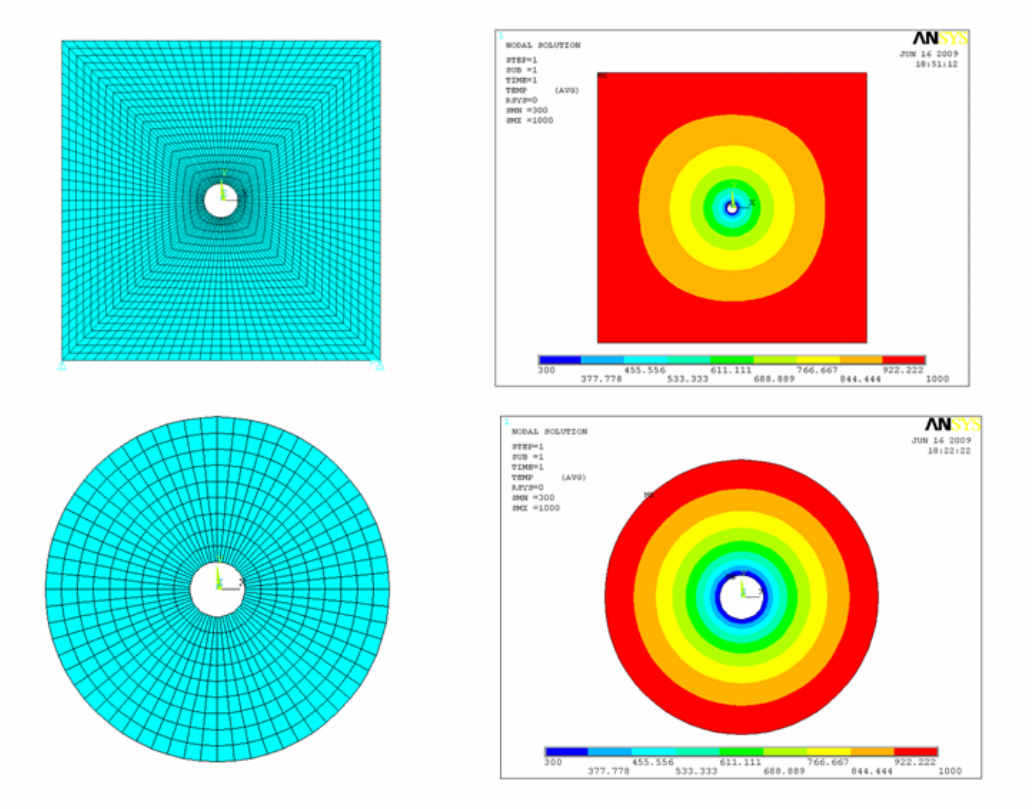


**Figure 3-13 CAD geometry and plot of the temperature distribution results**

Thermal analysis completed based on the steady-state heat transfer problem. The different sizes of the finite element mesh and singularity issues have been reviewed. The heat conduction problem with convection boundary conditions analyzed using ANSYS.

### 3.1.5.2 Thermal-stress analysis

The movement and rotation restriction displacement BC and thermal problem solution were applied to solve the structural problem. The size and shape of models can affect the Max stress and stress distribution fields. Figure 3-14.

The FEM results reveal that the existence of cooling holes causes the stress and strain concentrations near the holes. The FEM result is coincident with the stress appearance of the analytical solution.

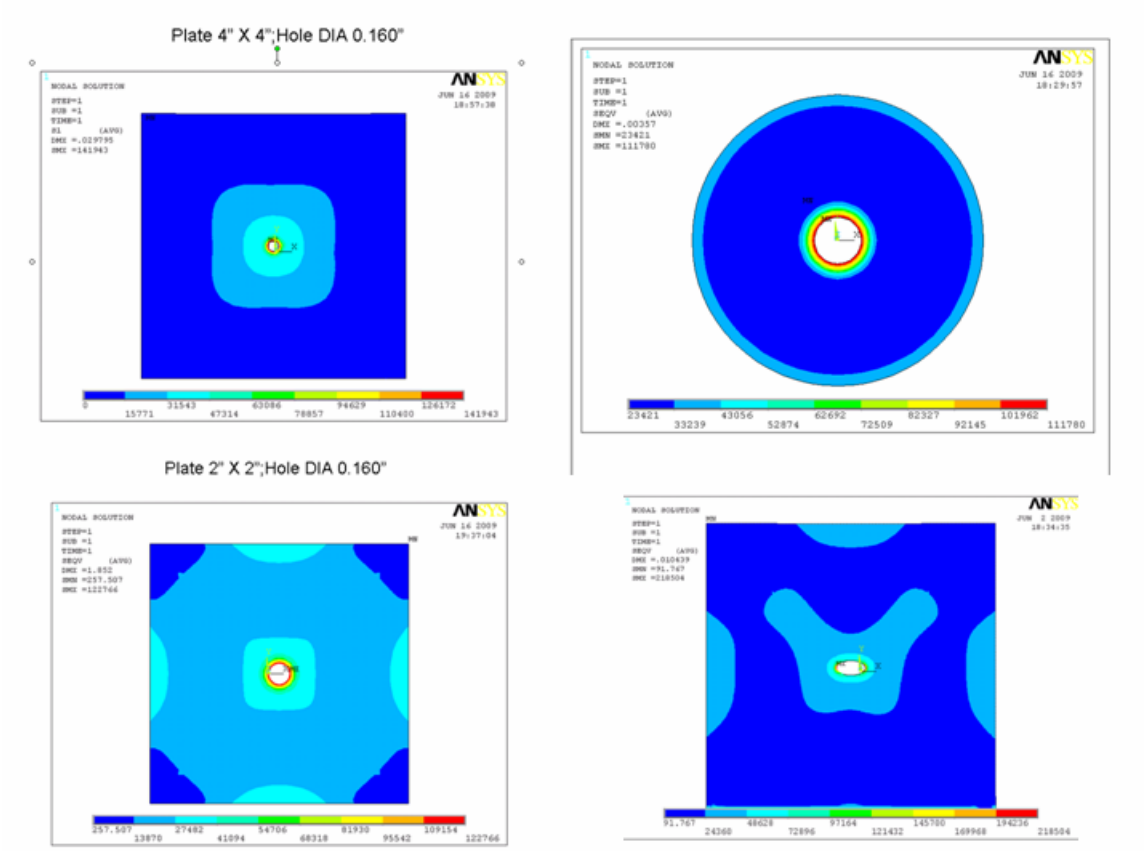


**Figure 3-14 Plot of Von Misses stresses for models with different geometry**

### 3.1.6 The sensitivity study for boundary conditions

The reason to review the different temperature – stress scenarios is a simulation of flight conditions that brings crack propagation at airfoil. This allows avoid full scale transient analysis. The discrete flight trajectory points were introduced by specifying temperature distribution and applying boundary conditions, and then analyzed to determine worst case loads for strain and deflection.

The sensitivity study of the boundary conditions was performed. The existence of a solution was evaluated by applying thermal loads and different boundary conditions. The finite element models were examined by performing thermal-structural analysis

For the 2D model the different loading constrains were reviewed to identify possible crack propagation conditions and eliminate improper displacement restrictions. The approach to simplify mechanical loading conditions by remain the one node fixed in

most applicable location an internal rib fixed in space for all two directions, and one other node at the same internal rib is fixed in the <010> axis or y-direction looks pretty much accurate for 3D study. Figure 3-15

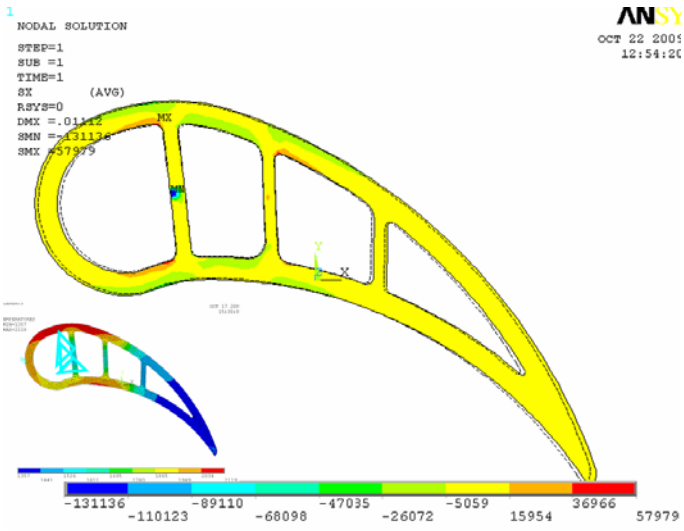


**Figure 3-15 Structural BC - the one node fixed in most applicable location an internal rib fixed in space for all two directions, and one other node at the same internal rib is fixed in the <010> axis or y-direction**

The criterions for the crack location were predetermined by observed failure results [3],[4],[10]-crack initiation possible from cooling hole; the location close to blade platform, pressure side of airfoils [3]. The LEFM crack propagation condition is expected on blade surface under tensile state of stress.

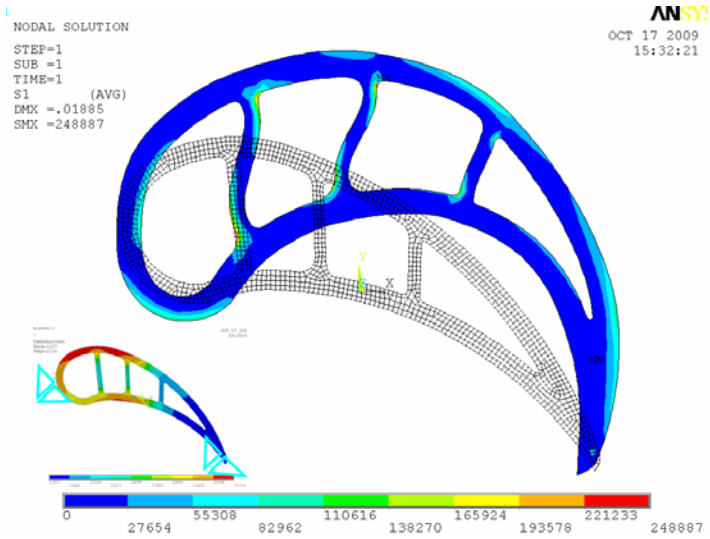


**Figure 3-16 The combined deflected and undeformed shape and stress contour plots. Deformed shape is exaggerated. Structural BC: the leading and trailing edges are fixed.**

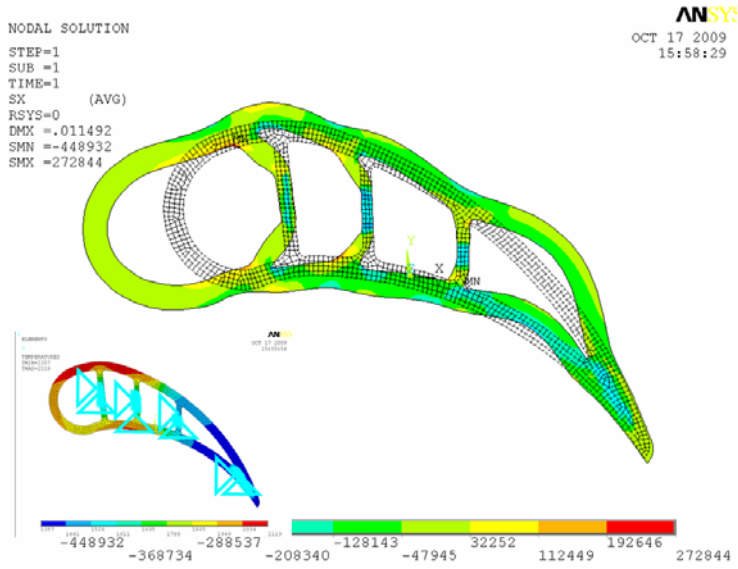


**Figure 3-17 The combined deflected and undeformed shape and stress contour plots. Deformed shape is exaggerated. Structural BC: the internal ribs and trailing edge are fixed**

The fixed internal ribs BC were analyzed Figure 3-17, another approach to fix the leading and trailing edges, Figure 3-16. The displacements were applied to leading and trailing edges with an internal rib fixed in space for all two directions, and one other node at the same internal rib is fixed in the <010> axis or y-direction.

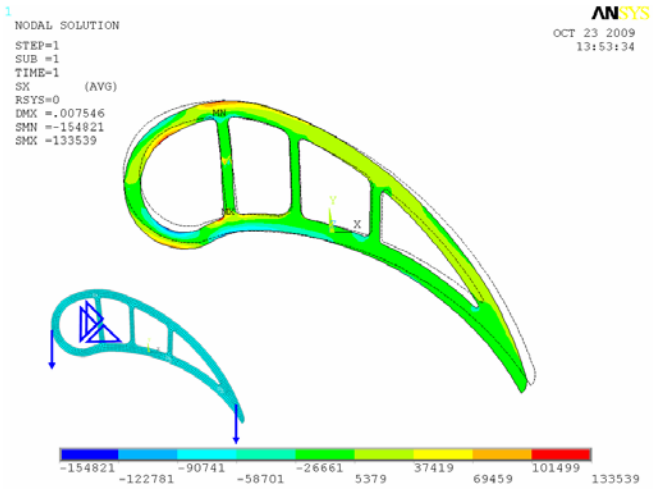


**Figure 3-18 Structural BC the vertical down displacements were applied to leading and trailing edges with an internal rib fixed in space for all two directions, and one other node at the same internal rib is fixed in the <010> axis or y. No temperature load.**

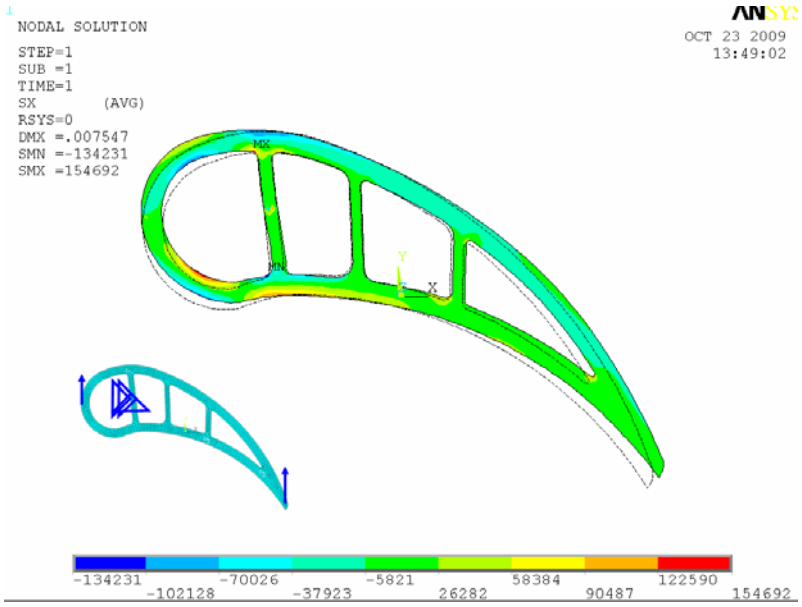


**Figure 3-19 Structural BC: the vertical up displacements were applied to leading and trailing edges with an internal rib fixed in space for all two directions, and one other node at the same internal rib is fixed in the <010> axis or y. No temperature load.**

Figures 3-18 and 3-19 analysis completed to define the local tensile stresses location due to mechanical blade deformation. A few more random constrain location have been reviewed. In creating these studies no thermal distribution properties were altered from one case to another.

### 3.1.7 Thermal-stress analysis results

According to test results [9], [16] the mechanical boundary condition will be sensitive to the crystal anisotropy and structural and body loads applied. For the real blade model are such that the bottom and top planes (nodal components with displacements) must be interpolated from full blade model by using ANSYS sub-modeling technique. The approach to simplify mechanical loading conditions by remain the bottom plane fixed in the direction of the blade stacking axis, the <001> axis or the z-direction; and one node fixed in most applicable location an internal rib fixed in space for all three directions, <100>, <010>, and <001>, and one other node near edge is fixed in the <010> axis or y-direction with top plane nodes are constrained to remain coupled and planar can be used if these boundary conditions can be replicated from full model structural analysis and can give the non accurate results.

The primary loading experienced by the blade section is the centrifugal force caused by the rotating mass of the blade; in order to simulate this, a uniformly distributed load is applied normal to the top face of the blade section. The planar boundary condition applied this way is a first approximation to boundary conditions that may be experienced by the blade section. The assumption is that there is sufficient constraint, because of the surrounding blade material, to counteract bending moments seen as a result of temperature gradients and non-uniform deformation rates [5]. The blade deformation will largely be controlled by the conditions at the ends of the blade. At the root, the blade will experience a relatively lower and more uniform temperature. Thus, if the root of the blade experiences a more uniform temperature, any other cross-section will be forced to deform at a uniform rate [5]. Therefore, to a first approximation, the constraint of planar sections has been applied in the blade model. The mechanical boundary conditions are prescribed to the model to determine the stress and strains fields from a subsequent ANSYS run. The thermal-mechanical results are then used as input for the following life analysis.

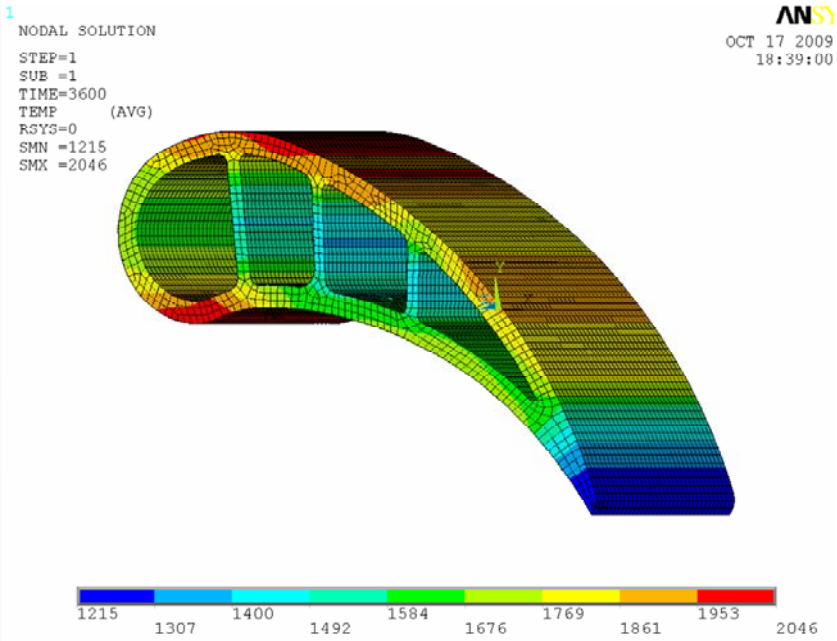


**Figure 3-20 Possible Temperature distribution were chosen for the thermo-structural analysis**

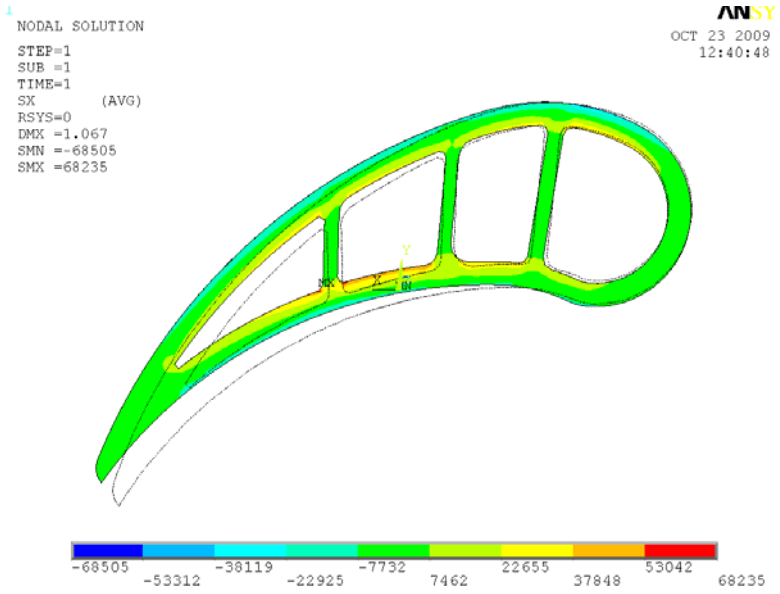


**Figure 3-21 The study model, plot of the X-stress component.**

After completing the 2D models thermal-structural analysis studies the 3D models were analyzed for possible crack prorogation condition. A few different structural BC scheme were selected and analyzed based on 2D models study for the boundary condition sensitivity study. The final thermal field distribution is shown on Figure 3-20.

For the thermal-structural analysis the 3D model with simplified mechanical loading conditions was selected. To BC scheme is implemented by one node fixed in most applicable location an  internal rib fixed in space for all three directions, and one other node at the same  internal rib is fixed in the <010> axis or y-direction, the bottom plane fixed in the direction of the blade stacking axis, the <001> axis or the z-direction. The final model is plotted for the start-up case with thermal loading and BC applied. Figure 3-21. After thermal structural analysis was completed the expected crack propagation zone were defined.

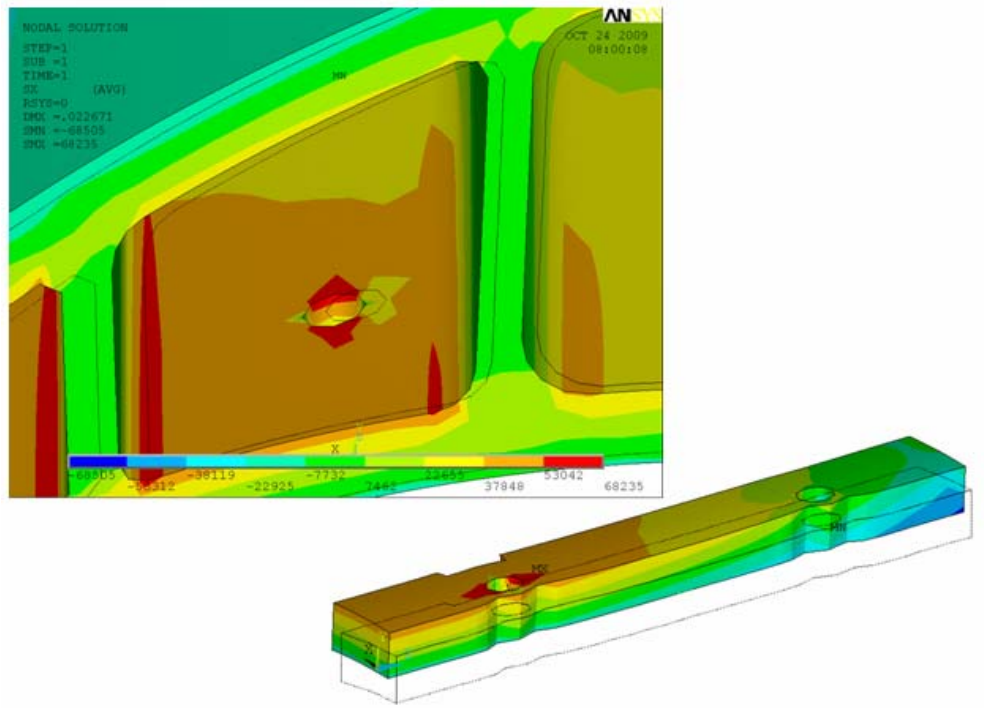


**Figure 3-22  The stress fields distributions in crack propagation location.**

The magnitudes and directions of stress indicate that the component has significantly high stresses in the locations of expected cracks and with the principal stresses suitably aligned. It can be observed that the highest stresses occur on the internal surfaces of the blade, Figure 3-22. These stresses combined with small surface defects could give rise to radial cracks which were observed in the crack nucleation study. Moderate stresses are present on the rib corner fillets and these should not give rise to cracking. However, the model has a finite radius of curvature in this region for modeling

purposes and the actual in-service blade had a much thinner and variable thickness in this region.

Figure 3-22 shows the distribution of the stress within the wall section. It is clear that the highest stress occurs in the vicinity of the transition between the cooling hole and the airfoil wall and this progress through the thickness of the wall at a consistently high magnitude. When combined with small surface irregularities may well be sufficient to propagate cracks. This could contribute to the type of failure seen in the real airfoil. Propagation would be dependent upon the stresses that will be generated at and around the crack tip and the stress intensity at the crack tip.

The finite element output has shown the areas of high stress resulting within internal blade section. Finite element results confirm the initial crack location at cooling hole and stress distributions aligned with model indicate the potential for failure.

# 4. Numerical fracture mechanics analysis.

The fatigue crack propagation is the subject of significant research, primarily dealing with the expansion of various methods and models to better explain the crack growth phenomenon. In realistic situations, structural members are often subjected to three-dimensional stresses and, therefore, mixed mode fractures, consisting of normal separating, in-plane sliding and out-of-plane sliding. Although the loading scheme may appear to be a simple one, a complex state of stress can exist inside the structure, mostly in the locality of mechanical defects or crack. The effects of stresses of this kind can frequently lead to unexpected failure. The problem of predicting the crack propagation in such stress state and modeling approach are most difficult.

The evaluation of SIFs and crack tip tresses for a non typical design structure are a challenging problem, involving the calculation of the crack path and the crack propagation rates at each step especially under mixed mode loading. The adaptive FEM-BEM method is selected to perform crack growth analyses.

For our task we analyzed one of the worst load case based on sensitivity studies of temperature distribution and boundary conditions at cooling hole location. The thermal cycle for our study is simplified to Cycle II, or in-phase TMF, that occurs when the maximum strain is directly in phase with the maximum temperature. The assumptions are the transient analysis was completed and the critical temperature distribution and structural BC were defined.

There are a wide diversity of FEA packages of which, the well-known being ANSYS, ABAQUS, NASTRAN, COMSOL. For the CAD applications, there are Pro/Engineer, Solid Works, and UG/NX. These packages are all inclusive, coming with all the necessary applications to create, apply loads to, mesh, and analyze a model. The software selected for the FEA discussed in thesis is ANSYS. ANSYS was selected because of its versatility, accuracy, user friendly GUI. The CAD software, UG/NX, was used for the parametric modeling. These programs were selected based on availability and compatibility with crack propagation software.

The Franc3D/NG, crack propagation simulation package was selected to investigate airfoil damage using linear elastic fracture mechanics based on Paris' model, and the maximum tensile stress and M-integral methods. Franck3D/NG supports the concept of

a sub-model; remeshing for crack growth is confined to this sub-model. The ANSYS has tools to define a sub-model. Confining the remeshing for crack growth to the sub-model greatly reduces the amount of data that needs to be transferred and processed, thus speeding the crack growth process. It also allows the thermal and complex mechanical loads interpolation using ANSYS.

The FRANC3D/ANSYS interface was implemented to complete the crack growth iterations. The initial model attributes are defined in ANSYS, and FRANC3D/NG is used to compute crack growth parameters and updates the geometry and mesh. After a model is analyzed using ANSYS, FRANC3D/NG computes the location of the new crack front, extends the crack, and updates the model geometry. Finally, remeshing is done and the process is continued until we have through wall crack.

## 4.1 Basics methods for crack propagation modeling

Figure 4-1 shows classification of methods for demonstration of crack propagation models. Demonstration means the manner in which the presence of a crack, or a crack nucleation process, is accommodated in the numerical procedure. Currently available approaches split into two major formats. In the first set of methods, the crack is a geometrical entity; the geometry model and the discretization model, if needed, are updated with crack growth.

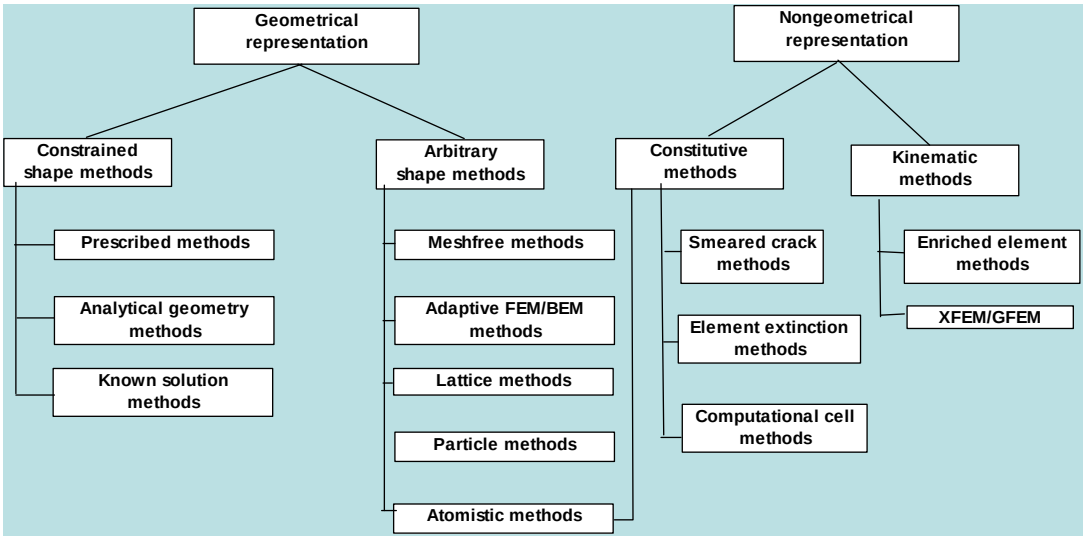


**Figure 4-1 The classification of methods of representation of cracking in a numerical model. [39]**

This is the left major branch of the classification in Figure 4-1. In the other approach, the original geometry model does not contain the crack, and neither it nor the discretization model, if needed, changes during crack growth. Rather, the crack is represented either in the material constitutive model or in a kinematic model as an intense localization of strain. This is the right main branch of the classification in Figure 4-1. [39]

The adaptive FEM-BEM method is selected to perform crack growth analyses. The method allows evaluate a non standard geometry of both structure and cracks by updating the mesh to conform to the crack shape. The sub modeling method is used in some cases. It does not take into account the redistribution of the loads in the structure thus requiring a large part of the structure to be included in the crack growth model.

Commonly large structures are modeled with finite element methods (FEM) because of the many varied types of structural elements. Modeling crack growth with FEM results in a particularly complex remeshing process as the crack propagates. Hence, self-adaptive remeshing is one of the major features that must be incorporated in the construction of a computational tool to properly perform crack propagation analysis with the FE method. [38]

The boundary element method (BEM) simplifies the meshing process and has the ability to correctly characterize the singular stress fields near the crack front. One challenge is how the two methods can work together capably for a large structure.

The adaptive FEM-BEM method is therefore proposed to perform crack growth analyses.

## 4.2 The review of 3D crack propagation software

The purpose of this study is the determination of the software to simulate 2D/3D crack propagation in elastoplastic materials. The program must evaluate the stress intensity factors and predict the cracks trajectories, crack paths and surfaces as a part of the damage tolerant assessment. The propagation process has to be driven by Linear Elastic Fracture Mechanics (LEFM) approach with minimum user interaction. The finite element code must generate results compared with sets of experimental or failure data, as well as numerical results of other researchers. The simulation of crack propagation

need include an automatic adaptive remising process in the vicinity of the crack front nodes and in the local element which represent the crack location. The software must to be compatible with major structural analysis codes.

### 4.2.1 FRANC2D, FRANC2D/L, FRANC3D/NG

FRANC2D/L is a highly interactive finite element program for the small deformation analysis of two-dimensional structures. Linear elastic fracture mechanics analyses can be performed with automatic remeshing as the crack grows. The layered capability allows the user to model riveted and adhesively bonded structures, such as lap joints and bonded repairs. Elastic-plastic material behavior is also available. This allows the user to model tearing with the critical crack tip opening angle approach. This provides the full capability of growing a fatigue crack and calculating residual (tearing) strength as a function of crack length.

FRANC2D/L is an extension of FRANC2D, which was originally written by Paul Wawrzynek at Cornell for the analysis of crack growth. A key concept in his work was the use of a winged-edge data structure to describe the geometry. This greatly facilitates automatic remeshing during crack growth.

FRANC3D/NG is designed to simulate crack growth in engineering structures where the component geometry, local loading conditions, and the crack geometry can be arbitrarily complex. It is designed to be used as a companion to a general purpose Finite Element (FE) package. Currently, interfaces to the ANSYS, ABAQUS, and NASTRAN commercial programs are supported.

The FRacture ANalysis Code 3D / Next Generation (FRANC3D/NG or F3D/NG for short) is designed to be used as a module to a general purpose Finite Element (FE) package.FRANC3D/NG is a successor to the original FRANC3D program (now referred to as FRANC3D/Classic), which was developed at Cornell University in the late 1980's. The two codes share a name, the next generation code benefits from over 20 years of experience developing and using the Classic code. The NG version is a complete rewrite employing different approaches for geometrical modeling and deformation analysis.

The integration of three-dimensional (3-D) crack modeling into engineering analysis adds accuracy to results. Using FEM software an engineer creates a mesh, and then uses

FRANC3D/NG to incorporate this mesh and insert a crack, identifying its size, shape, and orientation. FRANC3D/NG automatically remeshes the model around the specified crack geometry and sends the updated modeling data back to the FEM-based software for analysis. After reading the results, FRANC3D/NG "grows" the crack based on the analyzed data, creates a corresponding mesh, and repeats this process accordingly.

### 4.2.2 NASGRO life prediction software

NASGRO Fracture Analysis Software is a suite of programs based on fracture mechanics principles. NASGRO can be used to analyze crack growth, perform assessments of structural life, compute stresses, and process and store fatigue crack growth properties. The package includes a large set of crack growth rate and fracture data.

NASGRO was originally developed at NASA Johnson Space Center to perform fracture control analysis on NASA space systems. Later, after the NASA/FAA/USAF Aging Aircraft Program was formed and began supporting the development effort, NASGRO was developed further for use in damage tolerance analysis of aircraft, including that required for FAA certification.

The software is comprised of the following three modules:

• NASFLA - Life Assessment

• NASBEM - 2-D Boundary Element

• NASMAT - Database of da/dN & fracture test results

NASFLA is part of the NASGRO 3.0 suite of programs Stress Intensity Factor - These are computed for the crack geometry and loading chosen from the NASFLA library of models, and displayed in tabular or graphical form.

NASBEM is part of the NASGRO 3.0 suite of programs. It is a two-dimensional boundary element program used to perform the following analyses:

• Stress Intensity Factors - These can be calculated for any geometry and loading. Tables of stress intensity factors and corresponding crack lengths can be generated for use by the NASFLA module in performing life assessments.

• Stress Fields - These can be calculated for any collection of points in the two-dimensional uncracked object being modeled including its boundary.

NASMAT is used to store, retrieve and curve fit crack growth and fracture toughness data. It has a database containing over 9000 sets of data. This includes over 3000 sets of fatigue crack growth data and over 6000 fracture toughness data points. These data can be searched, plotted, and fitted to either the NASGRO crack growth rate equation or a user specified growth rate equation, or they can be entered into a growth rate table.

### 4.2.3 AFGROW fracture analysis software

The current multiple crack capability allows AFGROW to analyze two independent cracks in a plate (including hole effects), non-symmetric corner cracked holes under tension, bending, and bearing loading (corner cracks only for now). Finite element based solutions are available for two through or corner cracks at holes, and through cracks in plates1under tension loading. These solutions and more information are available in the open literature [27, 28], allow AFGROW to handle cases with more than one crack growing from a row of fastener holes. The COM capabilities in AFGROW have allowed it to be used with an external K-solver program to communicate with AFGROW to perform real time crack growth analysis for multiple cracks (more than two) and cracks growing in complex and/or unique structure. Additional stress intensity solutions and spectrum load interaction models have been added to AFGROW. Finally, user-defined plug-in modules may now be used by AFGROW to allow users to include proprietary or unique stress intensity solutions.

### 4.2.4 Cracks2000 structural integrity software

The CRACKS2000 program is based on the Linear Elastic Fracture Mechanics (LEFM) approach for estimating the fatigue life of a component with a crack. The LEFM approach uses the stress intensity factor parameter, as the driving factor for crack growth. The Cracks2000 program has considerable flexibility in the analytical modeling of crack growth analysis problems.

The program can solve both constant amplitude and variable amplitude crack growth analysis problems, with the user choosing the stress intensity factor, the type of

loading spectrum, the type of retardation model, and the type of crack growth rate behavior description.

Cracks2000 has fifty-one stress intensity factors solutions. There are closed form equations for stress intensity factor solutions for 25 geometries. Many of these solutions are the early Newman-Raju solutions, which are retained for comparisons with older analysis. For the latest stress intensity factor solutions, tables of β-factors are generated from the equations; the tables are used for the life analysis, and can be printed and plotted for β-factors comparison

### 4.2.5 DARWIN

Design Assessment of Reliability WIth INspection (DARWIN) is a risk analysis program for calculating the probability of failure in turbine engine disks. With a graphical user interface for problem setup and output, DARWIN integrates finite element analysis, fracture mechanics, non-destructive inspection, random defect occurrence and location, and other random variables to assess the risks of rotor fracture. Risk calculations incorporate both Monte Carlo and failure function/fast integration methods.

### 4.2.6 Franc3D/ANSYS thermal and mechanical loads interpolation

While it is possible to apply simple boundary conditions to the part (for example, uniform loading), typical usage of FRANC3D requires more complicated load scenarios including thermal and complex mechanical loads. Often, the mechanical loads include stress components arising from nonlinear contact analysis, and in some cases, the internal stresses may be altered due to a shakedown (elastic-plastic) analysis. Thermal and nonlinear analyses are not supported by FRANC3D directly, but the effects of these phenomena can be included in the SIF calculations by obtaining crack face tractions from an ANSYS analysis of the uncracked part. This method is based on the superposition principle illustrated in Figure 4-2.

From the uncracked ANSYS model, represented by case A below, we obtain the tractions, p(x) at the location of the crack. By superposition, we know that the total stress solution to the loaded, cracked part (B) is equal to the sum of the stress fields resulting

from the cracked part with no external load but with tractions p(x) applied at the faces (C), and the cracked part with external loads applied, but exactly shut (D). FRANC3D has the capability to interpolate the tractions along an arbitrary crack path from files output from ANSYS, thus allowing it to run case C. While the stress solution given by FRANC3D is not complete, the K solution is identical to that of the complete stress solution (because D has no singular component).

Note that the superposition assumption is strictly exact for thermal loads, residual stresses resulting from a shakedown analysis (if performed), and mechanical loads resulting linearly from pure load control. It is also valid for (rigid) displacement boundary conditions modeled in the FRANC3D analysis, though rigid boundary conditions are usually an approximate idealization of the real part boundary conditions. Contact nonlinearity and other forms of nonlinearity are not captured by the superposition approach. However, the user may assume the contact surface is either free or fixed in FRANC3D in order to bound contact problems. If the crack length is small compared to its distance from the contact area, contact nonlinearity is expected to have a small effect. Future development in FRANC3D is hoped to enable analysis of cases with nonlinear crack loading.

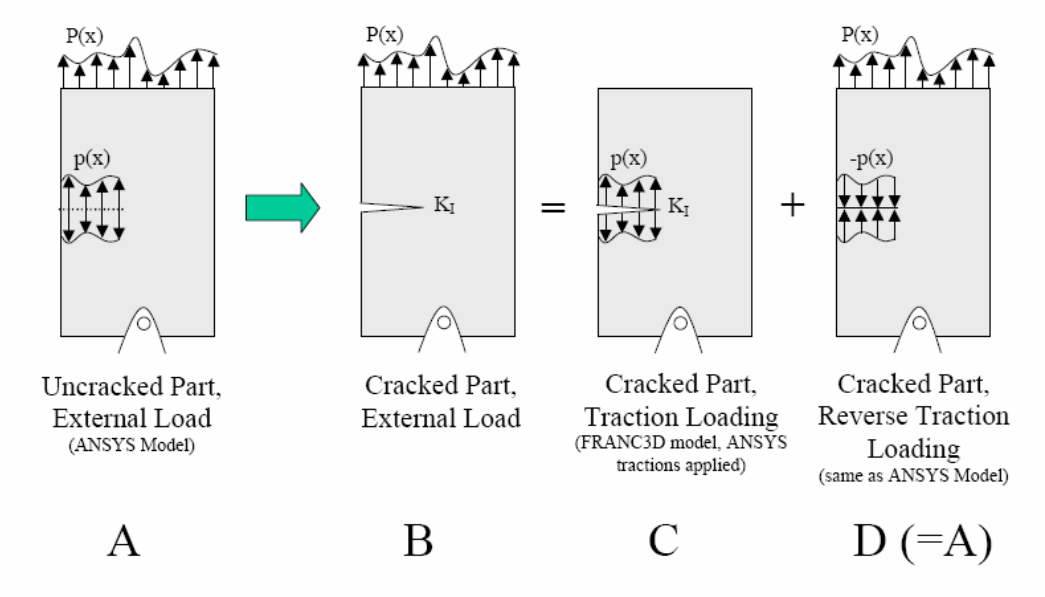


**Figure 4-2 Obtaining SIFs for Arbitrary Loading by Superposition [34]**

## 4.3 The typical work flow for crack propagation analysis.

In order to predict crack trajectories one should use an incremental approach. A series of finite element analyses are run which incrementally increase the crack length by a significant amount in relation to the model's geometry. For a given increase in crack length, the number of cycles to achieve that amount of growth can be calculated. For a given propagation step *i*, there are $N_i$ load cycles associated with it. The amount of crack growth for one cycle is calculated based on maximum stress in the load cycle. Because it is assumed the loading is proportional, it is straightforward to calculate the direction the crack will grow during the cycle. Simulation of fatigue crack growth starting from the initial geometries depicted in Figs. 3-4 consists of the major steps: 1)build and analyzed uncracked model, 2)build the local model and insert crack front elements, 4) mesh the cracked geometry, 5) compute the stress intensity factors, 6) incrementally advance the crack front nodes using a crack growth rate "law" based on the local stress intensity factors, 7) repeat steps 2 – 6 until the crack reaches a specified size or number of loading cycles.

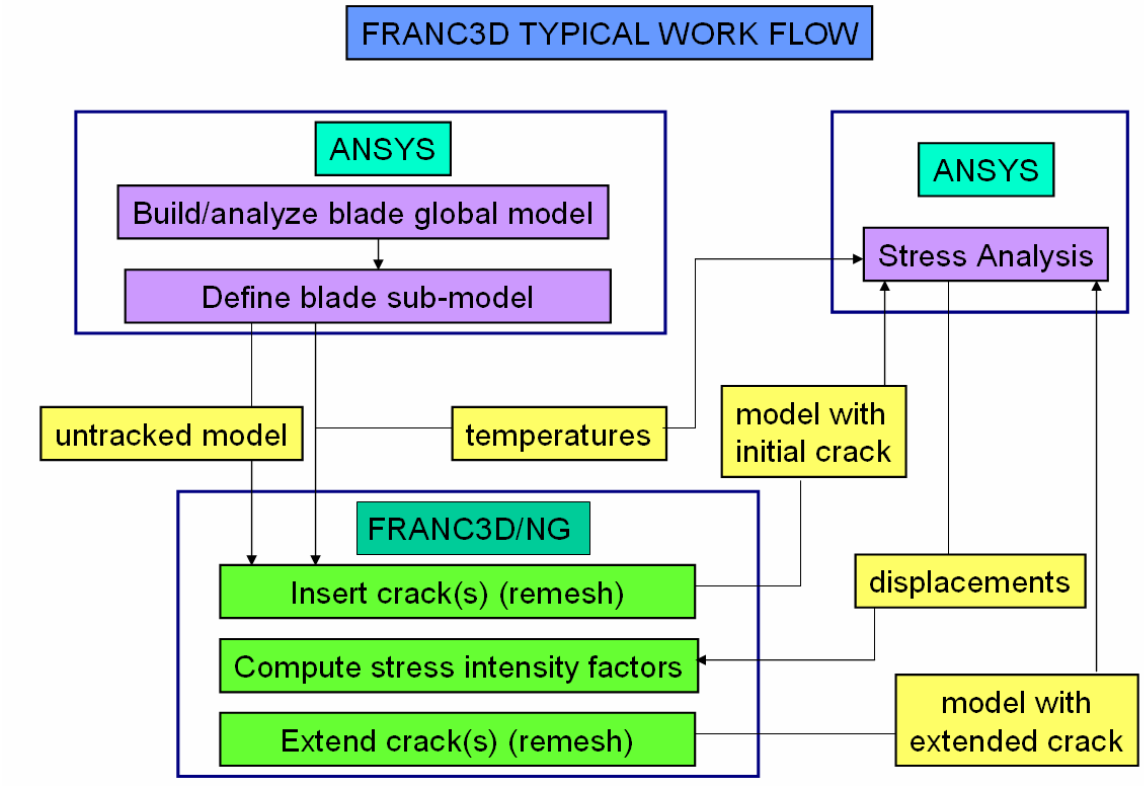


**Figure 4-3 The typical Frank3D work Flow for crack propagation analysis**

### 4.3.1 Sub-modeling approach

Franck3D/NG supports the idea of a sub-model remeshing for crack growth. The sub-model approach is illustrated in Figure 4-3. The ANSYS is capable to build a sub-model and interpolate temperatures and loads. Usually the size of a crack is small relative to the size of the structure. Confining the remeshing for crack growth to the sub-model greatly reduces the amount of data that needs to be transferred to, and processed by. It also allows depart undamaged portions of a model with different structural modeling, complex boundary conditions and are meshed with another elements.

Sub-modeling is used for mesh modification only; it does not affect the analysis strategy. The remeshed local sub-model is inserted back into the global model and the stress and deformation analysis is performed for the full combined model. The sub-model can be redefined at any step of a crack growth analysis.

The two ANSYS mesh models (.cdb files) have built. The smaller portion of the 3D airfoil span was extracted for fracture analysis. This is not necessary but it illustrates the process that will be useful for larger models.

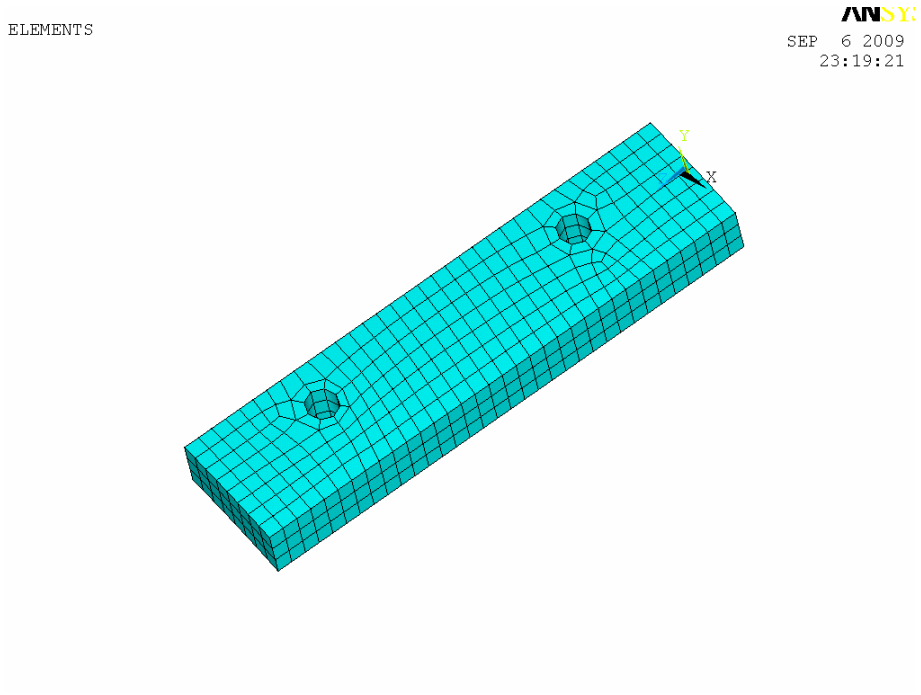


**Figure 4-4 The local ANSIS Sub-model**

Also the altered full model was built. Each element component was archived as a separate model, writing the DB information to .cdb files, which consists of the exterior elements and the boundary conditions, as a regular ANSYS. The global and local models have shown in Figures 4-4 and 4-5. The Ansys options used to create node components. The node component on the local portion of airfoil should be the same as node component on the outer blade model.

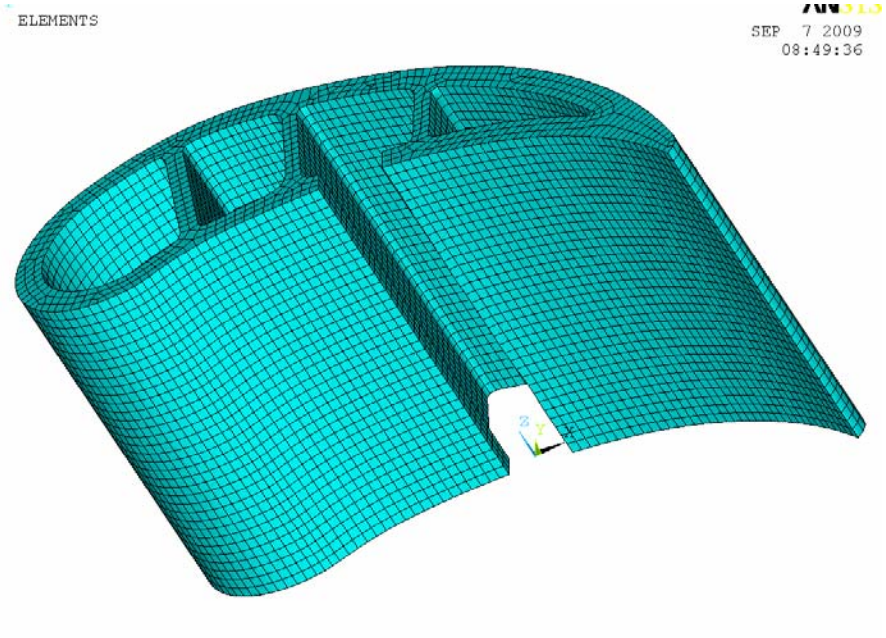


**Figure 4-5 The global ANSIS Sub-model**

### 4.3.2 Meshing, transferring a mesh description

The main form of communication between Franck3D/NG and ANSYS is through ASCII mesh description files. These are human-readable files that define a mesh, node coordinates, materials, and boundary conditions. These files use cdb format for ANSYS. Franck3D/NG expects a mesh file as input that describes an uncracked model or sub-model. It may also request a file of nodal temperatures in the case of thermal/mechanical loading, and possibly a file of nodal stresses if initial or residual stress fields are to be considered. The output from the program is a new file that describes a mesh for a model or sub-model containing a newly inserted or newly extended crack (and possibly a file of interpolated nodal temperatures).

Transferring a mesh description of a component between Franck3D/NG and ANSYS is sub-optimal because mesh descriptions encode geometrical information incompletely. For example, if a portion of the surface of a component is curved, then the mesh model will have replaced that surface with a collection of planar or polynomial patches. This means that Franck3D/NG must use heuristic algorithms to reconstruct a description of the local geometry from the mesh data. In most cases, the reconstructed geometry will be approximate.

In theory, a better approach would be for the FE package to send Franck3D/NG geometrical data with the mesh data. In practice, however, this would introduce unwanted complexities. The format of mesh files varies among venders, but the main information they contain (node coordinates and element descriptions) is essentially the same among popular FE packages, and they describe a relatively simple data model.

### 4.3.3 Initial crack geometry

To be sure that the studied crack placement really is a worst case, other crack placements, crack lengths and crack orientations might be interesting to study. This is done with a number of different locations, not shown in this thesis. An additional crack modeling has increased the understanding of the technique. To place a crack arbitrary is however not a good way to deal with the problem. To do it effective it is better to structure the work as proposed in chapter 3.3.

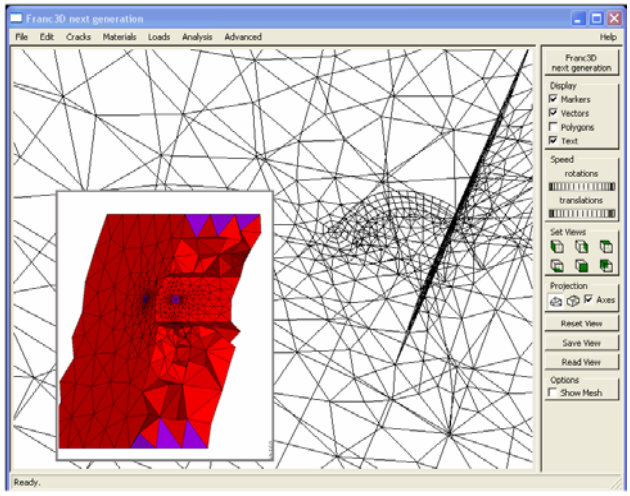


**Figure 4-6 Crack inserted in local sub-model**

Franck3D/NG used to insert both zero volume flaws (cracks) and finite volume flaws (voids) into a model. Both types of flaws are defined as a collection of triangular cubic Bézier spline patches. Using spline patches to describe flaws means that very complex, doubly curved crack surfaces can be modeled. Franck3D/NG provides a "wizard" Figure 4-6 to specify an initial flaw shape, orientation, and location. One first selects from a small library of parameterized flaw shapes (e.g. elliptical crack, part-through crack, center crack, ellipsoidal flaw), then specifies translations and rotations to position the flaw. The wizard provides visual feedback so that location can be confirmed. A representation crack insertion wizard is shown in Figure 4-6

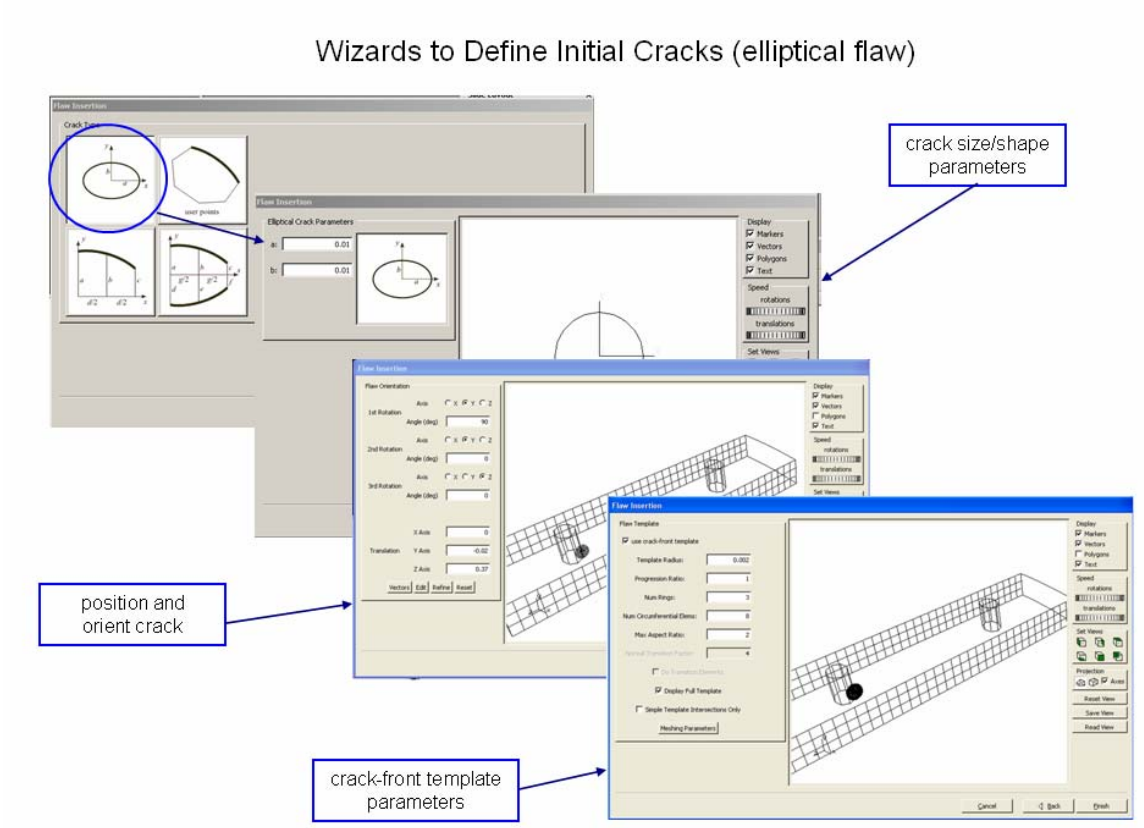


**Figure 4-7 Franck3D/NG rack insertion wizard**

### 4.3.4 Crack region meshing

A variety of element types is used within Franck3D/NG for meshing near cracks. The 15-nodes wedge elements are used adjacent to a crack front. By default, eight wedge elements are used circumferentially around the crack front and these elements have the

appropriate side-nodes moved to the quarter points, which allows the element to reproduce the theoretical stress distribution.

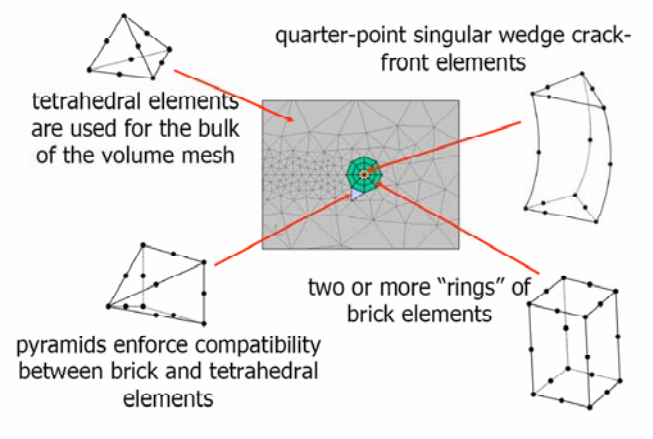


**Figure 4-8 An image from the flaw insertion wizard showing an elliptically shaped crack being positioned in a local blade sub-model**

The crack-front elements are surrounded by "rings" of 20-noded brick elements (two rings by default). Together, the wedge and brick elements comprise what is referred to as the crack front "template". The template is extruded along the crack front a shown in figure 4-7, Figure 4-8. This regular pattern of elements in the template is exploited when computing conservative integrals (e.g., J-integral and M-integral).

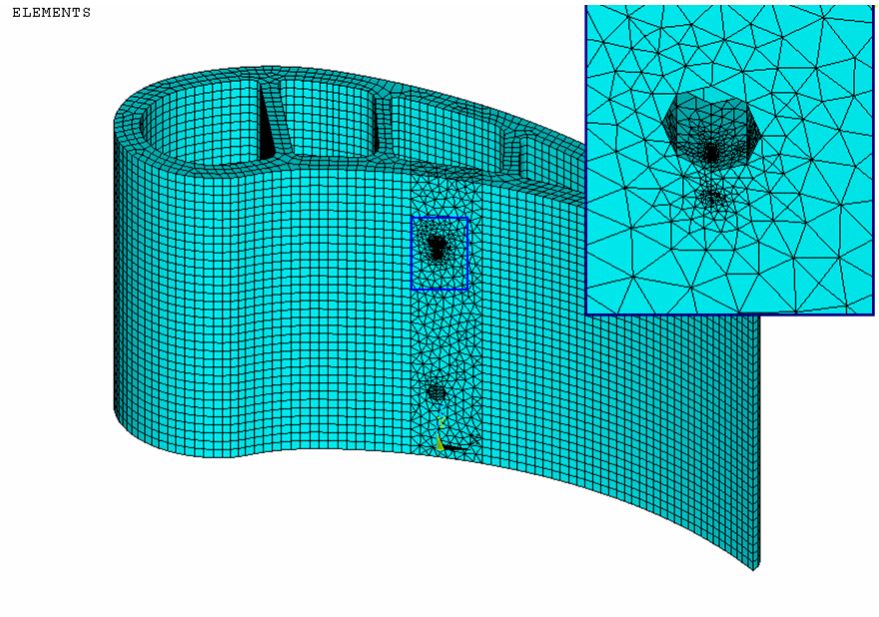


**Figure 4-9 The local model with crack inserted in global model**

The bulk of the sub-model is meshed with 10-noded tetrahedral elements. The triangular faces of the tetrahedral elements are not compatible with the quadrilateral faces of the brick elements;13-noded pyramid elements are used to transition from the template to the tetrahedra. Not all finite element packages support pyramid elements, so as an option the pyramid elements can be divided into two tetrahedra with the "hanging" node constrained.

### 4.3.5 Stress intensity factors definition

The M-Integral Method (default), most accurate method should generally be used. The Displacement Correlation Method is less accurate, but highly robust method useful as a check. Both methods determine SIF's from local displacement in the template region of mesh near the crack tip For the M-Integral method K's are computed by solving a system of three equations (full anisotropic solution shown)

For real cracks with a small amount of inelasticity, the plastic zone may be considered to be encapsulated within the elastic "K fields", thus the stress state at the crack tip is still approximately characterized by the SIFs. Higher order terms are indicated above, but are neglected, because the singular terms dominate the fields near the crack tip. Empirically, $K_I$ correlates with the crack growth rate, and $K_{II}$ effects crack direction. $K_{III}$ is generally neglected.

Stress intensities for all three modes are calculated by FRANC3D [33, 34] based on the displacement observed in the boundary element model. The crack tip displacements for plane strain are

$$\begin{Bmatrix} u \\ v \\ w \end{Bmatrix} = \frac{2(1+v)}{E}\sqrt{\frac{r}{2\pi}}\left( K_I \begin{Bmatrix} \cos\left(\frac{\theta}{2}\right)\left[1-2v+\sin^2\left(\frac{\theta}{2}\right)\right] \\ \sin\left(\frac{\theta}{2}\right)\left[2-2v-\cos^2\left(\frac{\theta}{2}\right)\right] \\ 0 \end{Bmatrix} + K_{II} \begin{Bmatrix} \sin\left(\frac{\theta}{2}\right)\left[2-2v+\cos^2\left(\frac{\theta}{2}\right)\right] \\ \cos\left(\frac{\theta}{2}\right)\left[-1+2v+\sin^2\left(\frac{\theta}{2}\right)\right] \\ 0 \end{Bmatrix} + K_{III} \begin{Bmatrix} 0 \\ 0 \\ 2\sin\left(\frac{\theta}{2}\right) \end{Bmatrix} \right)$$

At 180 degrees, along the crack flank,

$$\begin{Bmatrix} u \\ v \\ w \end{Bmatrix} = 4\frac{(1+v)(1-v)}{E}\sqrt{\frac{r}{2\pi}}\begin{Bmatrix} K_{II} \\ K_{I} \\ K_{III}(1-v) \end{Bmatrix}$$

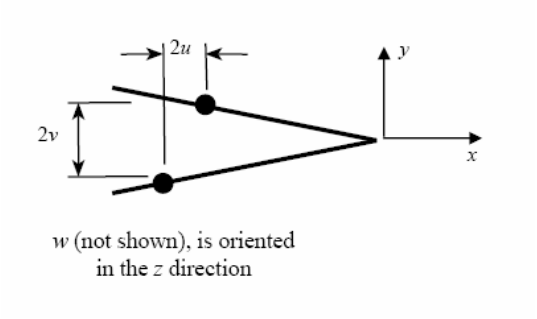


**Figure 4-10 The displacements for plane strain [34]**

Solving for the K's,

$$\begin{Bmatrix} K_{II} \\ K_{I} \\ K_{III} \end{Bmatrix} = \frac{E}{4(1+v)(1-v)}\sqrt{\frac{2\pi}{r}}\begin{Bmatrix} u_{FEM} \\ v_{FEM} \\ w_{FEM}/(1-v) \end{Bmatrix}$$

### 4.3.6 Crack propagating technique

Once the SIF solution for a given crack front is obtained, FRANC3D provides tools to estimate a new, propagated crack front. Because $K_I$ is in general not constant along the crack front, the crack will not propagate evenly across the front. The user specifies the maximum propagation increment anywhere along the crack, $\Delta a_{max}$, which would of course correspond to the point where $K_I$ is highest. The crack extension everywhere else on the crack front is calculated based on the local Paris law [69]

$$\Delta a = \Delta a_{\max}\left(\frac{K_I}{K_{I\max}}\right)^b$$

where the local Paris exponent, b, is actually a material property (the local slope of the da/dN curve in log-log coordinates), and can be affected by temperature and R-ratio.

However, for most engineering metals, b ranges between 3-4 throughout much of the crack growth range. Also, the K versus a curve eventually obtained from FRANC3D is not extremely sensitive to this value, thus in practice, a value of 4.0 is recommended. Nevertheless, sometimes it is necessary (and permissible) to use a smaller number to propagate the crack when the K distribution is highly (and usually temporarily) irregular.

A second issue with regard to the crack shape evolution concerns non-planar crack growth. The user may specify planar growth, for which case the local crack kink angle is always set to zero. This makes the problem a little simpler, and is an acceptable approach for symmetric problems, or where $K_{II}$ remains small compared to $K_I$. For non-planar growth, the Maximum Tangential (hoop) Stress algorithm should be used (and is the default set by the program) to calculate the local direction of crack growth, though the other options yield very comparable results. The Maximum Tangential Stress Theory [35] is derived from the in-plane asymptotic crack tip stress field in polar coordinates centered at the crack tip (Figure 4-11)

$$\begin{Bmatrix} \sigma_{rr} \\ \sigma_{\theta\theta} \\ \sigma_{r\theta} \end{Bmatrix} \cong \frac{1}{(2\pi r)^{1/2}} \cos\left(\frac{\theta}{2}\right) \begin{Bmatrix} K_I\left(1+\sin^2\left(\frac{\theta}{2}\right)\right)+\frac{3}{2}K_{II}\sin\theta - K_{II}\tan\left(\frac{\theta}{2}\right) \\ K_I\cos^2\left(\frac{\theta}{2}\right)-\frac{3}{2}K_{II}\sin\theta \\ K_I\sin\theta + K_{II}(3\cos\theta - 1) \end{Bmatrix}$$

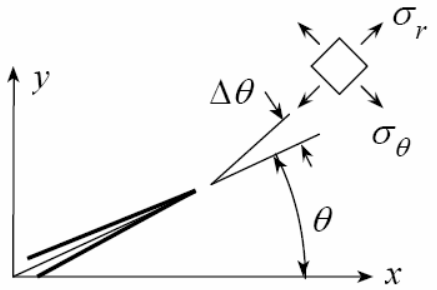


**Figure 4-11 Crack Tip Polar Coordinate System for Kink**

The theory assumes that the crack will grow from the existing crack tip toward the direction which maximizes $\sigma_\theta$ (which is the stress normal to the proscribed crack kink). Note that this condition also corresponds to the direction where $\sigma_{r\theta} = 0$. The predicted kink angle, $\Delta\theta_c$, is thus given by

$$\frac{K_{II}}{K_I} = \frac{-\sin\Delta\theta_c}{(3\cos\Delta\theta_c - 1)}$$

as shown in figure 34-11. This can also be given explicitly as [36]

$$\Delta\theta_c = 2\tan^{-1}\left(\frac{1-\sqrt{1+8(K_{II}/K_I)^2}}{4(K_{II}/K_I)}\right)$$

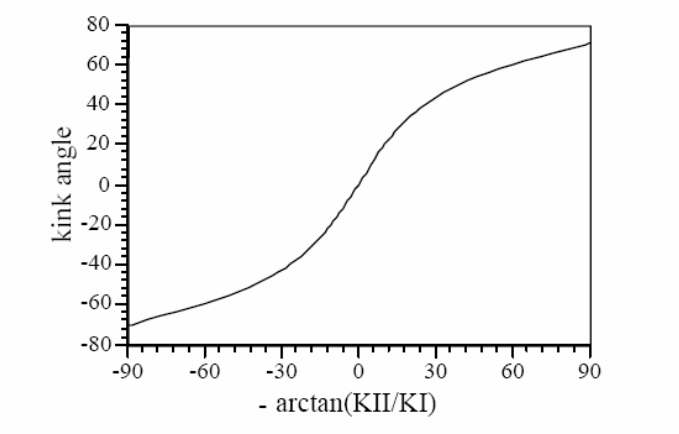


**Figure 4-12 Kink Angle as a Function of Mixed Mode Based on MTS Crack Turning Theory [34]**

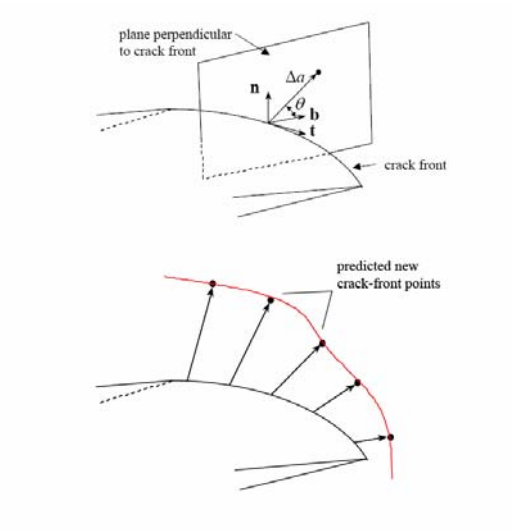


**Figure 4-13 Non-Planar Crack Propagation in Franc3D [34]**

FRANC3D computes the local crack increment and kink angle at several points along the crack front, and fits a polynomial curve through the new crack front points so determined as shown in Figure 4-13. Logic is built in to FRANC3D to support crack propagation with complex geometries, as shown in Figure 4-13.

### 4.3.7 Computing crack-front parameters

Franck3D/NG computes stress intensity factors using either a displacement correlation approach or an M-integral. It can also compute elastic strain energy release rates by way of a J-integral. In the displacement correlation approach, the finite-element-computed displacements for nodes on the crack faces are substituted into the theoretical expressions for the crack-front displacements fields written as functions of the stress-intensity factors.

In the displacement correlation approach, the finite-element-computed displacements for nodes on the crack faces are substituted into the theoretical expressions for the crack-front displacements fields written as functions of the stress-intensity factors.

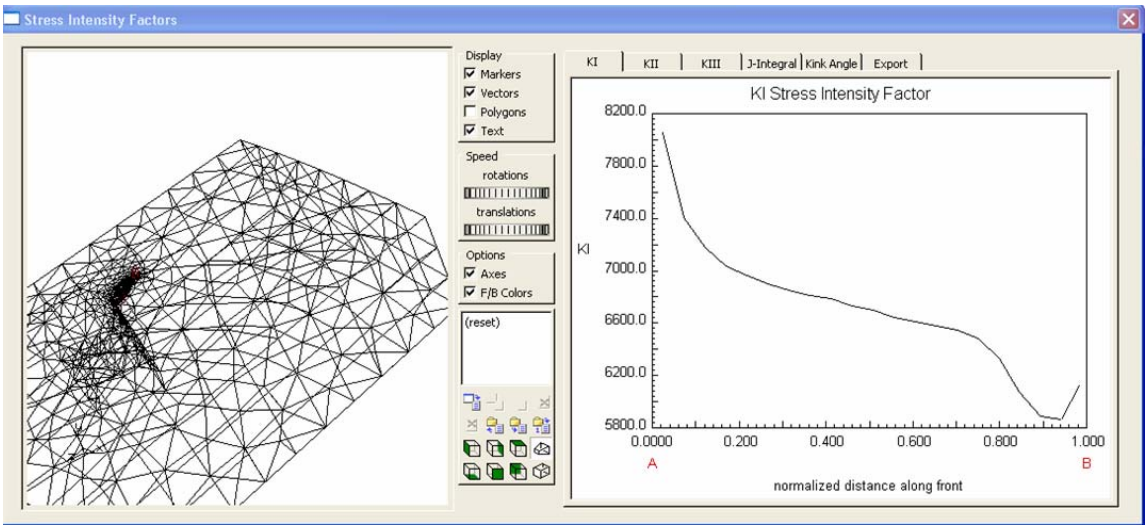


**Figure 4-14 Stress Intensity Factor Computations**

For a linear-elastic analysis, the J-integral is equivalent the total strain energy release rate. Franck3D/NG uses an equivalent domain formulation of the J-integral where the conventional contour formulation is replaced with a volume integral, which can be evaluated more accurately in a finite element context The M-integral, sometimes

called the interaction integral, computes the energy release rates segregated by modes so the modal SIF's ($K_I$, $K_{II}$, and $K_{III}$) can be computed. Franck3D/NG has M-integral formulations for both isotropic and orthotropic materials where the material axes can be oriented arbitrarily relative to the crack front [37].

## 4.4 Fatigue crack extension analysis

To study crack trajectory, a sub-model of an airfoil part of a generic turbine blade was modeled using UG/NX CAD. The airfoil modeled here is shown as Figure 3-1. The geometry shown in Figure 3-2 is similar to is a commercial turbine blade design. The boundary conditions applied to this model were the result of a global/local approach where displacements and temperatures were taken from the results of the global model and applied to the boundaries of the local sub-model studied here. To understand the major influences on crack trajectory, 3D model of airfoil section with edge boundary conditions, temperature distribution, global and local integrated sub-models and initial crack inserted was analyzed.

The model was used for fracture mechanics analysis. In the analyses, the model was simulated with a 0.010" inch penny shaped initial crack length, as shown in Figure 4-7. At the crack tip, quarter-point triangular elements were used. The mesh was then transitioned toward the boundaries using triangular elements and quad elements where bilinear mapping could be employed. Discrete crack growth steps were modeled in appropriate increments. At each step, the crack growth direction was computed using the max ($\sigma_{\theta\theta}$) criterion. The crack was then propagated in the computed direction, and, finally, the model geometry was updated with the new crack configuration and remeshed for subsequent analysis. The FRANC3D/ANSYS interface was implemented to complete the crack growth iterations. As shown in Figure 4-14, the initial model attributes are defined in ANSYS, and FRANC3D is used to compute crack growth parameters and updates the geometry and mesh. After a model is analyzed using ANSYS, FRANC3D computes the location of the new crack front, extends the crack, and updates the model geometry. Finally, remeshing is done and the process is continued until some criterion is met.

Stress intensity factors (SIF) associated with three modes of fracture are calculated using the displacement approach. Crack propagation trajectories under mode-I and mode-II conditions are obtained using maximum tangential stress crack-extension criteria.

### 4.4.1 Crack growth simulation process

For the crack propagation analysis we have used the five-step process embedded in Franc3D/NG as follows:

- SIF's are computed for all node points along the crack front.
- At each such point the direction and extent of growth is determined.
- A space curve is fit through the new crack-front points and, for the case of a surface crack, extrapolated, if necessary, to extend outside of the body.
- New Bézier patches are added to the crack surfaces.
- The extended crack is inserted into an uncracked mesh.

For our study the Maximum Tensile Stress (MTS) criterion is used to predict the local direction of crack growth. The relative amount of crack growth for points along the front, used by default, is a ratio of the corresponding SIF's raised to an analyst specified power. This is analogous to evaluating the Paris crack growth rate equation for two points where both points are subjected to the same number of load cycles.

### 4.4.2 Model for 3D finite element fracture mechanics

We have started with a pre-cracked model. The model has been created as described in section 4.3.3 and 4.3.4; this is a Franc3D/NG file with inserted crack geometry. Materials, coordinate systems, boundary conditions, constraint information, and node components for individual mesh facet groups were selected to be retained from ANSYS finite element (cdb) file.

The semi-elliptical corner crack was originated by entering the semi-axes lengths. The crack was placed by translations of the origin of the flaw to a location in the cooling hole edge. By rotations about the local axes crack was aligned to required position.

The 15-nodes wedge elements are used adjacent to a crack front. Sixteen wedge elements are used circumferentially around the crack front and these elements have the appropriate side-nodes moved to the quarter points, which allows the element to reproduce the theoretical stress distribution.

### 4.4.3 An incremental crack-extension analysis

Stress intensity factors (SIF) associated with three modes of fracture are calculated using the displacement approach. Crack propagation trajectories under mode-I and mode-II conditions are obtained using maximum tangential stress crack-extension criteria. Crack was grown in a series of crack propagation steps, sized by the user with a selected crack-extension criterion.

The stress intensity factors have been calculated in order to analyze the crack growth of an affected structural component. Crack-growth processes are simulated with an incremental crack-extension analysis. For each increment of the crack extension, a stress analysis is carried out in ANSYS by applying Macro file created in Franc3D/NG. The stress intensity factors are evaluated. The crack path, predicted on an incremental basis, is computed by a criterion defined in terms of the stress intensity factors.

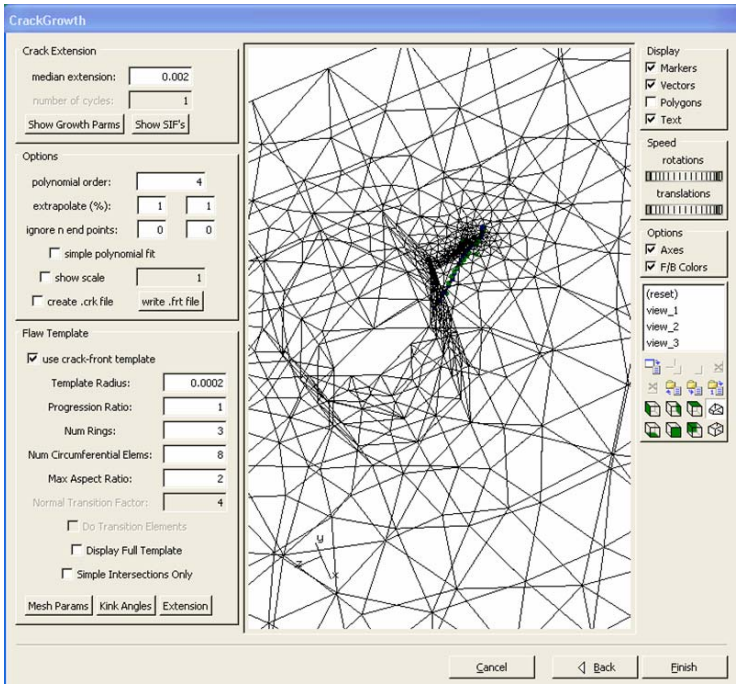


**Figure 4-15 Display Crack Growth panel for initial step**

We used M-Integral to compute the stress intensity factors and orthotropic toughness values based on material properties file. The thermal terms used for the M-Integral computation. We use a single static load case. We specify the load ratio (R=0) and load factor (P=1) where R is the ratio of minimum to maximum load and P provides a scaling factor. The form of the Mode I SIF was selected by entering the maximum K.

For the crack propagation direction the maximum stress criterion used to predict the angle $\theta$ at each point along the crack front. The following equation embedded in Frank3D/NG for kink angle calculation [34]:

$$\theta_{kink} = \theta \quad \text{such that}$$

$$MAX\left( \sigma_{\theta\theta}(\theta)\big|_{\max}, \sqrt{\left(\frac{K_{Ic}}{K_{IIc}}\right)^2 [\sigma_{r\theta}(\theta)]^2 + \left(\frac{K_{Ic}}{K_{IIIc}}\right)^2 [\sigma_{rz}(\theta)]^2}\Bigg|_{\max} \right)$$

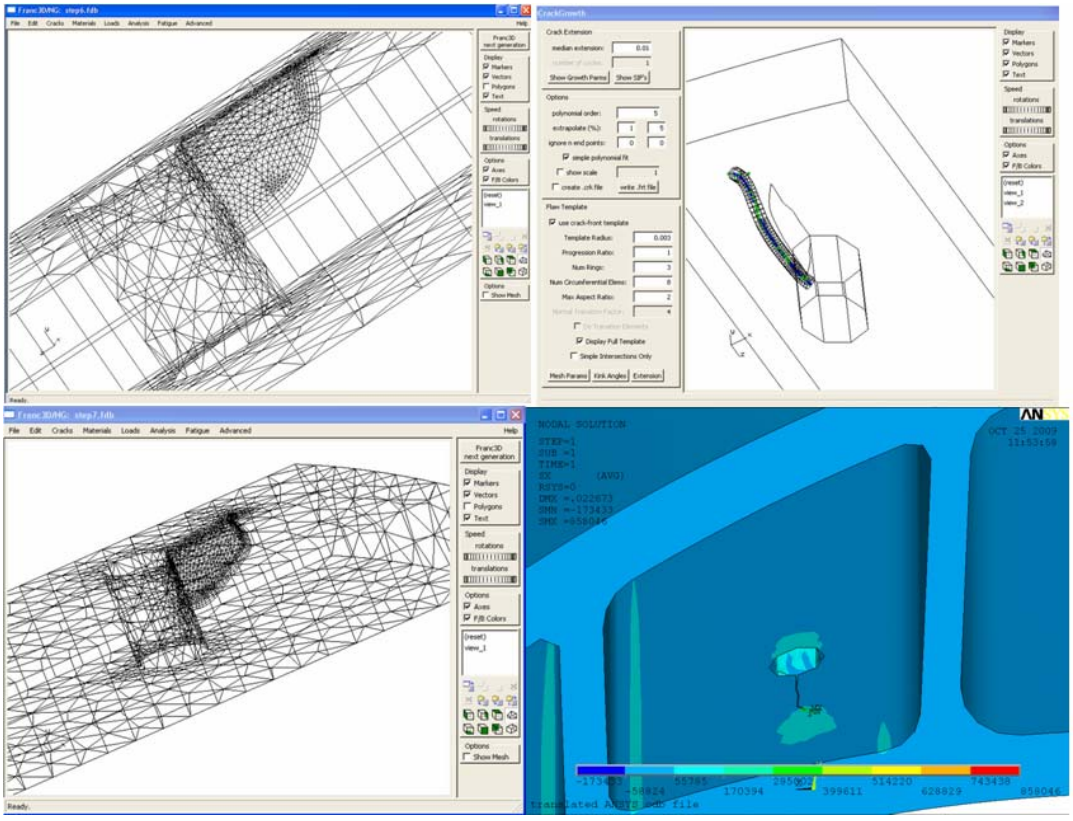

**Figure 4-16 The crack growth stages 6 and 7, crack growth definition for stage 7, the ANSYS model step6 for displacement analysis.**

The crack extension was specified by the crack propagation extension criterion; embedded in Frank3D/NG. The median extension has been selected to grow the crack based on a Paris power law. The relative extension at each point along the crack front is computed based on the chosen equation and a user-specified median extension. The median extension occurs at the point along the crack front with the median Mode I SIF value.

To complete crack growth definition the crack increment in the model scaled to define the length of extension; the polynomial fit was adjusted through the new crack front points; the polynomial extrapolation was fine-tuned to ensure intersection with the model surface, and the template radius was resized. Eight propagation steps were modeled in FRANC3D. Some propagation steps are shown in Fig. 4-16.

### 4.4.4 Crack growth results

Prediction of 3D crack propagation was conducted with thermal-mechanical stresses induced and boundary condition applied for comparison with experimental and failure results. The corner crack growth predictions linked well with the experimental and failure results for similar material, temperature and load conditions [3], [4], [5], [8], [10], [13], [14], [15]. Prediction of crack growth in the presence of the complex stress field that results from various temperature fields on geometries that imitate features in actual blade was achieved. Considerable decrease in crack growth life due to crack propagation from the cooling hole was successfully predicted using the 3D fracture mechanics code. The model predicts the propagation of the crack front assuming linear elastic behavior without the effect of possible residual stresses.

The complete history of the stress intensity factors is computed along the path as well as the crack tip. Under the applied loading scheme the crack is expected to grow towards the blade platform. In this application a crack is initiated from the corner of the hole and the crack path predicted. The accurate prediction of the crack growth is highly dependent upon the accuracy of the stress intensity factors. Any minor inaccuracy in

these values is accumulated during crack growth process which can lead to a completely unrealistic prediction.

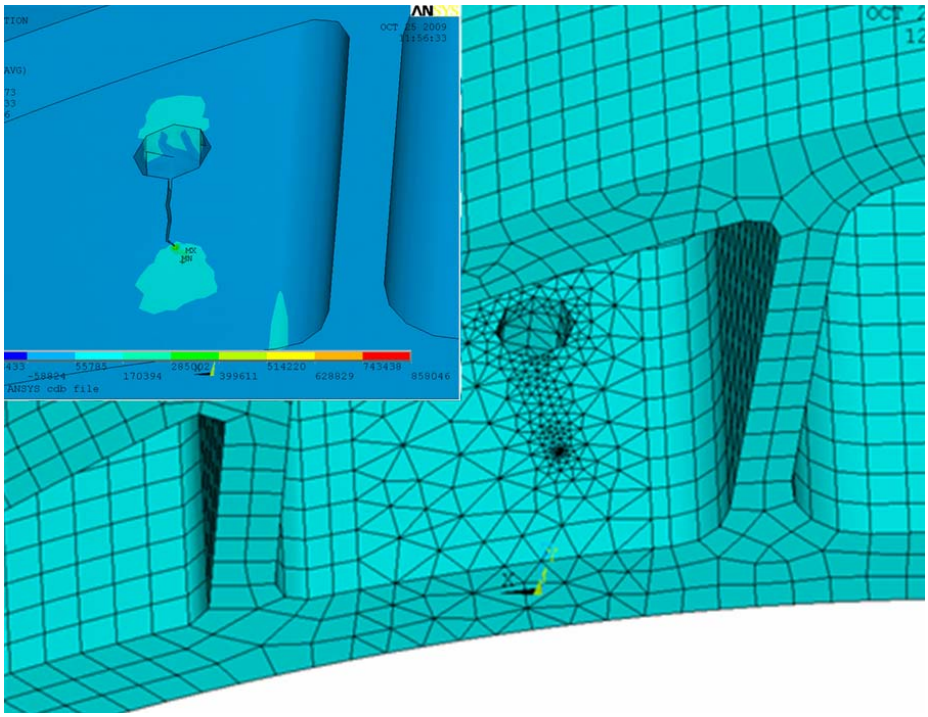

**Figure 4-17 Fractured blade after simulation, crack growth path**

The deformed crack shape shows a complex stress distribution as the cracks have approached each step. The crack has not maintained complete symmetry. A clearer view is shown by zooming into the crack area. Figure 4-17. The crack path becomes very complicated as the crack become longer as can be seen in the deformed shape display.

We have completed eight steps of propagation for this model. The crack propagates such that it not remains in the same radial plane. It has a tendency to transitions from a corner crack to a part-through crack after more steps of propagation (Figure 4-18).

The crack growth rate and crack growth direction have strong dependence on the state of stress Figure 3-21, 3-22. Once initiated the crack propagates instantaneously in the front direction, perpendicular to applied stresses. The crack propagation in lateral direction deviates depending on stress fields distribution at each step.

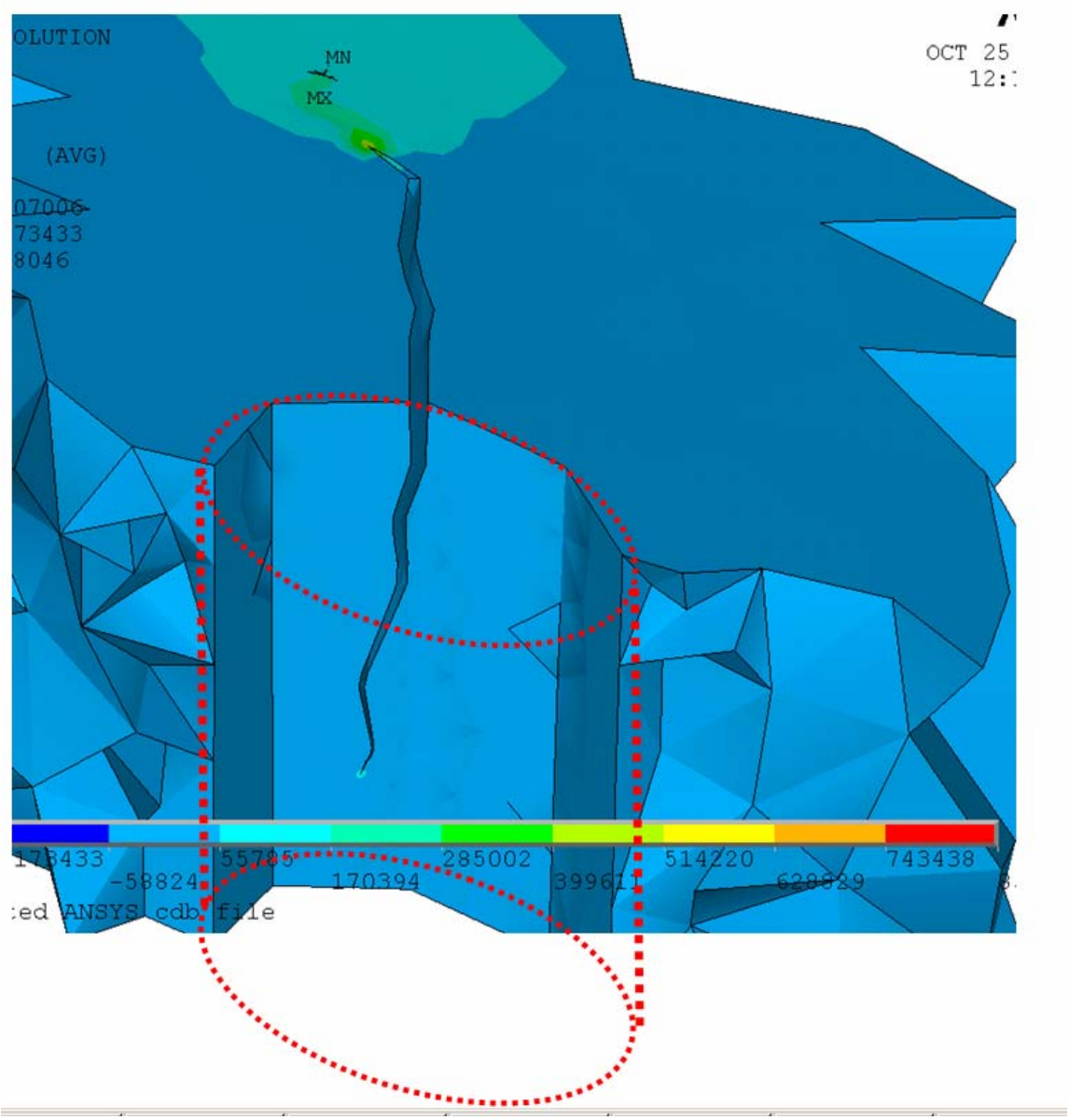


**Figure 4-18 Crack shape inside hole**

Several criteria have been proposed to describe the mixed-mode crack growth. Among them, one of the most commonly used is based on the maximum stress criterion at the crack tip. The maximum stress criterion postulates that the growth of the crack will occur in a direction perpendicular to the maximum principal stress. Thus, the local crack-growth direction is determined by the condition that the local shear stress is zero. In practice this requirement gives a unique direction irrespective of the length of the crack extension increment. Therefore the procedure adopted in the system is to use a

predictor corrector (the subroutine embedded in Franc3D/NG) technique to ensure the crack path is unique and independent of the crack extension increment used.

The results obtained from an incremental crack-extension analysis are a crack path definition, individual crack shapes displacements, and stress intensity factors for different stages of crack growth and/or stress intensity factor histories and life predictions. Figures 4-19, 4-20, 4-21 and 4-22.

Results of the linear elastic (LE) Franc3D/NG analysis are shown in Figures 4-19 and 4-20 includes the maximum stress intensity factors, plotted against crack length.

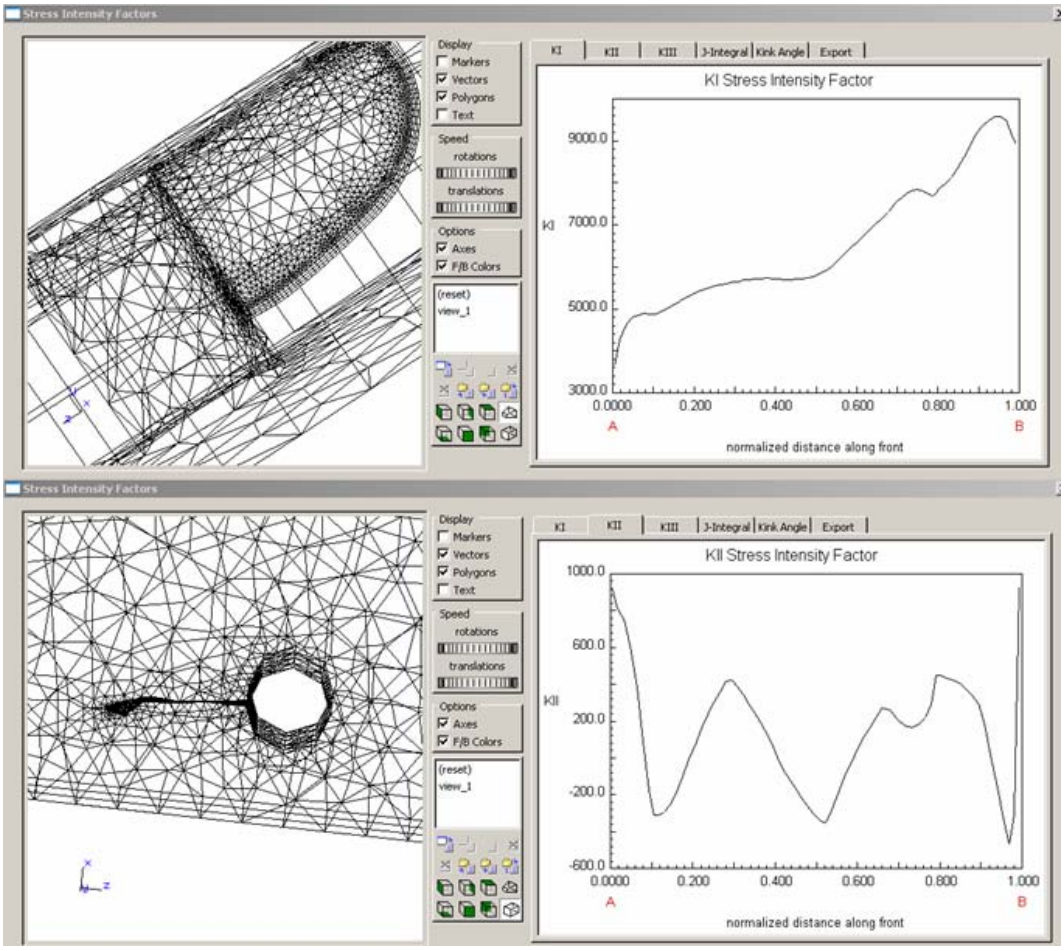


**Figure 4-19 The normalized KI and KII along the final crack front under analyzed stresses.**

The calculated stress intensity factors indicate a strong mode I (KI) and mode III (KIII) interaction and a weak mode II (KII) interaction on the contact surface. However, on the

free surface it is primarily a crack opening (KI) condition only.

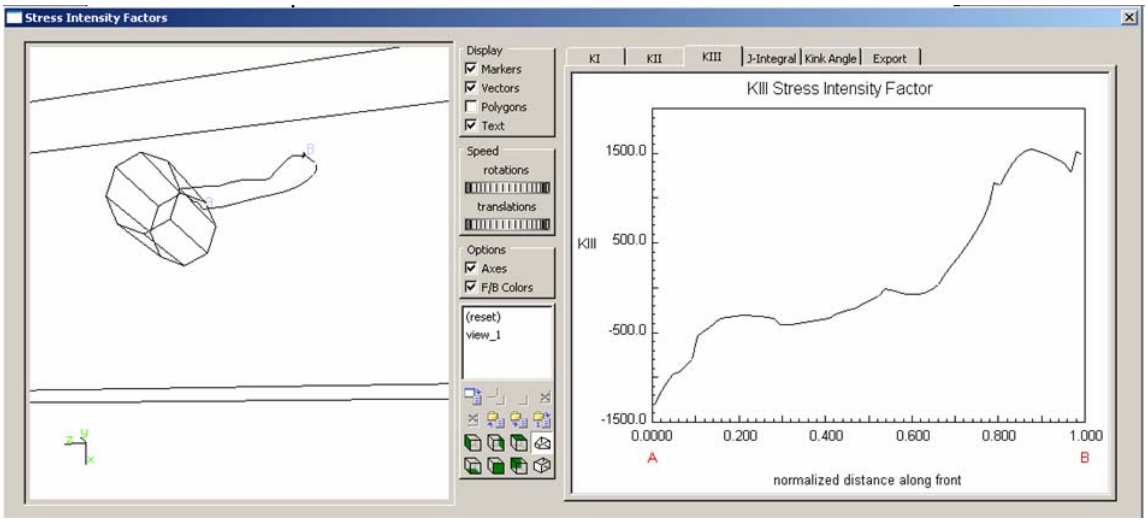


**Figure 4-20 The normalized KIII along the final crack front under analyzed stresses.**

The plots of mode I, II Ks (the vertical axes of Figure 4-19) were based on the geometric calculation points along the crack front. The horizontal axes of these plots represented a location along the crack front with a scalar, unit less, value that varied from zero to one. Zero represented one end of the crack front and one represented the other end, both of which were on the free surface (surfaces inside hole and adjusted wall surface) of the FRANC3D model. The mode I Ks were two to three orders of magnitude greater than both the mode II and mode III Ks. These mode I dominant K findings confirmed crack installation and shape were nearly ideal because energy release rates are highest from mode I cracks in local tension fields. The calculated stress intensity factors indicates that only KI play a strong role in propagation, this is of course expected since the stresses were perpendicular to crack area. The plot also indicates that the average stress intensity factor along the crack front exceeds the critical SIF could be occurred. This means mode I K values should be greater than modes II and III K values. A corollary to this, whenever mode I K values were not dominant then crack front shape and orientations were not ideal. Therefore, future crack front advances would alter the crack front shape and or orientation. The mode I through III K plots show the greatest changes in K values near the free surfaces of the crack front. This typical behavior was due to the singularity associated with the end of the crack front on the free surface of the

model. Thus, K values near the free surface contained the greatest degree of variation and uncertainty.

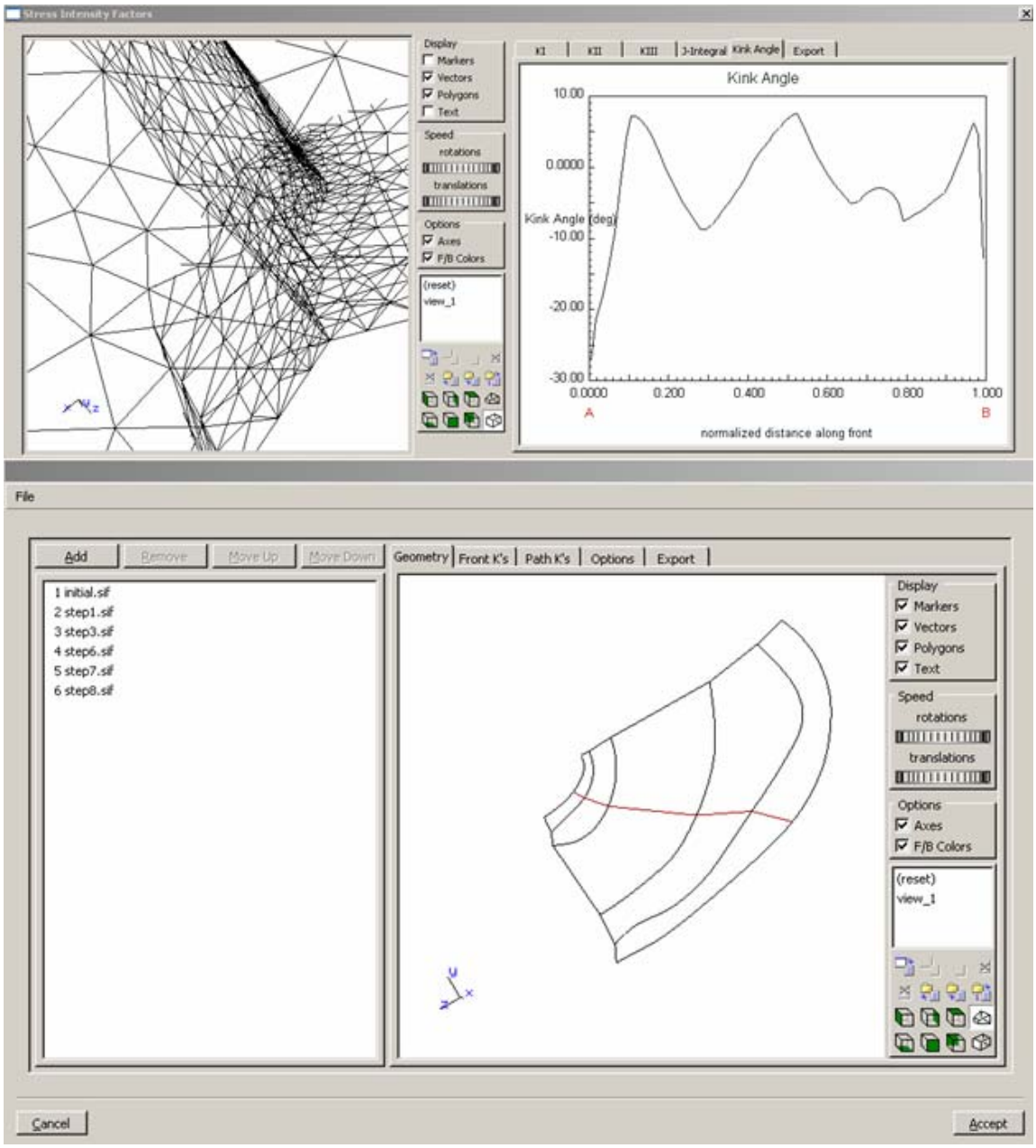


**Figure 4-21 Detailed evaluations crack size or shape and crack path geometry**

For the remaining life analysis, a $K_{eff}$ versus ***a*** plot was constructed after completing crack growth iterations using the Franc3D Stress Intensity Factor History mode Figure 4-21.The stress intensity calculations in center of crack front were used, crack growth is locally perpendicular to the crack front. All points along a given crack front occur at the

same life, N thus, the $\Delta a$'s were calculated for each step as each local $K_{eff}$ as well. Figure 4-22.

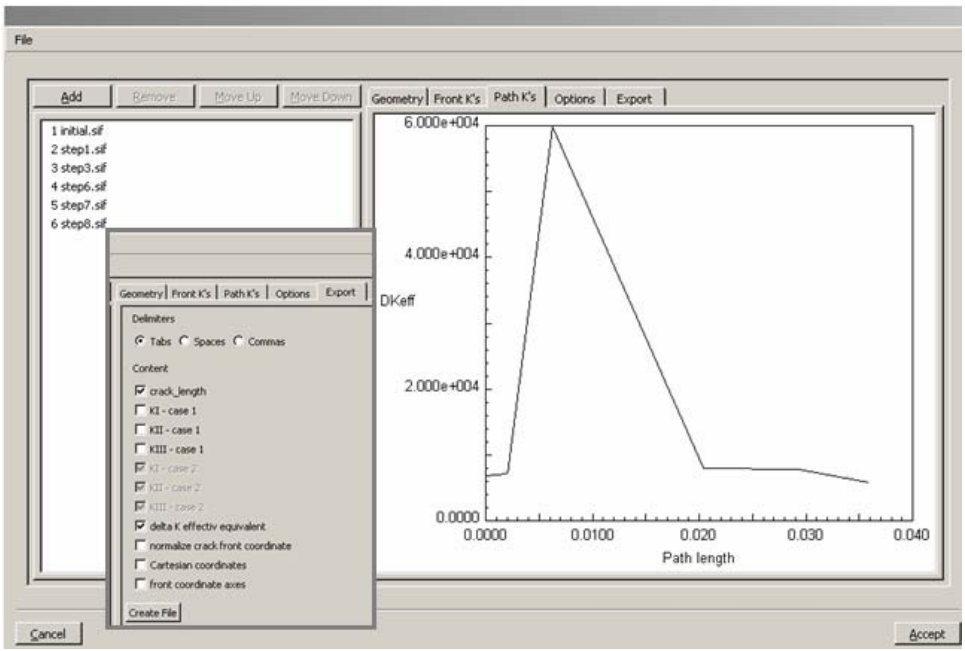


**Figure 4-22 Franc3D Stress Intensity Factor History mode, Path Length definition.**

The predicted fatigue life was preliminary estimated using the SURCK (UTC Pratt & Whitney lifing prediction code) Figure 4-23. The life prediction mode is available in Franc3D V 2.6. Crack lengths versus cycle count data are shown.

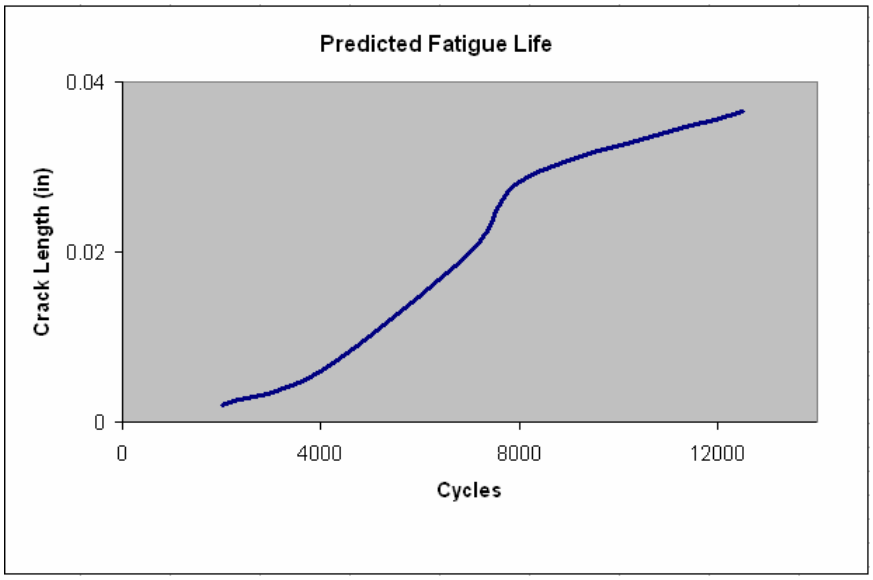


**Figure 4-23 The predicted fatigue life for the blade with an initial crack**

As expected the number of cycles increases as crack grows is reduced. Crack arrest develops before approaching compressive stress zone in airfoil wall. The crack size was changed from 0.010” to 0.040”.The shape of crack was mostly defined by local stress distribution.

This work shows that it is possible to predict crack growth for a penny shaped surface crack subjected to mixed-mode loading in general agreement with results obtained from published observations. The differences between the experimental results and the numerical predictions may partly depend on the material scatter and partly be due to deficiencies in the physical model. For instance crack closure may be developed in different ways for 3D surface cracks than for the 2D CT-specimens. Furthermore, with the implementation of fracture criteria, crack growth can be also directly analyzed with a fracture mechanics approach. No convergence difficulty has been encountered during the crack growth analyses.

# 5. Conclusions and recommendations

A new appropriate approach to the phenomenological modeling of fatigue damage behavior based on the well-known concepts of continuum damage mechanics is developed.

The thesis show how CAD modeling, finite element analysis, computational fracture mechanics, sub-modeling, meshing capabilities have been combined to create a methodology that provides an analyst with the capability to model realistically shaped cracks in existent turbine blades subjected to realistic loads.

For our task we analyzed one of the worst load cases based on sensitivity studies of temperature distribution and boundary conditions at cooling hole location. The thermal cycle for our study is simplified to Cycle II, or in-phase TMF, that occurs when the maximum strain is directly in phase with the maximum temperature.

The general thermal–stress problem separated into two distinct problems to be solved consecutively. The first is a problem (thermal analysis) in what is generally termed the theory of heat conduction and requires the solution of a boundary-value problem. When the temperature distribution has been found, the determination of the resulting stress distribution (thermal-stress analysis) is a problem in what is termed the non linear uncoupled quasi-static theory of thermoelasticity.

This thesis outlines a framework for damage tolerance assessment using computational mechanics software. The approach is presented through the methodology for simulating the growth of through cracks in the airfoil walls of turbine blade structures. In the framework of the thesis a comprehensive non-isothermal fatigue-damage model for a wide stress range is proposed in Chapters 3 and 4. It is based on the available thermal mechanical fatigue experimental studies and micro structural observations for advanced nickel based alloys. The proposed approach takes into account the features, which are important for the comprehensive TMF and crack propagation modeling for structural analysis of turbine blades components.

Comprehensive knowledge of the crack propagation characteristics of nickel based supper alloys is essential for the development of the structural integrity. For critical turbine blade applications, potential improvements in fatigue life, performance,

structural efficiency and maintenance offer incentives for the selection and development of materials with improved crack propagation resistance. In the aerospace industry, a fundamental understanding of the growth of long or macroscopic fatigue cracks under more realistic types of in-service loading is essential for the design, analysis, development and inspection of fail-safe structures.

The methodology currently being used in design and analysis is the defect-tolerant approach, where the fatigue lifetime is evaluated in terms of the time, or number of cycles, required to propagate the largest undetected crack to failure (defined by fracture toughness, limit load or allowable strain criterion). This approach relies on an integration of the crack growth expression, representing a fracture mechanics characterization of relevant data on fatigue crack propagation.

In the current study, as in [1], LEFM theories were used for fatigue crack growth predictions. Fatigue crack growth rates were determined using a modified Paris model accounting for crack closure. A crack is assumed to advance when its SIF is large enough to overcome closure and is larger than the SIF of the previous load step.

The analyses used both FRANC3D and ANSYS. FRANC3D was used to generate the complicated geometry of the blade, to specify the analysis attributes and to define the crack. Also, it was used as a post-processor to calculate the SIFs. ANSYS was utilized for finite element thermal-structural analysis of the model.

In order to perform thermal-structural analysis on models with cracks, features that complement FRANC3D and ANSYS were needed. In this respect FRANC3D was extended to include a capability of specifying the global and local models and to include a translator to convert the information regarding the geometry, mesh, boundary conditions, material properties and contact surfaces to an ANSYS input file.

The global/local model was meshed with quadratic tetrahedral rather than linear.. Volume meshing was done using Franc3D.

The model and meshes were generated with FRANC3D [10]. The finite element analysis was performed with ANSYS [11]. The computed nodal point displacements were read back into FRANC3D where the M integral was evaluated to determine the stress intensity factors.

## 5.1 The crack propagation prediction methodology

A methodology for incorporating the prediction capability into the lifing regimes for existing turbine blades must be developed.

The usages of different gas turbine blades are complex with many engine's throttle transients in each maneuver. Thus blade geometry features are subjected to various fatigue loading cycles applied at elevated and varying temperatures. The crack growth prediction methodology must identify the damage producing cycles from these histories and predict the life associated with a crack subjected to these cycles. The problem is further complicated by local yielding at regions of high concentrated stress and by the possibility of vibratory excitation.

The crack propagation prediction methodology was developed to provide a simplified and efficient means of predicting the residual life. The life predictions are based on the principles of Linear Elastic Fracture Mechanics (LEFM).

While FRANC3D provides a series of crack front configurations and the corresponding stress intensity profiles, the final outcome of a FRANC3D analysis is typically to determine the remaining life. Because FRANC3D/NG does not have built in crack growth models, this includes running another application for life estimation.

A quick step-by step description of the overall analysis is as follows. The sequence assumes that crack face traction loading will be used, though in practice, other loading approaches may be appropriate.

1. Determine most damaging (Type I) stress cycle.
    a. Analysis at most limiting surface flaw location.
    b. Pick most damaging Type I cycle to ratio other cycle pairs from.
2. Save ANSYS output from model of limiting time point
    a. Create Study Model from a Full Blade Model that was analyzed. Use sub-modeling techniques. Save ANSYS model to db file, With Powergraphics OFF, in Cartesian coordinates, save nodal stresses to .node file
    b. Create global and local models Save ANSYS model to .cdb file
3. Open local model (cdb file) in FRANC3D

4. Apply material properties, apply boundary conditions to restrain part if necessary
5. Insert initial crack in model using options available in FRANC3D
6. Mesh should transition gradually from fine mesh at crack tip to coarser mesh away from crack tip.
7. Save new meshed FRANC3D .fdb file.
8. Run macro created in FRANC3D using ANSYS.
9. Run FRANC3D. Analyze stress intensity factors.
10. Continue to grow crack, remesh and re-run FRANC3D to develop K vs a.
11. .K vs a profile should be calculated along path approximately normal to crack fronts.
12. Estimate and report crack growth rates and the predicted fatigue life for the blade with an initial crack. Currently available at FRANC3D V 2.6.

## 5.2 The future work

The knowledge obtained during this first work has shown the major interest crack propagation methodology that involves usage 3D finite element and fracture mechanics numerical tools. Results are promising and the perspectives are numerous to describe durability issues of turbine blades. This thesis has also underlined the great complexity of the material.

To continue the work the crack propagation simulations for the different initial flaws and crack-extension criteria need to be reviewed and compared. The dimensions and crack aspect ratios from the different simulations and the actual cracked blades are planned for evaluation. The contribution of KIII/KI and KII/KI interactions to the crack propagation needs to be defined.

The incorporation/simulation of typical and overspeed mission cycles under real life centrifugal, aerodynamic, thermal and thermal-mechanical loading conditions need to be introduced. Vibration modes also influence the crack growth rate.

Other aspects of feature work are the initiation of crack inside the wall from a flaw, the creation of multi cracks, the coupling of damage and crack evolution, the possible evolution of nodes in 3D.

The LEFM crack propagation model disregarded the effect of residual stresses. The creep deformation behavior of nickel-based single crystal superalloys also controls the service life of turbine blades used in modern turbine blades. The creep phenomenon takes place in general at high temperatures and is characterized by the fact that under constant stress and temperature, the material deforms viscoplastically. This time-dependent plastic deformation is governed by a changing in creep velocity which represents the response of the material to loading.

A few models for the creep deformation behavior of single crystal superalloys were presented in latest publications. Constitutive equations are constructed for single-crystal nickel-based superalloys [93]. The model allows the following features of superalloy creep to be recovered: dependence upon microstructure and its scale, effect of lattice misfit, internal stress relaxation, incubation phenomena, the interrelationship of tertiary and primary creep, and vacancy condensation leading to damage accumulation. In [94] an extension of the Cailletaud single crystal plasticity model to include modeling of tertiary creep was discussed. In [95] a general framework for advanced creep damage modeling is presented. The proposed approach consists in deriving a constitutive model at the continuum scale, where state variables and effects can be homogenized, based on microstructural features and deformation mechanisms. A time-independent formulation has been derived for creep damage and the procedure for identifying the material model parameters has been briefly indicated.

The creep involved crack propagation will be accomplished by performing an elastic-plastic stress analysis of the model without the crack local model. For the creep analyses the residual stresses will be computed in ANSYS or ABAQUS [106] prior to executing the crack growth analysis. Separate analyses will be performed incorporating bulk residual stresses that result from local yielding at the crack tip and by thermal mechanical fatigue. Each set of analyses will be conducted using the applied investigational conditions, and incorporated measured material properties including

plastic deformation at elevated temperature, fatigue crack growth rates for varying stress ratios and measured residual stress profiles, where applicable.

In the case where bulk residual stresses only will be incorporated, the residual stress calculation should include one full loading cycle at elevated temperature. Residual stresses will be present after unloading due to yielding at the cooling hole/or another location. The results of [96] study successfully demonstrated the potential to predict the effect of compressive residual stresses on crack growth retardation at corner cracks; elevated temperature corner crack growth experiments on notched Rene 88DT specimens were performed.

The development of methodology for the damage-tolerant approach based on finite element and fracture mechanics numerical crack propagation models can not be successful using the current numerical codes. The implementation in numerical modeling concepts of local microstructural features like the grain size and geometry, the crystallographic orientation relationship, and the grain boundary structure will be excellent approach.

# 6. References


1. R.M. Pelloux;N. Marchand: Thermal-Mechanical Fatigue Behavior of Nickel-Base Superalloys, *NASA-CR_175048.MIT 1986*
2. Broek D; Elementary engineering fracture mechanics, *Dordrecht: Martinus Nijhoff Publishers; 1982*
3. R. Nutzel ; E. Affeldt ; M. Goken: Damage evolution during thermo-mechanical fatigue of a coated monocrystalline nickel-base superalloy , *International Journal of Fatigue 30 (2008) 313–317*
4. Bernd Baufeld ; Marion Bartsch ; Michael Heinzelmann: Advanced thermal gradient mechanical fatigue testing of CMSX-4 with an oxidation protection coating, *International Journal of Fatigue 30 (2008) 219–225*
5. Bhattachar V.S.: Thermal fatigue behaviour of nickel-base superalloy 263 sheets, *International Journal of Fatigue Vol. 17, No. 6, pp. 407-413, 1995*
6. Bill, R.C.; Verrilli M.J.; McGaw, M.A. and Halford,G.R.: Preliminary Study of Thermomechanical Fatigue of Polycrystalline Mar-M 200*, NASA-TP 2280, 1984*
7. Swanson GA; Linask I; Nissley DM; Norris PP; Meyer TG; Walker KP: Life prediction and constitutive models for engine hot section anisotropic materials program, *NASA-CR-179594, 1987.*
8. Goswami, Tarun: Low cycle fatigue—dwell effects and damage mechanisms, *International Journal of Fatigue 21 (1999) 55–76*
9. Miner RV, Gayda J, Hebsur MG: Fatigue Crack Propagation of Nickel-Base Superalloys at 6S0°C, *ASTM STP 942. 1988:371*.
10. S.K. Bhaumik ; M. Sujata, M.A. Venkataswamy; M.A. Parameswara: Failure of a low pressure turbine rotor blade of an aeroengine, *Engineering Failure Analysis 13 (2006) 1202–1219.*
11. Reed, Roger C.: The Superalloys: Fundamentals and Applications, *New York: Cambridge University Press, 2006.*
12. Campbell, F.C.: Manufacturing Technology for Aerospace Structural Materials, *Elsevier Inc., San Diego, CA. 2006.*
13. C.M. Branco and J. Byrne: Elevated Temperature Fatigue on IN718 Effects of Stress Ratio and Frequency, *Proceedings of the 81st Meeting of the AGARD/SMP.*
14. C.C. Engler-Pinto Jr.; M. Blumm; F. Meyer-Olbersleben; B. Ilschner and F. Rezai-Aria:Non-Isothermal Fatigue: Methods, Results and Interpretation, *AGARD conference proceedings, v. 569, p. 71-79, 1996.*
15. G.F. Harrison; P.H. Tranter and; S.J. Williams: Modeling of Thermomechanical Fatigue in Aero Engine Turbine Blades, *AGARD conference proceedings, 1996.*

16. N.X. Hou,W.X; Gou, Z.X.Wen; Z.F. Yuell: The influence of crystal orientations on fatigue life of singlecrystal cooled turbine blade, *Materials Science and Engineering A 492 (2008) 413–418*

17. Q.M. Yu; Z.F. Yue ; Z.X. Wen: Creep damage evolution in a modeling specimen of nickel-based single crystal superalloys air-cooled blades, *Materials Science and Engineering A 477 (2008) 319–327*

18. L.M. Kachanov: Introduction to Continuum Damage Mechanics, *Martinus Nijhoff, Dotrecht, Netherlands (1986).*

19. Y.N. Rabotnov: Creep Problems in Structural Members, *North Holland Publishing Co., Amsterdam (1969).*

20. Heine, J.E.; Warren; J.R. and Cowles, B.A.:Thermal Mechanical Fatigue of Coated Blade Materials, *Final Report, WRDC-TR-89-4027, June 1989*.

21. J.E. Heine; E. Ruano and R.E. DeLaneuville: TMF Life Prediction Approach for Turbine Blades, *AGARD conference proceedings, v. 569*

22. T. Nicholas: Fatigue Crack Growth Under TMF, *AGARD conference proceedings, v. 569*

23. T.S. Cook; J.H. Laflen; R.H. Van Stone and P.K. Wright:TMF Experience With Gas Turbine Engine Materials, *General Electric Co., Thermal Mechanical Fatigue of Aircraft Engine19960301, AGARD-CP-569*

24. Huseyin Sehitoglu: Thermal and Thermomechanical Fatigue of Structural Alloys, *ASM Handbook.Volume19 Fatigue and Fracture*

25. Anderson, T.L.: Fracture Mechanics Fundamentals and Applications, *Second Edition CRC Press LLC, Florida, 1995.*

26. AFGROW USERS GUIDE AND TECHNICAL MANUAL AFGROW for Windows XP/VISTA, *Version 4.0012.15 AFRL-VA-WP-TR-2008-XXXX*

27. Heath, B.J.; Grandt, A.F.: Stress Intensity Factors for Coalescing and Single Corner Flaws Along a Hole Bore in a Plate, *Engineering. Fracture Mechanics*, *Vol 19, pp. 665-673, 1984*

28. Kuo, A.; Yasgur, D.; Levi, M.:Assessment of Damage Tolerance Requirements and Analyses *AFWAL-TR-86-3003 Volume II, Air Force Wright Aeronautical Laboratories Flight Dynamics Laboratory, Wright-Patterson AFB, OH, 1986*

29. Wawrzynek, P.A.; Carter, B.; Banks-Sills, L. :The M-integral For Computing Stress Intensity Factors in Generally Anisotropic Materials, *NASA/CR-2005-214006, 2005*

30. Ragupathy; Kannusamy; Shailendra; Bist: 3-D Crack Propagation Modeling and Analysis: Turbocharger components under TMF loading, *ANSYS 2009 Modeling Teqchnique, www.ansys.com*

31. Ani Ural; Gerd Heber; Paul A. Wawrzynek; Anthony R. Ingraffea; David G. Lewicki; Joaquim B.C.; Neto: Three-dimensional, parallel, finite element simulation of fatigue crack growth in a spiral bevel pinion gear, *Engineering Fracture Mechanics, Volume 72, Issue 8, May 2005, Pages 1148-1170*

32. .MacLachlan, D.W.; Knowles, D. M.: The Effect of Material Behavior on the Analysis of Single Crystal Turbine Blades: Part I – Material Model, *Fatigue Fracture Engineering Material Structures, Vol. 25, pp 385-398, Nov. 2001.*

33. Richard W. Hertzberg: Deformation and Fracture Mechanics of Engineering Materials, *Wiley, John & Sons, Incorporated,1996.*

34. FRANC3D Version 1.14 Menu & Dialog Reference, Cornell Fracture Group website *http://www.cfg.cornell.edu. (Version 1.14 manuals serve for V1.5 also).*

35. F. Erdogan; G. C. Sih: On the Extension of Plates under Plane Loading and Transverse Shear*, Journal of Basic Engineering, Vol. 85D, No. 4, pp. 519-527, 1963.*

36. G. P. Cherapanov: Mechanics of Brittle Fracture, *McGraw-Hill, New York, 1979.*

37. L. Banks-Sills;P. Wawrzynek; B. Carter; A.Ingraffea; I. Hershkovitz: Methods for computing stress intensity factors in anisotropic geometries: Part II – arbitrary geometry*, Engineering Fracture Mechanics, 74 (8)(2007) 1293-1307*

38. Elleithy, W.: Adaptive Coupled Finite Element-Boundary Element Method for Elasto-Plastic Analysis, *Seventh UK Conference on Boundary Integral Methods, Nottingham, UK, July 2009,*

39. Anthony R. Ingraffea; Paul A. Wawrzynek: Computational fracture mechanics: a survey of the field, *European Congress on Computational Methods in Applied Sciences and Engineering ECCOMAS 2004 Jyväskylä, 24—28 July 2004*

40. Rolls-Royce *TMF-Workshop 22 – 23 Sep. 2005*

41. Okazaki M ; Nakatani, H: On the Significance of Environment in Thermal Fatigue of a Unidirectional SCS-6/Ti-24Al-11Nb Metal Matrix Composite , *ASTM Thermo-mechanical fatigue behaviour of materials., v*ol. 3. *2003.*

42. M. Okazaki; M. Sakaguchi:Thermo-mechanical fatigue failure of a single crystal Ni-based superalloy, *International Journal of Fatigue 30 (2008) 318–323*

43. Carter B; Wawrzynek P; Ingraffea: A 2000 Automated 3D crack growth simulation, *Int. J. Numer. Methods Eng. 47, 229±53*

44. N.K. Arakere ; S. Siddiqui ; F. Ebrahimi : Evolution of plasticity in notched Ni-base superalloy single crystals, *International Journal of Solids and Structures 46 (2009) 3027–3044*

45. T. Sourmail: Coatings for Turbine Blades. Historical overview, *University of Cambridge www.msm.cam.ac.uk/.../coatings/index.html*

46. Denis Yurchenko and Pavel Krukovsky : Flow & thermal analysis of a turbine blade *Institute of Engineering Thermophysics, Kyiv, Ukraine Dynamics issue 2.01 Released: March 2008 http://www.cd-adapco.com*

47. Cetel, A.D.; Duhl, D.N.:Second-Generation Nickel-Base Single Crystal Superalloy, *Superalloys 1988, The Metallurgical Society, 235-244 (1988*).

48. Basquin, O.H., :The Exponential Law of Endurance Tests,. *American Society for Testing and Material Processes, 1910. 10: p. 625-630.*

49. Coffin, L.F.J.: A Study of the Effects of Cyclic Thermal Stresses on a Ductile Metal, *Transactions of the American Society of Mechanical Engineers, 1954. 76.*

50. Manson, S.S.: Behavior of Materials under Conditions of Thermal Stress, *Heat Transfer Symposium 1953. University of Michigan Engineering Research Institute*.

51. Bannantine, J.A.; Comer, J.J.; Handrock, J.L.: Fundamentals of Metal Fatigue Analysis. *1990, Englewood Cliffs, NJ: Prentice-Hall.*

52. Manson, S.S.:Behavior of Materials under Conditions of Thermal Stress, *Heat Transfer Symposium, University of Michigan Engineering, Research Institute, 1953, pp. 9-75*

53. Palmgren, A., "Durability of Ball Bearings". *ZVDI, 1924. 68(14): p. 339-341.*

54. M.A. Miner: Cumulative damage in fatigue, *Applied Mechanics., vol 12, 1945, p 159-164.*

55. Duhamel, J.M.C., Memoires de l'Institut de France, 1838.

56. A. Winkelmann, O. Schott: "Über thermischeWiderstandscoefficienten verschiedener Gläser in ihrer Abhängigkeit von der chemischenZusammensetzung (Dependence of the thermal resistance of various glasses from thechemical composition)", *;Annalen der Physikalischen Chemie, vol. 51, 1894, p 730-746, 1894.*

57. Schmid, E., Boas, W.: Kristallplastizitaet, *Verlag Julius Springer. 1935.Berlin.*

58. Bollenrath, F; Cornelius, H.; Bungardt, W.: Jahrbuch der Deutschen Luftfahrforschung, 1938. Vol.II.

59. Millenson, M.B., Manson, S.S., :Investigation of Rim Cracking in Turbine Wheels with Welded Blades. *NACA RME6L 17, National Advisory Committe for Aeronanautics,1947*

60. Sehitoglu, H.: Material Behavior under Thermal Loading, *Journal of Pressure Vessel Technology, Transactions of ASME, 1986..*

61. Neu, R.W.; Sehitoglu, H.: Thermomechanical Fatigue, Oxidation, and Creep, Part 1. Damage Mechanisms, *Metallurgical Transactions, 1989.: p. 1755-1767.*

62. Remy, L.; Bernard, H.; Malpertu, J.L.; Rezai-Aria, R., :Fatigue Life Prediction Under Thermomechanical Loading in a Nickel-Based Superalloy, *Thermomechanical Fatigue Behavior of Materials, ASTM STP 1186, ed. H. Sehitoglu. 1993, American Society for Testing and Materials: Philadelphia.p. 3-16.*

63. Marchand, N.J.; L'Esperance; Pelloux, R.M:. Thermal-Mechanical Cyclic Stress-Strain Responses of Cast B-1900+Hf, *Low Cycle Fatigue, ASTM STP 942, ed. H.D. Solomon. 1988, American Society for Testing and Materials: Philadelphia. 638-656.*

64. Inglis, C.E.:Stresses in a Plate Due to the Presence of Cracks and Sharp Corners, *Transactions of the Institute of Naval Architects, 1913.p. 219-241*

65. Griffith, A.A.,:The Phenomena of Rupture and Flow in Solids, *Philosophical Transactions, Series A, 1920. p. 163-198.*

66. Irwin, G.R.: Fracture Dynamics. Fracturing of Metals, *American Society for Metals. 1948, Cleveland. 147-166.*

67. Orowan, E.: Fracture and Strength of Solids, *Reports on Progress in Physics, 1948.*

68. Westergaard, H.M.:Bearing Pressures and Cracks, *Journal of Applied Mechanics, 1939.*

69. Dugdale, D.S.: AYielding in Steel Sheets Containing Slits, *Journal of Mechanics of Physical Solids, 1961.*

70. Paris, P.C.: Gomez, M.P., and Anderson, W.P., "A Rational Analytic Theory of Fatigue". *The Trend in Engineering, 1961.*

71. Chi-Ten Wang, :Applied Elasticity, *McGraw-Hill Book Company, inc, 1953*

72. Forman, R.G.; Kearney, V.E.; Engle, R.M.: Numerical Analysis of Crack Propagation in a Cyclic-Loaded Structure, *Journal of Basic Engineering, Transactions of the ASME, 1967*

73. Walker, K., The Effect of Stress Ratio During Crack Propagation and Fatigue for 2024-T3 and 7075-T6 Aluminum. Effects of Environment and Complex Load History on Fatigue Life, *ASTM STP 462. 1970, Philadelphia, Pa: American Society for Testing and Materials*. 1-14.

74. Elber, W.:"Fatigue Crack Closure under Cyclic Tension", *Engineering Fracture Mechanics, 1970*

75. Elber, W.: The Significance of Fatigue Crack Closure. Damage Tolerance in Aircraft Structures, *ASTM STP 486. 1971, Philadelphia, PA: American Society for Testing and Materials. 230-242.*

76. Rice, J.R.: A Path Independent Integral and Approximate Analysis of Strain Concentration by Notches and Cracks, *Journal of Applied Mechanics, 1968*.

77. Hutchinson, J.W.: Singular Behavior at the End of a Tensile Crack Tip in a Hardening Material, *Journal of Mechanics of Physical Solids, 1968.*

78. Rice, J.R.; Rosengren, G.F.:Plane Strain Deformation near a Crack Tip in a Power Law Hardening Material, *Journal of Mechanics of Physical Solids, 1968.*

79. Dowling, N.E.: Begley, J.A.:Fatigue Crack Growth during Gross Plasticity and the J-Integral, Mechanics of Crack Growth, *ASTM STP 590. 1976, American Society for Testing and Materials: Philadelphia.*

80. Dover, W.D.:Fatigue Crack Growth under C.O.D. Cycling, *Engineering Fracture Mechanics, 1973.*

81. McEvily, A.J.; Beukelmann, D.;Tanaka, K.: On Large-Scale Plasticity Effects in Fatigue Crack Propagation in Mechanical Behavior of Materials: *Symposium on Mechanical Behavior of Materials. 1974. Kyoto, Japan: Society of Material Science.*

82. Shih, C.F.: Relationships between the J-Integral and the Crack Opening Displacement for Stationary and Extending Cracks*, Journal of Mechanics of Physical Solids, 1981.*

83. Skelton, R.P.: The Prediction of Crack Growth Rates from Total Endurances in High Strain Fatigue, *Fatigue of Engineering Materials and Structures, 1979.*

84. Wareing, J.: *Creep-Fatigue Interaction in Austenitic Stainless Steels". Metallurgical Transactions, 1977.*

85. Landes, J.D.; Begley, J.A.: A Fracture Mechanics Approach to Creep Crack Growth. Mechanics of Crack Growth, *ASTM STP 590. 1976, Philadelphia, Pa: American Society for Testing and Materials.*

86. Saxena, A.: Evaluation of C* for Characterization of Creep Crack Growth Behavior of 304 Stainless-Steel, *12th Fracture Conference Proceedings, ASTM STP 590. 1980. Philadelphia: American Society for Testing and Materials.*

87. Blackburn, W.S.:Path-Independent Integrals to Predict the Onset of Crack Instability in an Elastic Material*". International Journal of Fracture Mechanics, 1972.*

88. Kishimoto, K.; Aoki, S.; Sakada, M.:On the Path-Independent Integral--J^, *Engineering Fracture Mechanics, Volume 13, Issue 4, 1980, Pages 841-850.*

89. Orange, T.W.:Elevated Temperature Crack Propagation, *Fatigue and Fracture of Aerospace Structural Materials, ASME, 1993.*

90. Atluri, S.N.; Nishioka, T.; and Nakagaki, M. : "Incremental Path-Independent Integrals in Inelastic and Dynamic Fracture Mechanics". *Georgia Institute of Technology, Atlanta, GA. GIT-CACM-SNA-83-27*

91. Kim, K.S.; Van Stone, R.H.:Hold Time Crack Growth Analysis at Elevated Temperatures*, Engineering Fracture Mechanics, 1995.*

92. Kim, K.S., Van Stone, R.H.: Crack Growth Under Thermo mechanical and Temperature Gradient Loads*,. Engineering Fracture Mechanics, 1997*.

93. A. Maa, D; Dyea, R.C.;Reed :A model for the creep deformation behavior of single-crystal superalloy CMSX-4, *Acta Materialia 56 (2008) 1657–1670*

94. Ivaylo N.Vladimirov, StefanieReese , Gunther Eggeler Constitutive modelling of the anisotropic creep behaviour of nickel-base single crystal superalloys *International Journal of Mechanical Sciences 51 (2009) 305–313*

95. Esposito:Time-independent-formulation-for-creep-damage-modeling-in-metals-based-on-void-and-crack-evolution, *Materials Science and Engineering (2009*

96. A. L. Hutson; M. Huelsman; D. Buchanan; R. John1; S. Haering: Corner Crack Propagation in the Presence of Residual Stresses, *AFRL-ML-WP-TP-2006-439*

97. .MacLachlan, D.W. ; Knowles, D.M.:Creep-Behavior Modeling of the Single Crystal Superalloy CMSX-4, *Metallurgical and Materials Transactions A,* 31A: 1401-1411 (2000).

98. Ott, M.; Mughrabi, H. : Dependence of the High Temperature Low Cycle Fatigue Behavior of the Monocrystalline Nickel Based Superalloys CMSX-4 and CMSX-6 on the Gamma/Gamma Prime Morphology, *Materials Science and Engineering, A272: 24-30 (1999).*

99. Sakaguchi, M. ; Okazaki, M. “Fatigue Life Evaluation of a Single Crystal Ni-Base Superalloy, Accompanying with Change of Microstructure Morphology,” *International Journal of Fatigue, 29: 1959-1965 (2007).*

100. A. Staroselsky ; L. Vestergaard ; B. Annigeri ; L. Favrow ; D.: Walls:Three-dimensional fatigue cracking under elastic–plastic deformation, *International Journal of Fatigue 23 (2001)*

101. Brice Cassenti; Alexander Staroselsky: The effect of thickness on the creep response of thin-wall single crystal components, *Materials Science and Engineering A 508 (2009) 183–189*

102. Ulrich Krupp: Fatigue Crack Propagation in Metals and Alloys, *Wiley-VCH Verlag GmbH & Co. KGaA, 2007*

103. Ramberg, W.; Osgood, W.R.: Description of Stress-Strain Curves by Three Parameters , *Technical Report No 902 NASA 1940)*

104. Ron S. Bunker; Lesley: Cooling Design Analysis, *The Gas Turbine Handbook, National Energy Technology Laboratory (NETL), http://www.netl.doe.gov/*

105. Je-Chin Han; Lesley M.Wright: Enhanced Internal Cooling of Turbine Blades and vanes, *The Gas Turbine Handbook, National Energy Technology Laboratory (NETL), http://www.netl.doe.gov*

106. VCCT for Abaqus.http://www.simulia.com/products/vcct.html